Robust Estimation of Low Frequency Modes for On-line Stability Monitoring of Power System

Shekha Rai

Robust Estimation of Low Frequency Modes for On-line Stability Monitoring of Power System

A

Thesis submitted

for the award of the degree of

Doctor of Philosophy

By

Shekha Rai

Department of Electronics and Electrical Engineering

Indian Institute of Technology Guwahati

Guwahati - 781 039, Assam, India

April 2017

Dedicated

To

My Family

Certificate

This is to certify that the thesis entitled "**Robust Estimation of Low Frequency Modes for Online Stability Monitoring of Power System**", submitted by **Shekha Rai** (11610239), a research scholar in the *Department of Electronics and Electrical Engineering, Indian Institute of Technology Guwahati*, for the award of the degree of **Doctor of Philosophy**, is a record of an original research work carried out by her under our supervision and guidance. The thesis has fulfilled all requirements as per the regulations of the institute and in our opinion has reached the standard needed for submission. The results embodied in this thesis have not been submitted to any other University or Institute for the award of any degree or diploma.

Date:

Place: Guwahati.

Dr. Praveen Tripathy
Assistant Professor
Dept. of Electronics and Electrical Engg
Indian Institute of Technology Guwahati
Guwahati - 781 039, Assam, India.

Date:

Place: Guwahati.

Dr. Sisir Kumar Nayak
Associate Professor
Dept. of Electronics and Electrical Engg
Indian Institute of Technology Guwahati
Guwahati - 781 039, Assam, India.

Acknowledgements

I feel it is as a great privilege in expressing my deepest and most sincere gratitude to my thesis supervisors Dr. P. Tripathy and Dr. S. K. Nayak for their excellent guidance throughout my study. Their kindness, dedication, hard work and attention to detail have been a great inspiration to me. I am highly obliged to Dr. P. Tripathy who has offered his infinite support and clarified my smallest of doubts and has been a mentor for me throughout these years.

I am highly obliged to Prof. S. C. Srivastava of IIT Kanpur for providing the Real Time Digital Simulator facility to carry out my research work. I am also thankful to the Power Grid Corporation of India for providing the real time PMU data located at one of the buses of the North-Eastern Regional Grid.

I am highly obliged to the Head of the Department, Dr. Tony Jacob and all the faculty members who have taught me various courses and provided me with active help and support, whenever needed. I am also very thankful to my doctoral committee members for sparing their precious time to evaluate the progress of my work. I am also grateful to the technical and non-technical staff members of the department for their assistance in carrying out various tasks associated with this research work.

I would like to thank Bhanu Priya, Dhaval, Umesh, Himanshu, Mridul, Venkat, Gautam, Anurag, Gayatri, Kannan and Reena and all the research scholars of the power control laboratory, IIT Guwahati, for their cooperation.

My deepest gratitude goes to my parents for their unending love and support. Their continuous encouragement have enabled me to sail through the most difficult times during my studies. I would like to thank my sister, my brother and my husband who have always motivated me during the course of my study. I would also like to thank my friend Puspanjalee for supporting me and making my stay in IITG memorable.

This acknowledgement will be incomplete without the mention of the Almighty Lord who has

always showered His divine blessings and unceasing love and grace upon me and has protected me against all odd circumstances.

Shekha Rai

Abstract

In recent times, lots of emphasis is given towards the utilization of renewable sources of energy to generate electrical power in the grid. The increasing capacity of generation from the renewable sources of energy has complicated the operational challenges related to stability, economic operation etc., of an interconnected power system. Thus, there is an urgent need of on-line stability monitoring tools that can capture the system dynamics and help the operators with a better decision support system and control. In recent times, with the advancement of phasor measurement unit (PMU) based wide area monitoring systems (WAMSs) which provides time-stamped phasors with high accuracy, it is now possible to develop a system for on-line monitoring of the small signal rotor angle stability of the power system. The present thesis mainly aims at developing robust algorithms to estimate low frequency critical modes corresponding to the oscillations in the power system.

Most of the methods reported in the literature to estimate the low frequency modes are mainly based on minimizing the l_2-norm of the error. It is observed that the estimated modes from these methods are severely affected in the presence of an outlier or bad measurements which can occur in wide area monitoring systems due to various environmental effects like lightning or temporary faults in the network or measuring instruments. Hence, there is a need to develop robust methods which can provide a good estimate of the modes even in the presence of outliers in the measurements. In order to mitigate the effect of such bad data or outliers, the first part of the thesis proposes a robust modified Prony estimator for estimating the low frequency modes of power system using the ring-down data obtained from PMU. The proposed method is based on minimum covariance determinant (MCD) technique to find the robust covariance matrix followed by improved Prony to estimate the modes. To further improve the performance, a total least squares -

estimation of signal parameter via rotational invariance techniques (TLS-ESPRIT) along with the use of robust covariance based on MM estimator is proposed in the second part of the thesis.

The events associated with major disturbances such as fault, adding/removing of a large load or generation provides the data associated with the free response that can be easily observed in the presence of ambient noise. As these major disturbance are less frequent, hence, the methods utilizing the ringdown data provides a very accurate estimation of the modes, but are updated typically after a long duration. Hence, there is a need to develop estimating algorithms which can continuously monitor the stability of the power system. These algorithms are mainly based on the use of ambient data corresponding to the flow of active power. The ambient data corresponding to the active power flow in the line is observed to have the presence of nonlinear trends along with noise of high variance, thus the proposed NwT-RD-TLS-ESPRIT method has used a combination of nonlinear filter, wavelet, random decrement (RD) and modified TLS-ESPRIT for mode identification.

Finally, a more accurate method which uses a sparse based signal recovery technique in conjunction with random decrement (RD) and modified TLS-ESPRIT for identification of inter-area oscillatory modes for the ambient data has been proposed. The proposed method is compared with NwT-RD-TLS-ESPRIT method for the sample test signal resembling ambient data.

Thus the present thesis tries to address some of the problems associated with the low frequency mode estimation using both ambient and ringdown data to have a better observability of the dynamics of the power system.

Contents

List of Figures

List of Tables

List of Acronyms:

AESOPS : Analysis of essentially spontaneous oscillations in power system

AR : Autoregressive

ARMA : Autoregressive moving average

ARMAX : Autoregressive moving average exogenous

CF : Cost function

DFT : Discrete Fourier transform

DOA : Direction of arrival

EMD : Empirical mode decomposition

EMS : Energy management system

ERA : Eigensystem realization algorithm

FDD : Frequency domain decomposition

FFT : Fast Fourier transform

GPS : Global positioning system

ICA : Independent component analysis

IF : Influence function

IRIG-B : Inter Range Instrumentation Group Time Code format B

ITD : Ibrahim time domain

KF : Kalman filter

KT : Kumaresan-Tufts

LS-ESPRIT : Least squares estimation of signal parameters via rotational invariance techniques

MCD : Minimum covariance determinant

MI : Multiple invariance

NEREB : North Eastern Regional Electricity Board

NExT : Natural excitation technique

N4SID : Numerical sub-space state space system identification

OMA : Operational modal analysis

OMP : Orthogonal matching pursuit

PDC : Phasor data concentrator

PEALS : Program for eigenvalue analysis of large systems

PMU : Phasor measurement unit

RD : Random decrement

R3LS : Regularized robust recursive least squares

RRLS : Robust recursive least squares

RTDS : Real time digital simulator

RTU : Remote terminal unit

SCADA : Supervisory control and data acquisition system

SNR : Signal to noise ratio

SSA : Small signal stability analysis

SSI : Stochastic subspace identification

SSSP : Small signal stability program

SVD : Singular value decomposition

TLS-ESPRIT : Total least squares estimation of signal parameters via rotational invariance techniques

TVE : Total vector error

UTC : Universal time coordinated

WAMS : Wide area monitoring system

WECC : Western Electricity Coordinating Council

YW : Yule-Walker

YWS : Yule Walker with spectral analysis

List of Symbols:

$s(n)$: Signal component

$w(n)$: Zero mean white Gaussian noise

a_k : Amplitude

ω_k : Angular frequency

ϕ_k : Initial phase

K : Number of sinusoids

b_k : Damping factor

α_j : Complex signal amplitude

β_j : Mode of the signal

$\mathbf{g}$: Vector of backward prediction coefficient

M : True signal components

$L - M$: Extraneous noise components

$G(z)$: Polynomial providing zeros

z_j : Zeros

ρ_i : i-th singular value

$K(i)$: Monotonously increasing index

$\mathbf{A}$: Hankel matrix

$\mathbf{T}_j$: Mean of the samples for the j-th iteration

$\mathbf{S}_j$: Covariance of the samples for the j-th iteration

$d_j(i)$: Mahalanobis distance for each sample for j-th iteration

$\mathbf{R_A}$	: Robust covariance matrix
$\mathbf{C_A}$	: Low rank approximation of $\mathbf{R_A}$
μ	: Mean
σ^2	: Variance
$\mathbf{p}(n)$, $\mathbf{q}(n)$ and $\mathbf{r}(n)$	: Time shifted data vectors
$\mathbf{\Gamma}$	: Diagonal matrix that relates the time shifted data vectors
$\mathbf{R}_{yy}$	: Autocorrelation matrix
$\mathbf{R}_s$	: Signal covariance matrix
$\mathbf{E_s}$	: Signal subspace
$\mathbf{E_n}$	: Noise subspace
$\boldsymbol{\lambda_s}$	: Singular value of the signal subspace
$\boldsymbol{\lambda_n}$	: Singular value of the noise subspace
$\boldsymbol{\mu}_n$	: Location vector
$\mathbf{\Sigma}_n$	: Covariance matrix
$\tilde{\boldsymbol{\sigma}}_n$	: Robust scale estimate
$w(k)$	: k-th window
l_w	: Length of the window and must be a multiple of 2
k	: Index of the window
w_s	: Samples by which the window is shifted
$x[i]$	: Input sample to the pre-filter
$\bar{w}(k-1)$	: Mean of samples in window $w(k-1)$

$\bar{w}(k)$: Mean of samples in window $w(k)$

$y[i]$: Output of the nonlinear filtered signal

$\psi_{a,b}(t)$: Wavelet function generated by scaling a and translation b of a single mother wavelet ψ

$w_{a,b}$: Wavelet coefficients corresponding to the wavelet basis function

T : Universal threshold

n_{TH} : Number of most significant wavelet coefficients

τ : Length of the segments

$\delta(\tau)$: RD signature

T_{th} : Threshold level for random decrement technique

c : Fraction of the standard deviation σ of the signal

X_r^e : Real values of the estimated quantity

X_i^e : Imaginary values of the estimated quantity

X_r^a : Real values of the actual quantity

X_i^a : Imaginary values of the actual quantity

$\boldsymbol{\gamma}$: Sparse vector

B : Number of non-zero elements in the sparse vector $\boldsymbol{\gamma}$

n : No of iteration

I^n : Indices of the atom selected

$\boldsymbol{\gamma}^n$: Sparse representation of $\mathbf{x}$

$\mathbf{r}^n$: Residue ($\mathbf{x} - \mathbf{D}\boldsymbol{\gamma}^n$)

$\boldsymbol{\zeta}^n$: Product of $\mathbf{D}^T\mathbf{r}^n$

$\mathbf{G}$: Product of $\mathbf{D}^T\mathbf{D}$

$\boldsymbol{\Upsilon}^n$: Product of $\mathbf{G}\boldsymbol{\gamma}^n$

$\mathbf{L}^n$: Cholesky factorization of $\mathbf{G}_{I^n,I^n}$

$\mathbf{c}^n$: Non zero coefficients of $\boldsymbol{\gamma}^n$, numbered by I^n

$\boldsymbol{\Phi}$: Estimated sparse matrix

$\mathbf{Y}_{\mathbf{reconstruct}}$: Reconstructed signal matrix

1

Introduction

1.1 General

In the present scenario of large interconnected power systems with continuously increasing electrical power demand, there is the requirement of rapid expansion of existing transmission network. However, the rapid expansion of transmission network is observed to be less feasible due to economical, environmental and the problems associated with right of way, thus forcing the system to operate close to its stability limits. Further, the situation gets more aggravated with the inclusion of renewable energy sources such as wind, solar etc, into the existing grid. The power system operating with the conventional generation, the load uncertainty and disturbances were the major causes of concern, but with the increasing generation through the renewable energy sources, the system operators have to consider the effect of uncertainty even in the generation. Under these circumstances, to operate the power system in a stable and economical way, better on-line monitoring and decision support systems are required. Earlier, supervisory control and data acquisition system (SCADA) have been used to collect data related to the power system through remote terminal unit (RTU) placed at various buses in the network. The estimated measurements from RTU such as magnitude of the bus voltage, branch currents and active and reactive power flows on lines are typically updated in the interval of $2 - 10$ seconds [1–3] at the control center. These measurements at the control center are given to a nonlinear

state estimator which updates the state of power system in an interval of 5 – 10 minutes. Thus, it is observed to be suitable for steady state observability of the power system.

With the rapid development of phasor measurement units (PMUs) based wide area monitoring systems (WAMSs) [4] which utilize GPS clock as time reference to estimate the phasors. Due to its high refreshing rate (i.e, one or two cycles) of the estimated phasors, it is possible to capture the dynamics of the system close in real time, thus enabling the online monitoring and assessment of system stability.

In the recent years, several projects on WAMS have been set up by countries like USA, China etc [5]. In India, establishment of WAMS and analysis of several off-line and on-line applications of synchrophasor measurements have been undertaken by the Ministry of Power, Government of India from 2010 [5]. One of those initiative is to develop tools for real time stability monitoring of Indian power system. Hence, the primary focus of the present thesis is on the development of algorithms for low frequency mode estimation both for ringdown and ambient data for real time assessment of small signal stability of the system using synchrophasor data.

1.1.1 Synchrophasor-based Wide Area Monitoring Systems (WAMSs)

Figure 1.1 shows the conventional SCADA/Energy Management System (EMS). Remote terminal units (RTUs) connected at a bus in a SCADA based wide area monitoring systems (WAMSs), measures the magnitudes of bus voltage, line currents and power flows in the lines. Typically, the measurements are received at control center with the time interval of 2 – 10 seconds. These measurements which are obtained from the RTUs are then fed to a nonlinear state estimator to estimate voltage magnitude and phase angle at various buses in the system. As the nonlinear estimator involves iterative steps for estimating the phasors, the estimated phasors gets updated in the interval of 2 – 10 minutes for a large interconnected power system. The SCADA based WAMSs finds its application for various static analysis but is found to be not suitable for observing the dynamics of the power system due to its significant delay in updating the states.

Recent trends is to have a phasor measurement units (PMUs)-based wide area monitoring system (WAMS), as shown in Figure 1.2. These PMUs placed at various buses measures the magnitude and phase angle of bus voltages, branch currents, frequency and rate of change of frequency with a report-

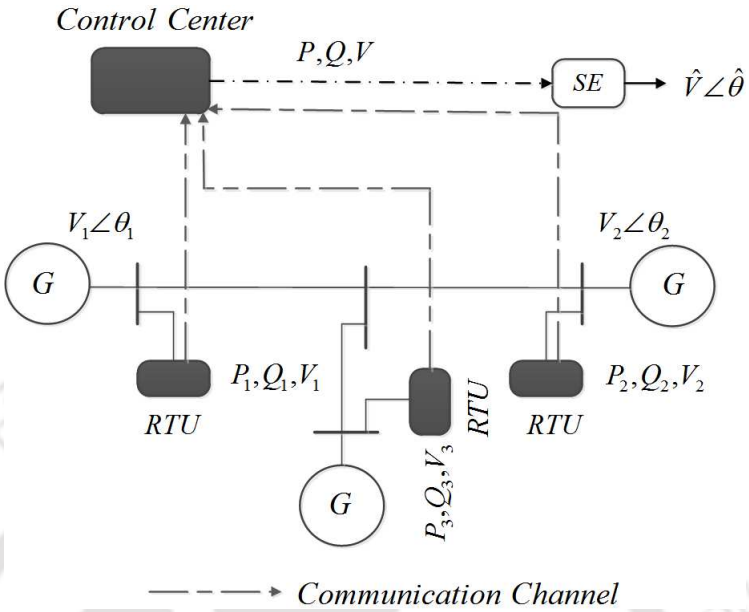

Figure 1.1: Block diagram of SCADA.

ing rate of 10/25/50 or 10/12/15/20/30/60 frames per second for 50 or 60 Hz systems, respectively. Phasor data concentrator (PDC) collects the measured data from the PMU by using links having high bandwidth and minimum noise interference, such as fiber optics etc. The high refreshing rate and time stamped measurements have made PMU-based WAMS suitable for observing the dynamic response of the power system in near real time. Based on these measurements, various control actions or the control strategies can be developed to enhance the stability, security and reliability of the power system.

A typical block diagram of a PMU is shown in Figure 1.3. The GPS clock utilizes Inter Range Instrumentation Group time code format B (IRIG-B) signal [6, 7] for providing the time tag for the estimated phasors by the PMU. The voltage and current from the secondary side of the potential and current transformers are converted to the corresponding voltage and current signals by the voltage and current sensors. These analog voltage and current signals are pre-processed by an anti-aliasing filter to filter out the unwanted high frequency components. The pre-processed analog signal is then converted into digital signal by the analog to digital converter. Finally, the phasor estimating algorithm running on the microprocessor estimates the phasors, frequency and rate of change of frequency from the converted digital signal and is transmitted to the PDC through communication links using the IEEE C37.118 format.

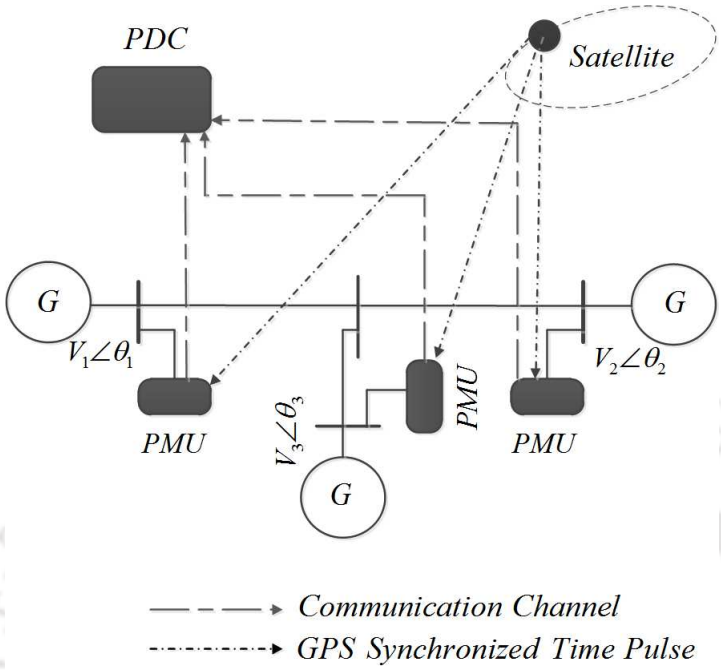

Figure 1.2: Block diagram of WAMS.

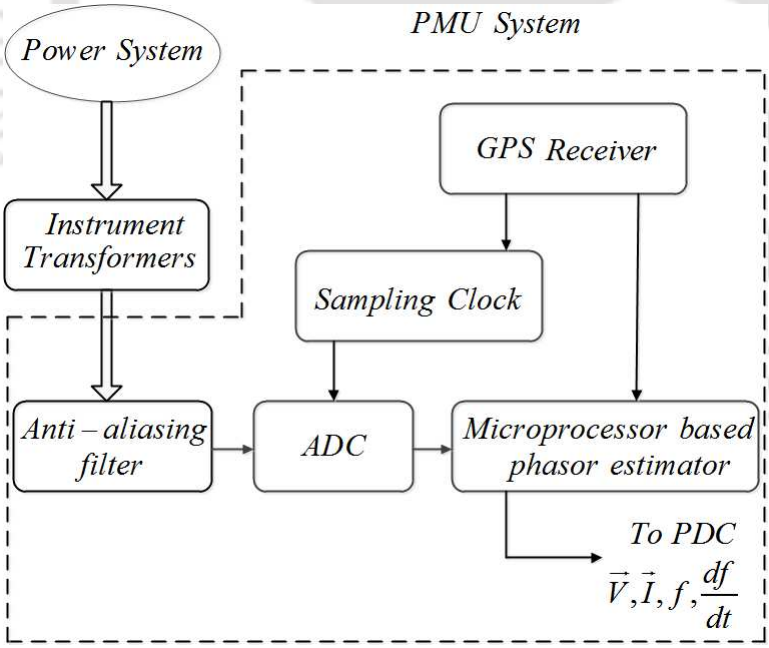

Figure 1.3: Block diagram of PMU.

1.1.2 Power system stability

The joint Task Force of the IEEE-CIGRE group has defined power system stability [8] as " *the ability of an electric power system, for a given initial operating condition, to regain a state of operating equilibrium after being subjected to a physical disturbance, with most system variables bounded so that practically the entire system remains intact*". The power system may experience different forms of instabilities, and it is difficult to analyse it by considering as a single problem and hence, requires proper classification. As cited in [8], the power system stability is mainly classified on the basis of 1) physical characteristics of the resulting mode of instability 2) size of the occurred disturbances and 3) the time duration during which the stability phenomena occurs. On the basis of these criteria, the power system stability is broadly categorized into three types:

1) Rotor angle stability

2) Frequency stability

3) Voltage stability

The classification of power system stability is shown in Figure 1.4. The voltage stability [8] is defined as " *the ability of a power system to maintain steady voltage at all buses in the system after being subjected to a disturbance from a given initial operating condition* ". It is again subclassified into small disturbance and large disturbance voltage stability. These instability problems may range from a few seconds to tens of minutes and therefore these phenomenon may either be a short term or long term. Frequency stability [8] is defined as " *the ability of a power system to maintain steady frequency following a severe upset resulting in a significant imbalance between generation and load*". It is further categorized into short term or the long term phenomenon. As the main focus of this thesis is on the estimation of the small signal rotor angle stability, a detail discussion of these instability phenomena is provided in the subsequent section.

1.1.2.1 Rotor angle stability

Rotor angle stability is defined [8] as " *the ability of synchronous machines of an interconnected power system to remain in synchronism after being subjected to a disturbance*". It depends on the ability to maintain or restore equilibrium between electromagnetic torque and mechanical torque of each synchronous machine connected to the power system. The change in electromagnetic torque of a

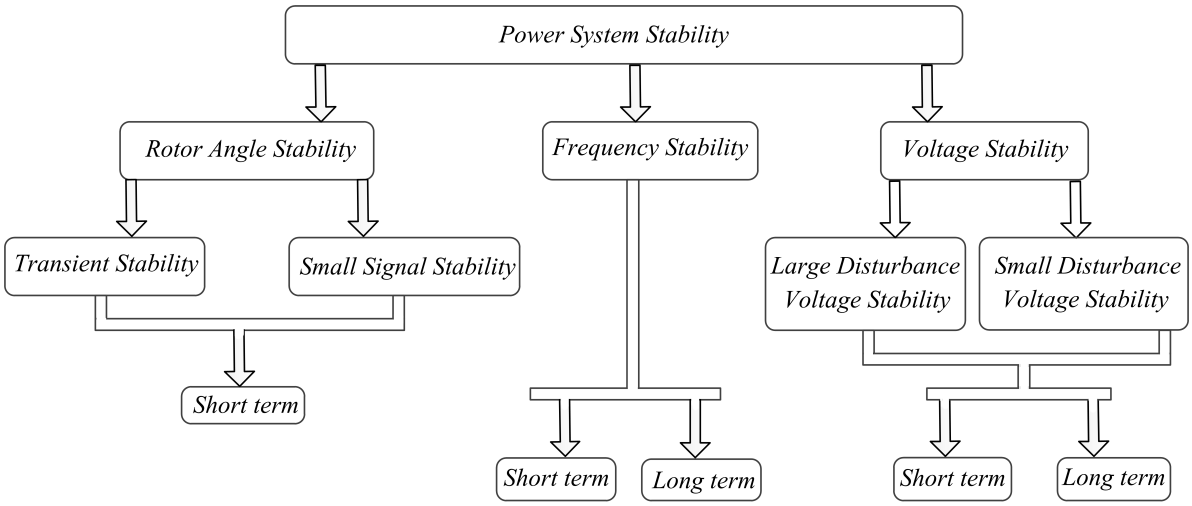

Figure 1.4: Classification of power system stability.

synchronous machine following a disturbance can be resolved into two components- 1) Synchronizing torque component which is in phase with the rotor angle deviation. 2) Damping torque component, which is in phase with the speed deviation. Lack of the first component causes non-oscillatory instability, while the latter causes oscillatory instability. The rotor angle stability is further characterized into two subcategories.

- **Small disturbance or small signal rotor angle stability:** It is defined as the ability of the power system to maintain synchronism under small disturbances. Small signal stability analysis is done using a linear time invariant model. This instability can be observed in two forms:

  1) Lack of synchronizing torque resulting in increase in rotor angle through non-oscillatory mode.

  2) Lack of damping torque resulting in rotor oscillations of increasing amplitude.

  Nowadays, rotor oscillations arising due to insufficient damping torque is mostly observed in the power system. The non-oscillatory instability problem has been eradicated to a great extent by using continuously acting exciters, yet, this problem may emerge on operation of generators with constant excitation, under the presence of field current limiters. Insufficient damping torque causing rotor oscillations, are further classified as,

  1) Local modes of oscillations- It involves swinging of units at a generating station against

rest of the power system. The damping of these oscillations depends upon the strength of the transmission system as seen by the power plant, the generator excitation control systems and the output of the plant [9]. Typically, the frequency range is 0.8 – 2 Hz.

2) Inter-area modes of oscillations- It involves swinging of many machines in one part of the system against machines in other parts. These oscillations have a short time duration, in the range of 10 – 20 s. Typically, the frequency range is 0.1 – 0.7 Hz.

- **Large disturbance rotor angle stability or transient stability:** It is defined as the ability of the power system to maintain synchronism, when subjected to a severe disturbance, such as a short circuit on a transmission line. It involves large rotor angles deviation which is influenced by the nonlinear power verses angle relationship. The system stability to these transients, depends both on the initial operating state of the system and the severity of the disturbance.

1.2 State-of-the-Art

Extensive literature and a few important books [9–11] related to power system stability phenomenon is available. These extensively referred books highlights the major aspects of angle stability. Recently, a wide number of literature and some books [12, 13] emphasizing the importance of synchrophasor for application in real time stability monitoring could be observed. A detail review of the existing literature on the topic of real time small signal stability prediction which are related to the present research work is presented below.

Modal identification algorithm for analyzing the low-frequency oscillatory modes associated with the large system has been cited in [14]. In this work, a computer program called as analysis of essentially spontaneous oscillations in power system (AESOPS) is developed which calculates the eigenvalues associated with electromechanical modes without constructing the system state matrix. However this algorithm works for 2000 buses and 350 machines system. In [15] an improvement over AESOPS called the program for eigenvalue analysis of large systems (PEALS) is presented, which employs the concept of modular modelling and sparsity to handle a system up to 12000 buses and 1000 machines. An extensive small signal stability program (SSSP) package has been developed in [16] which utilizes alternative programs like, QR transformation, the AESOPS and the modified Arnoldi

method for eigenvalue computation. Using sparsity the methods such as, simultaneous iterations and the modified Arnoldi for eigenvalue estimation has been cited in [17]. Other significant techniques for determining the eigenvalue mentioned in the literature are [18–22]. In a practical power system, the change of the operating conditions and system topology always induces a change in the oscillations characteristics. Therefore, the modes estimated using the off-line methods are suitable for analysis and design of the system, but do not provide the actual dominant modes present in an operating power system in real time.

In the recent times, with the development of phasor measurement unit (PMU) based wide area monitoring systems (WAMS), it is now possible to develop a system for on-line monitoring of low frequency modes present in the power system. These methods derives the real time data, namely ringdown and ambient data, from the phasor data concentrator (PDC) to estimate the low frequency modes. The data associated with the occurrence of large disturbances, such as line tripping, adding or removing of large load or generator fault is called as ringdown data, whereas, the ambient data is associated with small perturbation of power system due to random load variations. A brief literature review of PMU based on-line methods applicable to ringdown and ambient data are described below.

1.2.1 Low frequency critical mode estimation using ringdown data

Discrete Fourier transform (DFT) was frequently used for frequency analysis, as it employed Fast Fourier transform (FFT) [23], which had the advantage of being fast, noise resistant and easy to implement. However, FFT has a frequency resolution [24] problem for less number of data samples and fails to give information about the attenuation factor of the modes directly. The estimated signal parameter by the FFT has precision errors, owing to its picket-fence effect and energy leakage. To minimize the leakage phenomenon of FFT, interpolated window has been proposed in [25], yet the problem of frequency resolution still persist in this method to some level. Kalman filter [26] has also been used for mode identification, but as it follows an iterative system identification approach, it may cause numerical instability.

The Prony method [27–37] which is a high frequency resolution parametric method, is used to analyze the low frequency oscillations. This method extends the Fourier analysis by directly calculating the attenuation factor, frequency, amplitude and phase of the low frequency oscillations from

the real time measurements derived from the PMU. However, it is found to be sensitive to the presence of noise which results in incorrect mode identification. To minimize the effect of noise in the Prony method, several improvement are suggested in the literature like Kumaresan-Tufts (KT) algorithm [38, 39] which is based on the separation of signal and noise space, but still these methods are affected by the presence of noise. Improved Prony method [40] uses a median filter to minimize the variance of the estimated modes, therefore, it induces delay in the estimated modes and may provide inaccurate results. A nonlinear regression based Prony method is cited in [41–43], which is used to estimate the model parameters, but the iterative nature of these methods poses a problem for their convergence. A portable software tool based on ERA/Prony algorithm is referred in [44], which follows a least square minimization approach. A nonlinear least-squares optimization method known as variable projection method is proposed in [45], which is based on iterative orthogonal projection onto the signal space. However, in this method, the initial conditions of the parameters along with the partial derivatives of the basis functions needs to be defined.

A comparative assessment of Prony analysis and Hilbert transform based methods for mode estimation has been presented in [46]. In Hilbert transform based method, time domain data are preprocessed using an iterative signal decomposition procedure called as empirical mode decomposition (EMD) algorithm. Since Hilbert transform is usually obtained using the FFT of the signal, it also suffers from the drawback of frequency resolution and spectral leakage problems. Further, implementation of empirical mode decomposition (EMD) algorithm [46], makes this method very slow and may generate spurious modes due to the frequency-mixing phenomenon [47].

Recently, estimation of signal parameters via rotational invariance techniques (ESPRIT) [48–50] has been applied for estimating the attenuation factor and frequency. These signal subspace methods utilizes the rotational shift invariance property of the signals for the formation of an auto-correlation matrix, in order to recast the problem as a generalized eigenvalue problem. Various methods are applied to solve this generalized eigenvalue problem which leads to different types of ESPRIT. A sliding-window ESPRIT [51] has been proposed to estimate the inter-harmonics frequencies, however the selection of proper window to obtain the best tradeoff between frequency and time resolution is still an issue. Most of these work on the ESPRIT, have not considered the high variance noise and

outliers.

Total least squares estimation of signal parameters via rotational invariance techniques (TLS-ESPRIT) has been used for estimating the oscillatory frequency and attenuation factor for developing new islanding detection method [50]. Total least square approach takes into consideration the errors present in both the observation vector and the system matrix, while the least square method accounts for the error present in the observation vector. Hence the TLS-ESPRIT proves to be superior in estimating the modes as compared with the least squares estimation of signal parameters via rotational invariance techniques (LS-ESPRIT). However, this method has taken the assumption of noise to be Gaussian.

ESPRIT has been proposed for the direction-of-arrival (DOA) estimation [49] by exploiting the entire invariance structure for parameter estimation. In the original version of the ESPRIT, it is assumed that with each dimension of the parameter space, there exist only a single invariance in the data. An extension of the ESPRIT algorithm known as multiple invariance (MI) ESPRIT is presented in [49] for exploiting data with multiple invariance. This algorithm exploits multiple invariance along a single spatial dimension and it is based on a subspace fitting formulation of the DOA problem. This method outperforms the TLS-ESPRIT, but fails to provide the closed form solution, as it deals with minimization of complex nonlinear cost function. Hence, the computation time for estimating the parameters by this method is more as compared to the TLS-ESPRIT.

1.2.2 Low frequency critical mode estimation for ambient data

Several parametric approaches for mode identification of ambient data are available in the literature. A non recursive Yule-Walker (YW) algorithm of an autoregressive (AR) model is cited in [52] and the extension of this method to estimate an autoregressive moving average (ARMA) model is presented in [53]. As these are block processing algorithm, choice of proper block size remains a cause of concern for estimating the damping ratio. To enhance the convergence speed, an adaptive technology [54, 55] is adopted into the ARMA method. Random decrement (RD) technique in conjunction with TLS-ESPRIT, known as RD-TLS-ESPRIT has been proposed in [56] which performs better as compared to RD-Prony method. However, these methods do not include an effective method to address the issues related to the presence of nonlinear trends in the ambient data.

A robust recursive least squares (RRLS) algorithm as proposed in [57] is found to have better convergence than LMS algorithm [54]. An extension of this method known as regularized robust recursive least squares (R3LS) has been cited in [58], where the AR model is extended to an autoregressive moving average exogenous (ARMAX) model, which has the advantage of processing probing data and including moving average (MA) terms for the noise. A dynamic regularization term is also included in this algorithm while solving the least squares problem for enhancing the numerical efficiency. However, these methods are found to be sensitive towards the choice of initial filter states.

In [26], the AR model parameters are determined recursively by using a combination of AR algorithm and Kalman filter (KF), but it gives reliable damping estimates provided a known excitation is applied to the power system [59]. Hence, this method is not suitable for ambient data.

Extended modified Yule Walker with spectral analysis (YWS) for mode identification has been proposed in [60]. The performance of YWS has been compared with extended modified Yule Walker (YW) and sub-space system identification (N4SID) [61] methods. It is observed from the simulation results that the performance of YW and the YWS methods are superior as compared to the N4SID method in estimating the oscillatory modes. However, YWS method is sensitive to the order of the model.

A frequency domain decomposition (FDD) method has been proposed [62, 63], in which singular value decomposition (SVD) is applied to decompose the power spectrum density (PSD) matrix. However, a proper threshold technique is needed in order to decide the dominant singular values. Moreover, due to truncation and leakage phenomenon, damping may not be correctly estimated.

In [64], analysis of inter-area oscillations is performed based on system identification by utilizing subspace techniques which performs better for non-Gaussian excitation in the system. However, these system identification based methods requires both the input and the output response of the system. Random decrement (RD) technique in combination with wavelets has been proposed in [65], where the criteria for selecting the most optimal mother wavelet functions for damping estimation for power system under study is defined and the wavelets satisfying the required criteria are selected. However, the estimated damping may deteriorate significantly for high damping ratio due to limited time resolution of the wavelet function. Independent component analysis method in conjunction with

random decrement (RD-ICA) has been cited in [66], but it involves computation of higher order statistics and is also not valid for scarce data. A comparative review of [64], [65] and [66] has been presented in [67].

In [68], natural excitation technique (NExT) [69] in combination with eigensystem realization algorithm (ERA) [70] is used for mode identification which utilizes the cross-correlation functions to extract the impulse responses of the system. However, this method requires proper selection of reference variable for computing the cross-correlation functions.

Random decrement (RD) technique in combination with Ibrahim time domain (ITD) known as RD-ITD has been proposed in [71]. This method requires less computational time as compared to the stochastic subspace identification (SSI) method, while having similar accuracy, but requires a zero-phase band-pass filter to minimize the effect of the measurement noise present in the signal which doubles the filter order.

1.3 Motivation

Rotor angle instability phenomenon is often found to be the main cause for most of the blackouts in the world, such as the major blackout on 10^{th} August, 1996 [72] of the Western Electricity Co-ordinating Council (WECC). Conventionally, the low frequency oscillatory modes are analyzed by the small-signal analysis [14], [16], [17] which utilizes a linearized time-invariant model. Since, the generation or demand characteristics in a practical power system always varies with some changes in system topology, the off-line identification based methods may fail to provide the real-time critical modes present in the system.

With the development of synchrophasor based WAMS, the methods based on on-line identification of the modes have widely gained popularity. Measurement based methods applicable to low frequency critical modes estimation for ringdown data, includes the Fast Fourier transform (FFT) [24], the Prony methods [27], [29], [30], [32], [33], [34], [35] and the estimation of signal parameters via rotational invariance techniques (ESPRIT) [48], [49], [50]. The computational complexity and noise sensitivity of FFT is less and it is easy to implement. However, it has a drawback of frequency resolution problem for data having less number of samples and is unable to provide the attenuation factor of the modes directly. The Prony method [27] can provide the estimate of attenuation factor, amplitude, phase

and frequency of oscillations from measurements derived from the PMU. However, its use is limited due to its sensitivity towards the presence of noise. A few modifications are suggested based on signal and noise space separations, like the Kumaresan and Tufts (KT) method [38], but these are also found to be sensitive towards noise. These Prony based methods as available in the literature, have not considered high variance noise and outliers. Recently, some works have recommended the use of ESPRIT for mode estimation [48], [49], [50]. These ESPRIT based methods mostly exploits the rotational shift invariance property of the signals for the formulation of an auto-correlation matrix and, thus, it transforms the problem to a generalized eigenvalue problem. Different types of ESPRIT are proposed based on the methods used to provide solution to this problem. A sliding-window ESPRIT as proposed in [51] induces significant delay in estimating the inter-harmonic frequencies because of the use of sliding windows. The ESPRIT based methods differs from the Prony based methods as the former uses the correlation matrix, while the later directly uses the data samples for constructing the data matrix. Therefore, even though the ESPRIT based methods are computationally more expensive than the Prony based methods, they can provide higher noise immunity. Most of these ESPRIT based works have considered white Gaussian noise to represent the noise but have neglected the presence of outliers and high variance noise in the measurements.

Several mode estimating techniques applicable to ambient data are suggested in the literature. In [56], Random decrement (RD) technique in combination with TLS-ESPRIT has been used for estimating the modes from the free response of the system. In [52], an autoregressive (AR) model has been proposed and several modification of this algorithm has been presented in [53], [54], [55]. These methods have used downsampling and filtering techniques to remove the nonlinear trends. Other approaches include extended modified Yule Walker with spectral analysis (YWS) [60] and stochastic subspace based methods which also depends on proper model order selection. Random decrement technique in combination with wavelets as proposed in [65] may provide inaccurate damping estimate owing to limited time resolution. Other methods applicable for ambient analysis like NExT-ERA and RD-ITD requires a reference variable and use of zero-phase band-pass filter respectively, to obtain correct mode estimation. It is necessary to separate the signal from the high amplitude noisy ambient data without depending much on the model order or use of reference variable or zero-phase band-pass

filter.

In view of the limitations of the existing methods in the real time monitoring of the small signal rotor angle stability of the power system, the objectives behind the research work carried out in the present thesis are as follows:

- To modify improved Prony based estimator suitable for estimating the low frequency modes with the presence of high variance noise and outliers in the measured ringdown data.
- To further enhance the performance of the above estimator, the MM estimator and modified TLS-ESPRIT are utilized to mitigate the presence of outliers and high variance noise in the ringdown data.
- To develop a suitable method which can be effective towards the presence of high variance noise and nonlinear trends in the ambient data.
- To develop an improved estimator which exploits the sparsity of the signals in the ambient data.

1.4 Thesis Organization

The work carried out in this thesis is organized into six chapters. A few basic concepts of synchrophasor based wide area monitoring system (WAMS) and power system rotor angle stability are discussed in the present chapter. A state-of-the-art survey of some of the important published literature, on the estimation of low frequency modes for ringdown and ambient data are presented and also the motivation behind the present research work is highlighted in this chapter.

In Chapter 2, a robust modified Prony method has been proposed to reduce the effect of the high variance noise and outliers present in the signal utilizing the synchrophasor measurements derived from the phasor measurement units (PMUs). This method uses a minimum covariance determinant (MCD) technique to mitigate the effect of outliers followed by low rank approximation of the estimated covariance to obtain a robust estimation of the modes. The estimated modes by the proposed method has been compared with improved Prony and modified TLS-ESPRIT utilizing Monte-Carlo simulations. The effectiveness of the proposed method is studied on two sample test signals corre-

sponding to local and inter-area mode, two-area system and real time probing data of the Western Electricity Coordinating Council (WECC) system in presence of outliers.

Chapter 3 proposes a robust covariance approach based TLS-ESPRIT method using a MM estimator to mitigate the effect of outliers on mode estimation. A comparative analysis of the estimated modes by the proposed robust TLS-ESPRIT method with modified TLS-ESPRIT and robust Modified Prony method are carried out using Monte-Carlo simulations. The robustness of the proposed method in dealing with outliers has been demonstrated, for inter-area as well as local modes of oscillations, on the two sample test signals, on a two-area system and real time probing test data of the Western Electricity Coordinating Council (WECC) system.

In Chapter 4, a nonlinear filter to mitigate the effect of nonlinear trends, along with wavelet method has been proposed to provide an accurate estimate of low frequency oscillatory modes in the ambient data. The performance of the proposed method, i.e., NwT-RD-TLS-ESPRIT is compared with the nonlinear filtering, natural excitation technique- eigensystem realization algorithm (NExT-ERA) and random decrement technique- Ibrahim time domain (RD-ITD) for the test signals, simulated second order system corresponding to the modes present in a two-area system, two-area system simulated on real time digital simulator (RTDS) facility at IIT Kanpur, and real time PMU data for Indian power systems and WECC.

Chapter 5 uses a sparsity based de-noising technique to extract the signal from a low dimensional space. A comparative analysis of the proposed S-RD-TLS-ESPRIT method with the NwT-RD-TLS-ESPRIT method has been done for the test signals, simulated second order system corresponding to the modes present in a two-area system, two-area system simulated on RTDS facility at IIT Kanpur, and real time PMU data for Indian power systems and WECC.

Chapter 6 provides the general conclusion of the thesis with major contributions and some potential future research problems.

2

Estimation of Low-Frequency Modes in Power System with Robust Modified Prony

2.1 Introduction

In the present scenario, increasing power demand leads to a vast and complex network of power which consist of interconnected generating stations, renewable energy sources, transmission lines and the control centers. The major challenges faced by power system operational engineers is to ensure stability and sustainability with increasing generation and demand. These complex network poses many challenges, such as maintaining small signal rotor angle stability with proper damping for the critical modes. Hence, it is important to identify the critical modes and design suitable controllers to minimize the poorly damped low-frequency oscillations, which otherwise may result into islanding or blackout. Conventionally, the small signal rotor angle stability analysis is done using modal analysis to find the critical modes. Traditionally, the technique based on eigen value analysis is used for mode identification by using a linear time invariant model approximated in the neighborhood of the operating point of the nonlinear system [14, 16, 17]. This method utilizes an off-line approach for modal analysis and suffers from the drawback of inaccurate model. With the development of synchrophasor based wide area monitoring systems (WAMSs), it is possible to develop an on-line method

for monitoring modes corresponding to the power oscillations. Major classes of these online estimation methods are based on spectral estimation algorithms such as the Fast Fourier transform (FFT), the Kalman filter [26], Prony analysis [27, 29, 30, 32, 34, 36] and estimation of signal parameters via rotational invariance techniques (ESPRIT) [51, 73]. The computational complexity and sensitivity towards noise is less for FFT, but it has less frequency resolution if the available data points in a window are less [24] and also the model does not support damped exponentials. The use of Kalman filter for mode identification is also reported in the literature, but the recursive nature of the filter may lead towards numerical instability. The model used in Prony method is better than FFT in terms of modeling the response of complex modes [27], however, it is found to be sensitive to the presence of noise. To improve the performance of Prony method in presence of noise, several modifications are proposed in the literature like Kumaresan-Tufts (KT) algorithm [35, 38, 39] which is based on separation of signal and noise spaces. Improved Prony method [40] tries to minimize the variance of the estimated modes by using median filter, hence, induces delay in the estimated modes and may not be very accurate. In [41–43], a nonlinear regression based Prony method is utilized to estimate the parameters of the model, but because of its iterative approach these methods have an issue related to their convergence. In [74], N4SID method is utilized for mode estimation, but it can only be used for probing data as it is based on system identification which requires both input and output responses of the system. In [45], a variable projection method is used for mode estimation which is based on iterative orthogonal projection on the signal space. In presence of noise, TLS-ESPRIT [51, 75] method seems to be less sensitive as compared to the Prony method in estimating the modes. In [44], a portable software tool based on eigensystem realization algorithm (ERA)/Prony algorithm is proposed which gives reliable estimate of modes in presence of noise. However, the performance of all these methods are based on minimizing the l_2-norms of the error between the estimated signal and original signal which are very much sensitive to the presence of the outliers.

All these conventional estimation techniques are based on classical least square technique. Some of these approaches have prior assumption about the Gaussian noise model, and tends to fail under high variance noise or noise with a flat tail distribution [76]. These estimates are also biased under anomalies which is referred in statistical terminology as outliers. These outliers are common in sensor

networks, the main source of these bad data are environmental effects like lightning or electromagnetic pulses, hardware faults, data corruption or data packet loss over communication networks or man-made data injection attacks. The basic idea behind least square minimization technique is to minimize the l_2-norm of the estimation error $||y - \hat{y}||_2$. It has a quadratic cost function (CF) and linear influence function (IF), i.e. large sample will have large influence on the estimation. There are many robust techniques to handle such issues which includes l_1 minimization, Huber loss functions etc. l_1 minimization (least absolute deviation) has a linear cost function and a step influence function which gives equal influence to all the errors as shown in Figure 2.1 and 2.2, respectively, but it involves an optimization problem with high computational cost, high convergence time and also the convergence is not guaranteed. Huber function combines the characteristics of both l_1 and l_2 minimization [77]. It is defined as

$$\begin{aligned} f(x) &= x^2 \quad if\ |x| \leq \delta \\ f(x) &= 2\delta|x| - \delta^2 \quad if\ |x| > \delta \end{aligned} \tag{2.1}$$

This function has a quadratic cost characteristic for absolute value of the sample less than δ, otherwise has a linear cost characteristic. Figure 2.1 and 2.2 uses δ which is equal to 0.5. Here, δ sets a limit over the range of outliers and the crucial part lies in deciding the δ value for a particular estimation. The problem becomes more complex when the error distribution is itself changing over the period of time. So, there is a need to have data independent methods for modal analysis of power system oscillations.

This chapter proposes a robust covariance based improved Prony method which uses a minimum covariance determinant (MCD) technique to mitigate the effect of outliers followed by low rank approximation of the estimated covariance to estimate the low frequency modes corresponding to the power oscillations. The proposed method is compared with the improved Prony [38,40] and modified TLS-ESPRIT [75] methods for different types of signals with and without outliers, followed by the estimation of the modes for a two-area system [9]. Further, a comparative analysis of the proposed method with the improved Prony [38, 40] and modified TLS-ESPRIT and ERA/Prony [44] is carried out for real time data of the Western Electricity Coordinating Council (WECC) system [78, 79].

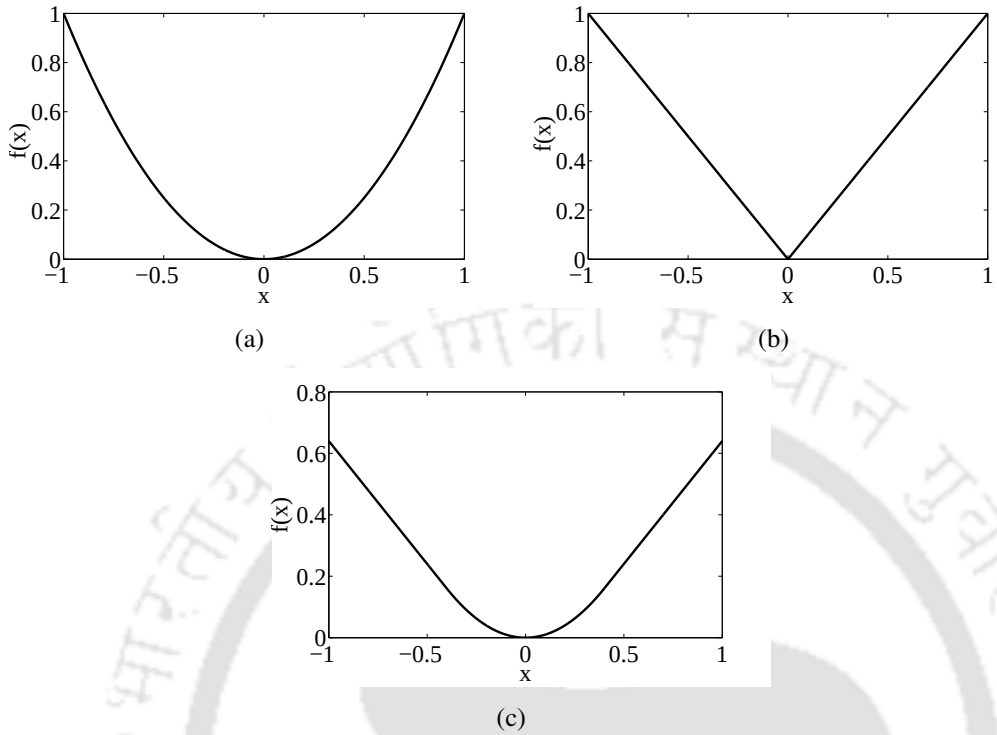

Figure 2.1: Cost function (CF) comparison for (a) l_2 minimization; (b) l_1 minimization; (c) Huber minimization.

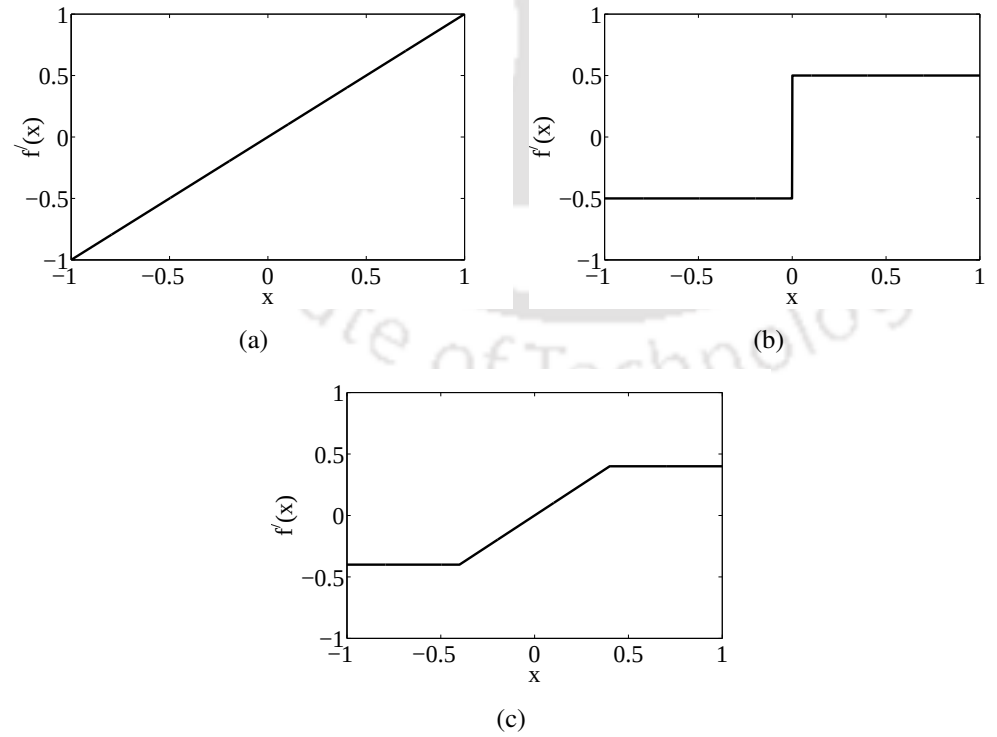

Figure 2.2: Influence function (IF) comparison for (a) l_2 minimization; (b) l_1 minimization; (c) Huber minimization.

This chapter motivates towards the modification of the existing improved Prony method, so that it can provide good estimate of power system modes corresponding to the low frequency power oscillation in the presence of outliers in the measured data. Section 2.2, briefly explains improved Prony method. Section 2.3, explains how the presence of outlier distorts the structure of the covariance matrix. Section 2.4, explains the proposed method. Section 2.5, discusses the results followed by the conclusions in Section 2.6.

2.2 Improved Prony

2.2.1 Power system signals

The power system response is represented as a linear combination of damped sinusoidal signals with white Gaussian noise. The measured signal $y(n)$, at time instant n, for a given block of data is represented as

$$\begin{aligned} y(n) &= s(n) + w(n) \\ &= \sum_{k=1}^{K} a_k e^{b_k n} cos(n\omega_k + \phi_k) + w(n) \end{aligned} \tag{2.2}$$

where $s(n)$ is the signal component and $w(n)$ is the zero mean white Gaussian noise. Here $\{a_k\}$, $\{\omega_k\}$, $\{\phi_k\}$, K and $\{b_k\}$ are the amplitude, angular frequency, initial phase, number of sinusoids and unknown attenuation factor respectively.

Complex exponential representation of equation (2.2) is given as

$$\begin{aligned} y(n) &= s(n) + w(n) \\ &= \sum_{j=1}^{M} \alpha_j e^{\beta_j n} + w(n), \quad n = 0, 1, 2...., N-1 \end{aligned} \tag{2.3}$$

where $\alpha_j = (a_j/2)e^{i\phi_j}$, $M = 2K$. For real signal there are two complex conjugate exponents $\beta_j = b_j \pm i\omega_j$, where $\alpha_j > 0$ and $\omega_j \in [-\pi, \pi]$.

2.2.2 Prony estimation and modifications

Since α_j is independent of β_j, the nonlinear estimation problem can be written as a linear regression problem as suggested by Hildebrand [80]. The original work of Prony [27] uses one dimensional

null space to find the coefficients of the characteristic polynomial, where the roots are the modes present in the signal. The recent trends is to formulate the problem as a backward or forward linear predictive model, which utilizes a high dimensional null space, as shown in equation (2.4).

$$\begin{bmatrix} y(1) & y(2) & \dots & y(L) \\ y(2) & y(3) & \dots & y(L+1) \\ \vdots & \vdots & \ddots & \vdots \\ y(N-L) & y(N-L+1) & \dots & y(N-1) \end{bmatrix} \begin{bmatrix} g_1 \\ g_2 \\ \vdots \\ g_L \end{bmatrix} = - \begin{bmatrix} y(0) \\ y(1) \\ \vdots \\ y(N-L-1) \end{bmatrix}$$

$$\mathbf{A} \cdot \mathbf{g} = -\mathbf{h} \tag{2.4}$$

$$\mathbf{g} = -[\mathbf{A^T A}]^{-1} \mathbf{A^T h} \tag{2.5}$$

where, **g** is the vector of backward prediction coefficient. L is chosen such that $M \leqslant L \leqslant N-M$, where M are true signal components and the rest $L-M$ are extraneous noise components. This also provides noise immunity as it tries to fit the noise components by additional exponent terms of the model. The above equation can also be written in augmented form as $A'\, g' = 0$, where $A' = (h|A)$ and $g' = (1, g^T)^T$. If the data is noiseless, then solution to polynomial $G(z) = 1 + g_1 z^{-1} + g_2 z^{-2} + .. + g_L z^{-L}$ will provide zeros $z_j = e^{-\beta_j}$, $j = 1, 2, ..., L$. The location of these extraneous zeros depends on the choice of g' belonging to the null space of A'. By constraining **g** vectors as min $\sum_{i=1}^{L} |g_i|^2$, the extraneous zeros lies inside the unit circle [39], hence, the signal modes could be estimated by reflecting the identified modes inside the unit circle. Further to reduce the sensitivity of zeros towards noise, Kumaresan-Tufts [38] have suggested a subspace decomposition based technique which reduces the effect of noise on the location of zeros. They have used singular value decomposition (SVD) to determine a low rank approximation of the matrix **A**. The approximation is done by considering only larger singular values, as they corresponds to the signal subspace while ignoring other smaller singular values as they corresponds to the noise subspace.

For doing so, in [35], an index is defined as

$$K(i) = \left[\frac{\rho_1^2 + \rho_2^2 + \cdots + \rho_i^2}{\rho_1^2 + \rho_2^2 + \cdots + \rho_L^2} \right]^{\frac{1}{2}} \tag{2.6}$$

where ρ_i is the i-th singular value and $K(i)$ is monotonously increasing index. As i approaches to the real signal order, $K(i)$ is very close to unity.

2.3 Effects of outliers

To explain the sensitivity of the improved Prony (as explained in the above Section 2.2) and robustness of the proposed method towards outlier, we have taken a test signal $x(t) = e^{-0.4t}cos(2\pi t)$ with an additive Gaussian noise. Figure 2.3(a) shows the zeros corresponding to the signal zeros and extraneous zeros obtained with improved Prony without outlier. The signal zeros fall outside the unit circle and hence could be identified. Figure 2.3(b) shows the zero plot obtained by improved Prony for the signal corrupted with outlier. It is hard to identify the signal zeros as both signal zeros and extraneous zeros are inside the unit circle. Figure 2.3(c) shows the effectiveness of the proposed method, which is a robust version of improved Prony method by utilizing the robust estimation of covariance matrix. Here, we have used the data with outliers, and could see that signal zeros fall outside the unit circle and hence can be identified.

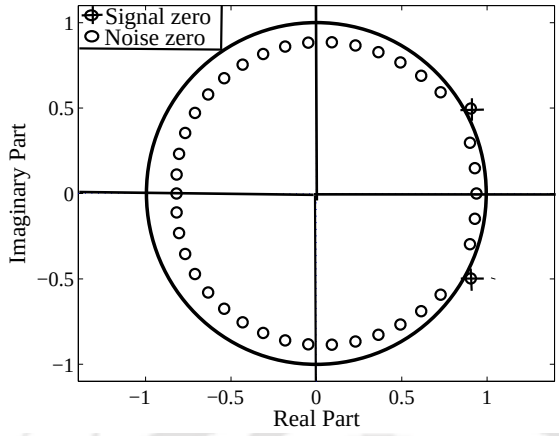

(a)

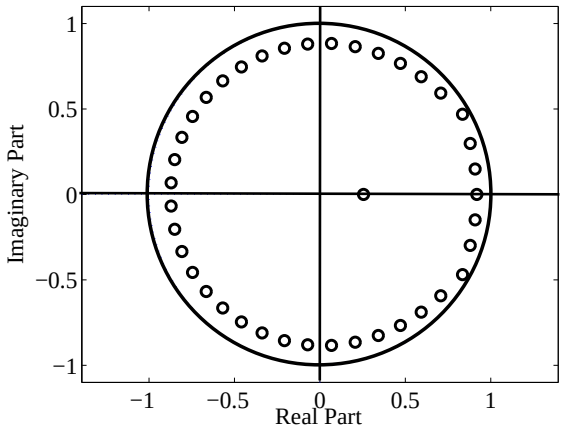

(b)

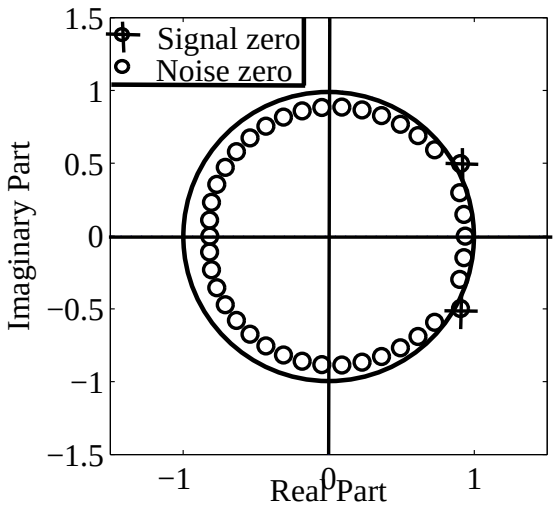

(c)

Figure 2.3: Zero plot of signal and noise for (a) Prony method without outlier; (b) Prony method with outlier; (c) Proposed method with outlier.

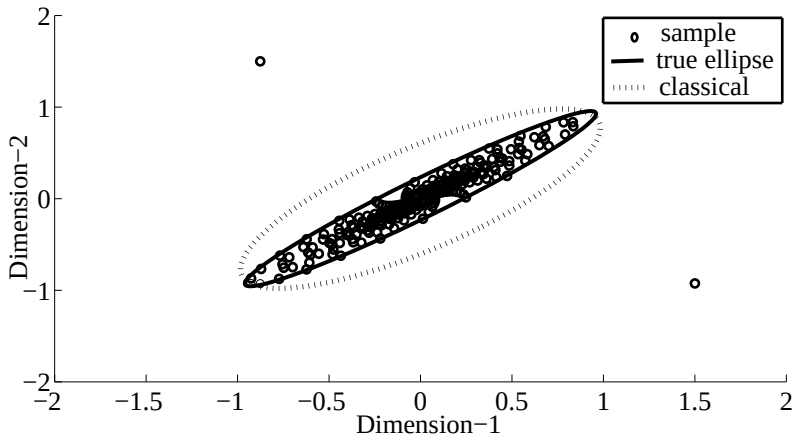

Figure 2.4: Covariance ellipsoidal using classical technique for clean data and outlier corrupted data.

Figure 2.4 shows the scatter plot of data matrix $\mathbf{A}$ obtained from the signal $x(t) = e^{-0.4t}cos(2\pi t)$ having an order $L = 2$ along with a single outlier and the covariance ellipsoid constructed using the classical technique of covariance estimation (i.e., covariance ellipsoid containing 98% of data points) on the data de-noised using SVD. The classical technique being the solution of an optimization problem involving squared error [81–83] is known to be very sensitive to outliers or high variance noise. As seen in Figure 2.4, the covariance ellipse strongly changes its direction depending on the position of the outliers and also area of the ellipse increases by a significant factor. Thus the correlation between the variables is affected along with the increase in the volume of the covariance ellipse. This leads towards error in the estimated modes.

2.4 Proposed Robust Modified Prony

The proposed method i.e., robust modified Prony for mode identification is based on robust estimation of the covariance matrix used in (2.4) and (2.5) which can be rewritten as

$$\mathbf{A}^{\mathbf{T}}\mathbf{A} \cdot \mathbf{g} = -\mathbf{A}^{\mathbf{T}}\,\mathbf{h} \tag{2.7}$$

$$\mathbf{R_A} \cdot \mathbf{g} = -\mathbf{R_h} \tag{2.8}$$

where $\mathbf{R_A}$ is the covariance matrix of $\mathbf{A}$ and $\mathbf{R_h}$ is $\mathbf{A}^{\mathbf{T}}\mathbf{h}$. Since the covariance matrix $\mathbf{R_A}$ is corrupted by noise and outliers, the proposed robust method utilizes the robust estimation of the covariance matrix using minimum covariance determinant (MCD) followed by low rank approximation as shown in the

following subsection.

2.4.1 Minimum Covariance Determinant (MCD)

Rousseeuw and Driessen [84] suggested this technique and is found to be useful for time series data analysis. It searches iteratively for the best samples to represent the covariance structure with the lowest possible covariance determinant.

The basic computation steps are as follows:

Step 1: The rows of matrix $\mathbf{A}$ are considered as samples $\mathbf{a}_i$ and columns as dimensions, where L is the dimension of each sample and $(N-L)$ are the number of samples. A set of random k samples are taken as K_1.

$$k = \lfloor 2 * \lfloor (n+L+1)/2 \rfloor \rfloor - n + 2 * (n - \lfloor (n+L+1)/2) \rfloor * 0.75)$$

where n is the number of observations.

Mean and covariance are calculated as,

$$\mathbf{T_1} = \frac{1}{k} \sum_{i \in K_1} \mathbf{a}_i \tag{2.9}$$

$$\mathbf{S_1} = \frac{1}{k} \sum_{i \in K_1} (\mathbf{a}_i - \mathbf{T}_1)^T (\mathbf{a}_i - \mathbf{T}_1) \tag{2.10}$$

where $K_1 \subset 1, ..., (N-L)$ and $|K_1| = k$

Step 2: The Mahalanobis distance is computed for each sample as $d_1(i) = \sqrt{(\mathbf{a}_i - \mathbf{T}_1)^T \mathbf{S}_1^{-1} (\mathbf{a}_i - \mathbf{T}_1)}$ for $i = 1, 2, ..., (N-L)$ and $\det(\mathbf{S_1}) \neq 0$

Step 3: Distances are sorted in increasing order and only the samples with first k shortest distances are considered and a set of new samples K_2 is taken.

Step 4: The new mean and covariance $\mathbf{T_2}$ and $\mathbf{S_2}$ are computed and the same procedure is followed iteratively until $\det(\mathbf{S}_{j+1}) \simeq \det(\mathbf{S}_j)$ for the j-th iteration. Now, $\mathbf{S}_j$ is the estimate for the covariance matrix.

Each step iteratively selects samples with decreasing covariance determinant. These steps are known as C-step where C represents the concentration steps. This is because in each step the area of ellipsoidal decreases and hence more concentrated samples with less covariance determinants are

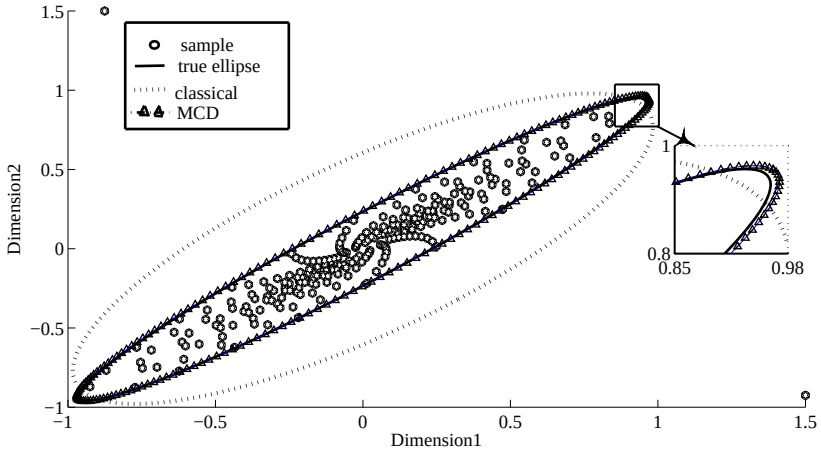

Figure 2.5: Comparison of the classical and MCD algorithm based covariance ellipse for outlier data with covariance ellipse with clean data.

obtained. Similar simulation is done with matrix **A** obtained from the signal $x(t) = e^{-0.4t}cos(2\pi t)$ having an order $L = 2$ along with a single outlier. The two-dimensional scatter plot and classical and robust ellipsoidal are plotted together in Figure 2.5. Here outlier free ellipse and the robust covariance ellipse with outlier overlaps with each other with almost similar covariance ellipse, whereas the classical covariance ellipse becomes circular. This shows the robust performance of MCD algorithm in presence of outlier where the classical technique fails.

2.4.2 Low rank approximation

The minimum covariance determinant (MCD) calculated using MCD algorithm is designed to estimate a covariance matrix which is close to the covariance corresponding to the original data in terms of their determinant, it tends to retain the effect of the noise in the original data. Since, outliers would have been eliminated by MCD and the estimated covariance matrix is affected only by noise, an SVD is utilized to determine the low rank approximation by considering only larger singular values, as they corresponds to signal subspace and ignoring other smaller singular values as they corresponds to noise subspace [85].

2.4.3 Identification of Power System Modes using the Proposed robust modified Prony Method

Block diagram in Figure 2.6 shows the various steps for on-line monitoring of low frequency modes of power system corresponding to the generator's swing. The estimation of these low frequency mode can be done using power signal acquired through the phasor measurement units (PMUs),

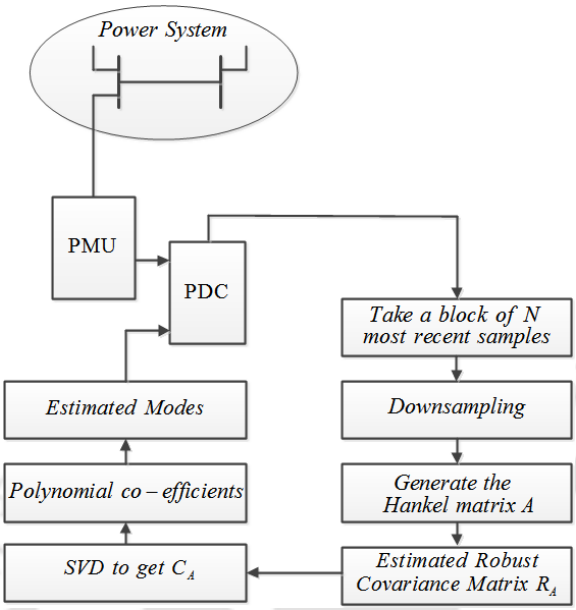

Figure 2.6: Block diagram for on-line estimation using proposed method i.e, robust modified Prony.

which may contain bad data.

The steps for estimating the modes using the proposed method are as follows:

Step 1: The proposed technique i.e., robust modified Prony method uses a block of N recent samples of the active power acquired through the PDC, where N is approximately taken as the ratio of the phasor data rate of the PMU and the minimum limit of the frequency of the estimator.

Step 2: These samples are then down sampled.

Step 3: The proposed method is mainly concentrated on estimating the robust covariance matrix $\mathbf{R_A}$ of the Hankel data matrix $\mathbf{A}$ using minimum covariance determinant technique [84]. The best samples having the lowest possible covariance determinant is iteratively searched using C-steps to represent the covariance structure of the matrix. Thus, the estimated covariance matrix is free from the effect of outlier which depicts the robust performance of the MCD algorithm.

Step 4: As the proposed method requires an accurate estimation of the signal components to mitigate the effect of noise, equation (2.6) is used to estimate the signal order. SVD is done on the robust matrix $\mathbf{R_A}$ and polynomial co-efficient are calculated from $\mathbf{C_A}$ i.e., low rank approximation of $\mathbf{R_A}$.

Step 5: The estimated modes which corresponds to a block of N most recent samples, are stored in the PDC.

Step 6: The whole process is repeated for the arrival of N new recent samples.

2.5 Simulation Results

To illustrate the effectiveness of the proposed method i.e., robust modified Prony, the simulations are done on two synthetically generated sinusoidal signals with known attenuation factor and frequency in the presence of outlier (=10× the peak of the signal value) at different SNR corresponding to local mode and inter-area mode of oscillations. Performance evaluation is done by performing 10000 Monte Carlo simulation for the proposed method, the improved Prony and the modified TLS-ESPRIT method. The simulation also includes the comparison of the proposed method with the other methods on two-area system and real data obtained from the PMU connected in the WECC system. For a comparative analysis of the effect of an outlier, the present work has taken a signal with different values and position of outlier. For the synthetic test signal, a time window having a duration of 20 s with 251 samples of active power acquired from the PMU at the sampling frequency of 12.5 Hz, while for two-area system, a time window of 10.16 s with 128 samples of active power acquired at a sampling rate of 12.5 Hz. For WECC system a time window having a duration of 8.55 s is utilized for estimations of low frequency modes.

2.5.1 Test signal Corresponding to Local Mode

A test signal $x(t) = e^{-0.1t}cos(2\pi t + \phi)$ corresponding to local mode is considered for mode estimation to carry out simulation in this section.

Table 2.1: Mean and Variance of the estimated mode for the improved Prony, the modified TLS-ESPRIT and the Proposed Method for outlier (=10 × peak value) placed towards the end of the signal at different SNR (Test signal- local mode)

Improved Prony				
	Estimated Attenuation factor (True value= -0.1)		Estimated Frequency (True value= 1 Hz)	
SNR (dB)	μ (Mean)	σ^2 (Variance)	μ (Mean)	σ^2 (Variance)
40	0.0229	9.206×10^{-8}	1.006	1.984×10^{-9}
30	0.0229	9.209×10^{-7}	1.006	1.984×10^{-8}
20	0.0231	9.226×10^{-6}	1.006	1.983×10^{-7}
Modified TLS-ESPRIT				
	Estimated Attenuation factor (True value= -0.1)		Estimated Frequency (True value= 1 Hz)	
SNR (dB)	μ (Mean)	σ^2 (Variance)	μ (Mean)	σ^2 (Variance)
40	-0.0869	3.292×10^{-8}	1.0011	4.342×10^{-9}
30	-0.0869	3.267×10^{-7}	1.0011	3.464×10^{-8}
20	-0.0870	3.301×10^{-6}	1.0011	3.396×10^{-7}
Proposed Method (Robust Modified Prony)				
	Estimated Attenuation factor (True value= -0.1)		Estimated Frequency (True value= 1 Hz)	
SNR (dB)	μ (Mean)	σ^2 (Variance)	μ (Mean)	σ^2 (Variance)
40	-0.1000	5.571×10^{-8}	1.0000	1.482×10^{-9}
30	-0.1000	5.622×10^{-7}	1.0000	1.471×10^{-8}
20	-0.1000	5.774×10^{-6}	1.0000	1.456×10^{-7}

Performance comparison among all the methods for this test signal for the estimated attenuation factor and frequency with the outlier injected at the end of the sample is shown in Table 2.1. It is observed that the estimated mean value of attenuation factor degrades highly for improved Prony while the proposed method provides much more close results (i.e, estimated mean value of attenuation factor is equal to -0.1) than that of modified TLS-ESPRIT (which has a mean value of -0.0869 for SNR= 40 dB and SNR=30 dB and -0.087 for SNR= 20 dB). For estimated frequency all the methods gives good results with the proposed method estimating much more accurate results as depicted by its mean and variance values as provided in Table 2.1.

Table 2.2: Mean and Variance of the estimated mode for the improved Prony, the modified TLS-ESPRIT and the Proposed Method for outlier (=10 × peak value) placed towards the beginning of the signal at different SNR (Test signal- local mode)

Improved Prony				
	Estimated Attenuation factor (True value= -0.1)		Estimated Frequency (True value= 1 Hz)	
SNR (dB)	μ (Mean)	σ^2 (Variance)	μ (Mean)	σ^2 (Variance)
40	0.0093	6.484×10^{-8}	1.0024	1.651×10^{-9}
30	0.0093	6.364×10^{-7}	1.0024	1.657×10^{-8}
20	0.0095	6.354×10^{-6}	1.0024	1.576×10^{-7}
Modified TLS-ESPRIT				
	Estimated Attenuation factor (True value= -0.1)		Estimated Frequency (True value= 1 Hz)	
SNR (dB)	μ (Mean)	σ^2 (Variance)	μ (Mean)	σ^2 (Variance)
40	-0.0676	1.831×10^{-8}	1.0028	3.144×10^{-9}
30	-0.0676	1.787×10^{-7}	1.0028	2.450×10^{-8}
20	-0.0676	1.752×10^{-6}	1.0028	2.454×10^{-7}
Proposed Method (Robust Modified Prony)				
	Estimated Attenuation factor (True value= -0.1)		Estimated Frequency (True value= 1 Hz)	
SNR (dB)	μ (Mean)	σ^2 (Variance)	μ (Mean)	σ^2 (Variance)
40	-0.1000	1.533×10^{-7}	1.0000	3.896×10^{-9}
30	-0.1000	1.513×10^{-6}	1.0000	3.932×10^{-8}
20	-0.1000	1.551×10^{-5}	1.0000	3.857×10^{-7}

Performance check of all the methods for this test signal corresponding to the estimated mean value of attenuation factor and frequency for outlier injected towards the beginning of the sample is shown in Table 2.2. Improved Prony gives incorrect attenuation factor while the proposed method gives correct mean, i.e, the estimated mean value of attenuation factor is equal to -0.1 as compared to the modified TLS-ESPRIT which is equal to -0.0676. For estimated frequency, it is observed that all the methods gives good results even with high noise level with the proposed method giving more accurate mean, i.e, estimated mean value of frequency is equal to 1 Hz.

Table 2.3: Estimated Attenuation factor and Frequency for the improved Prony, the modified TLS-ESPRIT, ERA/Prony and the Proposed Method for test signal without noise and without outlier (Test signal- local mode)

Methods	Attenuation factor (True value= -0.1)	Frequency (True value= 1 Hz)
Improved Prony	-0.1000	1.000
Modified TLS-ESPRIT	-0.1000	1.000
ERA/Prony	-0.1000	1.000
Proposed Method	-0.1000	1.000

Table 2.4: Estimated Attenuation factor and Frequency for the improved Prony, the modified TLS-ESPRIT, ERA/Prony and the Proposed Method for test signal without noise but with outlier (=10 $\times$ peak value) (Test signal- local mode)

Methods	Attenuation factor (True value= -0.1)	Frequency (True value= 1 Hz)
Improved Prony	0.0229	1.0006
Modified TLS-ESPRIT	-0.0869	1.0011
ERA/Prony	-0.1223	1.0009
Proposed Method	-0.1000	1.0000

Performance comparison for all the methods for the test signal without noise and without outlier is shown in Table 2.3. It is observed that all the four methods gives accurate attenuation factor and frequency estimates. Performance analysis is also done for test signal without noise, but with outlier (whose value is 10 times the peak signal value) as shown in Table 2.4. Improved Prony method provides more erroneous estimates in presence of large outliers as seen in the estimated attenuation factor value from Table 2.4, while the proposed method is better as compared to the modified TLS-ESPRIT and ERA/Prony method in estimating the attenuation factor and frequency.

Table 2.5: Mean and Variance of the estimated mode for the improved Prony, the modified TLS-ESPRIT, ERA/Prony and the Proposed Method for outlier (=10 × peak value) placed towards the beginning of the signal at different SNR (Test signal- inter-area mode)

Improved Prony				
	Estimated Attenuation factor (True value= -0.07)		Estimated Frequency (True value= 0.4 Hz)	
SNR (dB)	μ (Mean)	σ^2 (Variance)	μ (Mean)	σ^2 (Variance)
40	0.0365	1.477×10^{-7}	0.3973	2.747×10^{-9}
30	0.0365	1.482×10^{-6}	0.3973	2.733×10^{-8}
20	0.0368	1.482×10^{-5}	0.3973	2.813×10^{-7}
Modified TLS-ESPRIT				
	Estimated Attenuation factor (True value= -0.07)		Estimated Frequency (True value= 0.4 Hz)	
SNR (dB)	μ (Mean)	σ^2 (Variance)	μ (Mean)	σ^2 (Variance)
40	-0.0811	4.105×10^{-8}	0.3981	5.475×10^{-9}
30	-0.0811	3.992×10^{-7}	0.3981	4.793×10^{-8}
20	-0.0811	3.953×10^{-6}	0.3981	4.712×10^{-7}
ERA/Prony				
	Estimated Attenuation factor (True value= -0.07)		Estimated Frequency (True value= 0.4 Hz)	
SNR(dB)	μ (Mean)	σ^2 (Variance)	μ (Mean)	σ^2 (Variance)
40	-0.0929	2.249×10^{-8}	0.3995	1.630×10^{-8}
30	-0.0929	2.189×10^{-7}	0.3995	1.668×10^{-7}
20	-0.0929	2.259×10^{-6}	0.3995	1.672×10^{-6}
Proposed Method (Robust Modified Prony)				
	Estimated Attenuation factor (True value= -0.07)		Estimated Frequency (True value= 0.4 Hz)	
SNR (dB)	μ (Mean)	σ^2 (Variance)	μ (Mean)	σ^2 (Variance)
40	-0.07	5.148×10^{-8}	0.4000	1.336×10^{-9}
30	-0.07	5.093×10^{-7}	0.4000	1.351×10^{-8}
20	-0.07	5.055×10^{-6}	0.4000	1.339×10^{-7}

Table 2.6: Mean and Variance of the estimated mode for the improved Prony, the modified TLS-ESPRIT and the Proposed Method for outlier (=10 × peak value) placed towards the end of the signal at different SNR (Test signal- inter-area mode)

Improved Prony				
	Estimated Attenuation factor (True value = -0.07)		Estimated Frequency (True value = 0.4 Hz)	
SNR (dB)	μ (Mean)	σ^2 (Variance)	μ (Mean)	σ^2 (Variance)
40	0.0736	2.922×10^{-7}	0.4032	4.243×10^{-9}
30	0.0737	2.999×10^{-6}	0.4032	4.203×10^{-8}
20	0.0744	3.024×10^{-5}	0.4032	4.315×10^{-7}
Modified TLS-ESPRIT				
	Estimated Attenuation factor (True value = -0.07)		Estimated Frequency (True value= 0.4 Hz)	
SNR (dB)	μ (Mean)	σ^2 (Variance)	μ (Mean)	σ^2 (Variance)
40	-0.1230	1.072×10^{-7}	0.4036	1.048×10^{-8}
30	-0.1230	1.070×10^{-6}	0.4036	1.001×10^{-7}
20	-0.1230	1.067×10^{-5}	0.4036	9.796×10^{-7}
Proposed Method (Robust Modified Prony)				
	Estimated Attenuation factor (True value = -0.07)		Estimated Frequency (True value= 0.4 Hz)	
SNR (dB)	μ (Mean)	σ^2 (Variance)	μ (Mean)	σ^2 (Variance)
40	-0.07	1.157×10^{-7}	0.4000	2.727×10^{-9}
30	-0.07	1.154×10^{-6}	0.4000	2.729×10^{-8}
20	-0.07	1.179×10^{-5}	0.4000	2.733×10^{-7}

2.5.2 Test signal Corresponding to Inter-Area Mode

This section uses a test signal $x(t) = e^{-0.07t}cos(2\pi0.4t + \phi)$ corresponding to inter-area mode for mode estimation.

The mean and variance of the estimated mode in terms of attenuation factor and frequency by the improved Prony, modified TLS-ESPRIT, ERA/Prony and the proposed method for outlier placed towards the beginning of the test signal is provided in Table 2.5. Estimated attenuation factor with improved Prony method gives inaccurate attenuation factor while the proposed method has a mean

value of −0.07 which is better than modified TLS-ESPRIT and ERA/Prony which have mean of −0.0811 and −0.0929 respectively. For estimated frequency, the mean estimated by the proposed method is 0.4 Hz and has low variance as compared with the other methods. Table 2.6 provides the performance of all the methods for this test signal corresponding to estimated attenuation factor and frequency for the outlier placed towards the end of the samples. It is observed that the mean of the estimated modes by the proposed method is accurate as compared to the other methods.

2.5.3 Mode estimation for different ranges and position of outliers

The test signal of Section 2.5.1 i.e., $x(t) = e^{-0.1t}cos(2\pi t + \phi)$ is used for the analysis in this section with a SNR of 40 dB.

Table 2.7 provides a comparison of all the methods without outlier. It is observed that the proposed method works well for a signal with no outliers and is comparable in performance with the other methods. Figure 2.7(a) and 2.7(b), shows the plot of estimated attenuation factor and frequency, respectively for all the methods with varying magnitudes of outliers. It is observed that the proposed method is almost insensitive to the presence of outliers, whereas the error in the estimated modes by the other methods increases significantly. Table 2.8 shows the effectiveness of the proposed method in estimating modes for different position of the occurrence of outlier in the signal. It is observed that the proposed method is almost insensitive towards the location of the outlier.

Table 2.7: Mean and Variance of the estimated attenuation factor and frequency for the improved Prony, the modified TLS-ESPRIT, ERA/Prony and the Proposed Method for test signal without outlier with SNR=40 dB (Test signal- local mode)

Estimated Attenuation factor (True value= -0.1)		
Methods	μ (Mean)	σ^2 (Variance)
Improved Prony	-0.1000	4.46×10^{-8}
Modified TLS-ESPRIT	-0.1000	4.05×10^{-8}
ERA/Prony	-0.1000	1.88×10^{-8}
Proposed Method (Robust Modified Prony)	-0.1000	4.41×10^{-8}
Estimated Frequency (True value= 1 Hz)		
Methods	μ (Mean)	σ^2 (Variance)
Improved Prony	1.000	1.15×10^{-9}
Modified TLS-ESPRIT	1.000	1.29×10^{-9}
ERA/Prony	1.000	4.29×10^{-9}
Proposed Method (Robust Modified Prony)	1.000	1.14×10^{-9}

Table 2.8: Mean and Variance of the estimated attenuation factor and frequency for the improved Prony, the modified TLS-ESPRIT and the Proposed Method for the test signal for different position of outlier with SNR=40 dB (Test signal- local mode)

Estimated Attenuation factor (True value= -0.1)						
Outlier Position	Improved Prony		Modified TLS-ESPRIT		Proposed Method	
(Sample No)	μ (Mean)	σ^2 (Variance)	μ (Mean)	σ^2 (Variance)	μ (Mean)	σ^2 (Variance)
50	0.0093	6.321×10^{-8}	-0.0676	1.881×10^{-8}	-0.1000	1.533×10^{-7}
100	0.0149	6.916×10^{-8}	-0.0753	2.495×10^{-8}	-0.1000	1.109×10^{-7}
150	0.0194	8.347×10^{-8}	-0.0818	2.878×10^{-8}	-0.1000	7.189×10^{-8}
200	0.0229	9.077×10^{-8}	-0.0869	3.343×10^{-8}	-0.1000	5.414×10^{-8}
Estimated Frequency (True value= 1 Hz)						
Outlier Position	Improved Prony		Modified TLS-ESPRIT		Proposed Method	
(Sample No)	μ (Mean)	σ^2 (Variance)	μ (Mean)	σ^2 (Variance)	μ (Mean)	σ^2 (Variance)
50	1.0024	1.621×10^{-9}	1.0028	3.205×10^{-9}	1.0000	3.899×10^{-9}
100	1.0017	1.362×10^{-9}	1.0021	3.214×10^{-9}	1.0000	2.982×10^{-9}
150	1.0011	1.630×10^{-9}	1.0016	3.642×10^{-9}	1.0000	1.857×10^{-9}
200	1.0006	2.053×10^{-9}	1.0011	4.395×10^{-9}	1.0000	1.474×10^{-9}

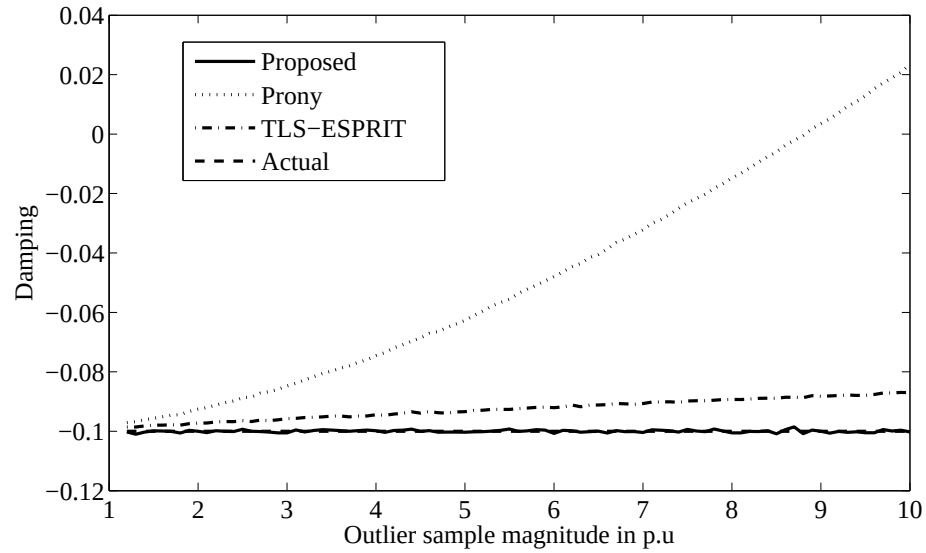

(a)

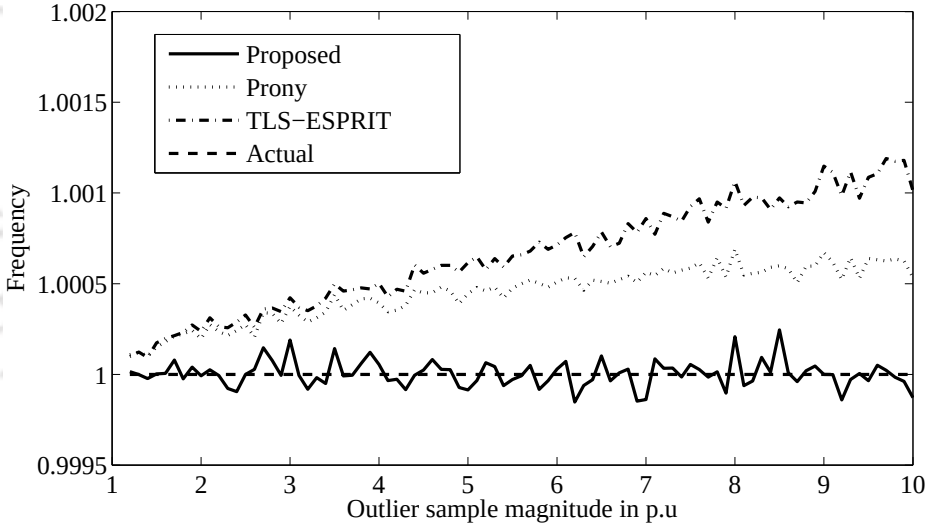

(b)

Figure 2.7: Test signal- local mode (a) Estimated attenuation factor against outlier; (b) Estimated frequency against outlier.

2.5.4 Mode estimation for the two-area test system

Mode estimation is done for a two-area power system [9], as shown in Figure 2.8. Table 2.9 shows the estimated modes for the two-area system which corresponds to low-frequency oscillations of the power in line $10-9$. The data for estimating the modes is obtained by considering the loss of 40 MW of load at bus 8 which causes low-frequency oscillations. The measurements corresponding to the power oscillations are taken from a PMU installed at bus 9 with an outlier of magnitude 1.2 times the peak value of signal injected into the measurements. The mean and variance of the estimated mode is shown in Table 2.9 at SNR= 20 dB by running 10000 Monte Carlo runs. Since, the magnitude of an outlier is very small, the mode estimated by the other methods are also comparable to the proposed method. The modes estimated by the proposed method are very close to the values obtained from the small signal stability analysis (SSA) based on the eigen values of the state matrix [9] as compared to the other methods. Table 2.10, which shows the effect of large outlier (=10× the peak value) on various methods. It could be observed from the comparison provided in the Table 2.10 that the proposed method is insensitive to outlier while the estimation of modes by the other methods is severely affected with the presence of outlier.

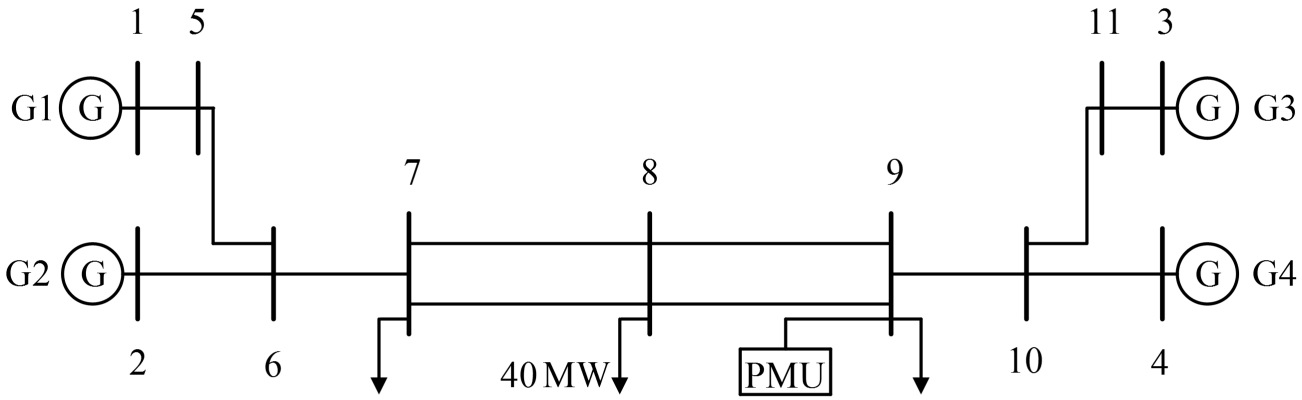

Figure 2.8: Single line diagram of the two-area system.

Table 2.9: Estimated Critical Modes of Low-frequency oscillations for a 2-Area System with loss of 40 MW for SNR=20 dB with outlier (=1.2× peak value of the signal, Test signal- inter-area mode)

Mode 1 (Attenuation factor= -0.25, freq= 0.5374 Hz) obtained from SSA				
	Attenuation factor		Frequency	
Methods	μ (Mean)	σ^2 (Variance)	μ (Mean)	σ^2 (Variance)
Improved Prony	-0.2520	1.826×10^{-4}	0.5352	4.983×10^{-6}
Modified TLS-ESPRIT	-0.2442	9.457×10^{-5}	0.5363	1.854×10^{-6}
Proposed Method (Robust Modified Prony)	-0.2482	1.890×10^{-4}	0.5355	4.515×10^{-6}
Mode 2 (Attenuation factor= -0.25, freq= 1.1950 Hz) obtained from SSA				
	Attenuation factor		Frequency	
Methods	μ (Mean)	σ^2 (Variance)	μ (Mean)	σ^2 (Variance)
Improved Prony	-0.1923	2.40×10^{-3}	1.1648	1.515×10^{-4}
Modified TLS-ESPRIT	-0.0974	3.00×10^{-3}	1.1640	6.079×10^{-4}
Proposed Method (Robust Modified Prony)	-0.2101	2.50×10^{-3}	1.1800	4.384×10^{-4}
Mode 3 (Attenuation factor= -0.25, freq= 1.2047 Hz) obtained from SSA				
	Attenuation factor		Frequency	
Methods	μ (Mean)	σ^2 (Variance)	μ (Mean)	σ^2 (Variance)
Improved Prony	-0.1064	2.30×10^{-3}	1.225	1.433×10^{-4}
Modified TLS-ESPRIT	-0.1554	1.33×10^{-2}	1.2074	5.10×10^{-3}
Proposed Method (Robust Modified Prony)	-0.1772	5.70×10^{-3}	1.220	2.038×10^{-4}

Table 2.10: Estimated Critical Modes of Low-frequency oscillations for a 2-Area System for outlier (=10× peak signal value) without noise

Mode 1 (Attenuation factor= -0.25, freq= 0.5374 Hz) obtained from SSA		
Methods	Attenuation	Frequency
Improved Prony	1.3599	0.5628
Modified TLS-ESPRIT	0.0958	0.5416
Proposed Method (Robust Modified Prony)	-0.2651	0.5355
Mode 2 (Attenuation factor= -0.25, freq= 1.1950 Hz) obtained from SSA		
Methods	Attenuation	Frequency
Improved Prony	0.4405	1.1484
Modified TLS-ESPRIT	-0.0318	1.1698
Proposed Method (Robust Modified Prony)	-0.1531	1.1813
Mode 3 (Attenuation factor= -0.25, freq= 1.2047 Hz) obtained from SSA		
Methods	Attenuation	Frequency
Improved Prony	1.2628	1.667
Modified TLS-ESPRIT	0.1162	1.3864
Proposed Method (Robust Modified Prony)	-0.2443	1.2325

2.5.5 Mode estimation utilizing the probing test data of the WECC system

A data corresponding to the probing test of the WECC system obtained on September 14, 2005 [78] is used for the performance evaluation of the proposed method as shown in Figure 2.9 [75]. Window 1 (20 : 10 : 11.993 – 20 : 10 : 20.526 UTC) and Window 2 (20 : 15 : 13.324 – 20 : 15 : 21.857 UTC) corresponds to the data acquired after the first and second sequential signal mode probing of ±125 MW respectively. Window 3 (20 : 00 : 03.333 – 20 : 00 : 11.866 UTC) corresponds to ambient data. The estimated modes for the North-South Swing was reported in literature to be 0.318 Hz and 8.3% damping [79]. Each analysis window of real probing data utilized for mode estimation is artificially corrupted by an outlier of strength 3 times the peak value. From the Table 2.11, it is observed that for each analysis window the improved Prony method fails to give correct mode estimation. For the analysis window 1, the proposed method gives a better estimate of the frequency

as compared to TLS-ESPRIT and ERA/Prony algorithm. For analysis window 2, the proposed method gives the value of damping (8.86% damping) almost same as the reported value [79] (8.3% damping) as compared to the other methods. For analysis window 3, the proposed method gives a better mode estimate as compared to the other methods. Table 2.12 compares the methods without an outlier, it is observed that the estimated modes are comparable to each other.

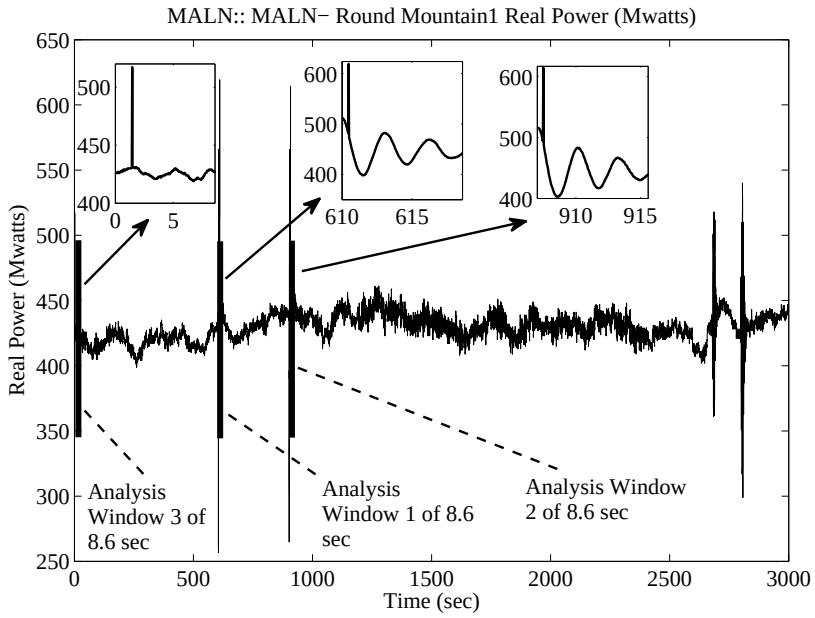

Figure 2.9: Probing data corresponding to the real power flow.

Table 2.11: Estimated mode analysis for outlier (= 3× peak signal value) placed in each window

Estimated mode for Analysis window 1			
	Attenuation	Frequency	% Damping
Improved Prony	-2.66	0.0318	99.71
Modified TLS-ESPRIT	-0.1313	0.323	6.45
ERA/Prony	-0.2204	0.3267	10.67
Proposed Method (Robust Modified Prony)	-0.1204	0.3179	6.01
Estimated mode for Analysis window 2			
	Attenuation	Frequency	% Damping
Improved Prony	-2.1711	0.0246	99.74
Modified TLS-ESPRIT	-0.1527	0.3178	7.62
ERA/Prony	-0.1533	0.3155	7.70
Proposed Method (Robust Modified Prony)	-0.1753	0.3135	8.86
Estimated mode for Analysis window 3			
	Attenuation	Frequency	% Damping
Improved Prony	-2.1779	0.3216	73.32
Modified TLS-ESPRIT	-0.0443	0.2984	2.36
ERA/Prony	-0.0555	0.2804	3.14
Proposed Method (Robust Modified Prony)	-0.0669	0.3199	3.32

Table 2.12: Estimated mode analysis without outlier for Analysis window 2

Methods	Attenuation	Frequency	% Damping
Improved Prony	-0.1513	0.3159	7.61
Modified TLS-ESPRIT	-0.1867	0.3153	9.38
ERA/Prony	-0.1817	0.3062	9.40
Proposed Method (Robust Modified Prony)	-0.1529	0.3114	7.79

2.6 Conclusion

This chapter proposes to modify improved Prony method by suggesting to use robust covariance matrix based on minimum covariance determinant (MCD) algorithm to take care of the outliers in the

sample data followed by low rank approximation to mitigate the effect of noise. Thus, the proposed method i.e., robust modified Prony can estimate modes very effectively in the presence of sample outliers, and also suitable for high variance Gaussian noise. To show the effectiveness of the proposed method, the performance of the method has been evaluated on known test signals, 2-area system and real PMU data taken from WECC system with the data sample corrupted with outlier.

From the simulation results as shown in Section 2.5, it could be inferred that the proposed method is indeed robust towards the presence of outliers as compared with the other methods such as improved Prony and modified TLS-ESPRIT. Simulation results are also included for a test signal with varying magnitude and different position of outlier sample on the mode estimated by different methods. It is observed that when the magnitude of outlier is less, i.e., 1.2 times the peak value of the signal, the performance of all the methods are comparable, but as the magnitude of outliers increases the proposed method tends to give more accurate results as compared with the other methods, since, the other methods are not designed to mitigate the effect of the presence of outlier sample.

3

Estimation of Low-Frequency Modes in Power System with Robust TLS-ESPRIT

3.1 Introduction

Robust modified Prony based low frequency critical mode estimation method, as proposed in Chapter 2, uses minimum covariance determinant (MCD) technique to find the robust covariance to mitigate the effect of an outlier. This method is more effective as compared to the improved Prony, modified TLS-ESPRIT and ERA/Prony methods. MCD algorithm involves computing the determinant of the sample covariance matrix for all the subsamples which comprises of 50% of the initial data [86]. To make it more suitable for its implementation, the code FAST-MCD [84] utilizes the p-subset algorithm which considers only a reduced number of subsets. However, this algorithm may lead to a relatively unstable results, particularly for small datasets. The MCD estimator has high breakdown point, but comes at the expense of low Gaussian efficiency. Even though the MCD estimator is widely used, there are other highly robust estimators which are more efficient than MCD and have smooth influence function [87]. One of the method among them is a MM estimator [82, 88]. Since, TLS-ESPRIT [51, 75] method is less sensitive to noise as compared to the Prony method in estimating the modes, this chapter has combined the advantage of MM estimator and TLS-ESPRIT

for estimating modes, where the MM estimator is utilized to minimize the effect of outliers.

This chapter motivates towards the improvement of the existing modified TLS-ESPRIT method, so that it can provide more accurate estimate of the low frequency oscillatory modes in the presence of outliers in the measured data. Section 3.2, briefly explains the modified TLS-ESPRIT method. Section 3.3, explains briefly how the covariance matrix used in the modified TLS-ESPRIT method is affected by outliers. Section 3.4, explains the proposed robust TLS-ESPRIT method. Section 3.5, discusses the results. Comparison of the modified TLS-ESPRIT [75] with the proposed method are performed for two test signals in the presence of an outlier with different SNR corresponding to local mode and inter-area mode, respectively. The proposed method is further compared with robust modified Prony for different position of outliers in the signal and also for two-area system [9]. The effectiveness of the proposed method is also demonstrated for real time signal of the WECC system [78, 79]. Section 3.6, presents the conclusions.

3.2 ESPRIT Estimation

3.2.1 Power system signals

The model of the power system signal used in the proposed method is same as presented in Chapter 2, Section 2.2.1. This consists of exponentially-damped sinusoids with additive white noise. The complex exponential form representation as given in equation (2.3), is expressed below as

$$\begin{aligned} y(n) &= s(n) + w(n) \\ &= \sum_{j=1}^{M} \alpha_j e^{\beta_j n} + w(n) \end{aligned} \tag{3.1}$$

3.2.2 Modified TLS-ESPRIT

The details about the modified TLS-ESPRIT is given in reference [75]. Considering the complex exponential signal model and assuming a data vector of size L, equation (3.2) is obtained as

$$\begin{aligned} \begin{bmatrix} y(n) \\ y(n+1) \\ . \\ . \\ y(n+L-1) \end{bmatrix} &= \begin{bmatrix} s(n) \\ s(n+1) \\ . \\ . \\ s(n+L-1) \end{bmatrix} + \begin{bmatrix} w(n) \\ w(n+1) \\ . \\ . \\ w(n+L-1) \end{bmatrix} \\ &= \sum_{k=1}^{M} \begin{bmatrix} s_k(n) \\ s_k(n+1) \\ . \\ . \\ s_k(n+L-1) \end{bmatrix} + \begin{bmatrix} w(n) \\ w(n+1) \\ . \\ . \\ w(n+L-1) \end{bmatrix} \end{aligned} \tag{3.2}$$

The signal is expressed as a linear combination of M basis vectors which are exponentially damped. $s(n) = \sum_{k=1}^{M} s_k(n)$. The k^{th} component of the signal vector can be expressed as

$$\mathbf{s}_k(n) = \begin{bmatrix} s_k(n) \\ s_k(n+1) \\ . \\ . \\ s_k(n+L-1) \end{bmatrix} = \alpha_k e^{n\beta_k} \begin{bmatrix} 1 \\ e^{\beta_k} \\ . \\ . \\ e^{(L-1)\beta_k} \end{bmatrix} \tag{3.3}$$

Substitution of equation (3.2) in (3.3) yields

$$\mathbf{y}(n) = \mathbf{AS} + \mathbf{w}(n) \tag{3.4}$$

Here **A** is denoted as

$$\mathbf{A} = \begin{bmatrix} 1 & 1 & . & . & . & 1 \\ e^{\beta_1} & e^{\beta_2} & . & . & . & e^{\beta_M} \\ . & . & . & . & . & . \\ . & . & . & . & . & . \\ e^{(L-1)\beta_1} & e^{(L-1)\beta_2} & . & . & . & e^{(L-1)\beta_M} \end{bmatrix}$$

$$= [\mathbf{a}(\beta_1), \mathbf{a}(\beta_2), ...\mathbf{a}(\beta_M)] \tag{3.5}$$

S=$[\hat{a}_1, \hat{a}_2, ...\hat{a}_M]^T$ and $\hat{a}_k = \alpha_k e^{n\beta_k}$

The vectors are defined below as

$$\mathbf{p}(n) = [y(n), ..., y(n+L-1)]^T$$

$$= \mathbf{AS} + \mathbf{w}_1 \tag{3.6}$$

$$\mathbf{q}(n) = [y(n+1), ..., y(n+L)]^T$$

$$= \mathbf{A\Gamma S} + \mathbf{w}_2 \tag{3.7}$$

$$\mathbf{r}(n) = [y(n+2), ..., y(n+L+1)]^T$$
$$= \mathbf{A}(\mathbf{\Gamma})^2\mathbf{S} + \mathbf{w}_3 \tag{3.8}$$

The vectors $\mathbf{p}(n)$, $\mathbf{q}(n)$ and $\mathbf{r}(n)$ are related to each other by the $\mathbf{\Gamma}$ matrix which is defined as $\mathbf{\Gamma} = diag[e^{\beta_1} e^{\beta_2} ... e^{\beta_M}]$ and $\mathbf{w_1}$, $\mathbf{w_2}$ and $\mathbf{w_3}$ are the noise vectors of $\mathbf{p}(n)$, $\mathbf{q}(n)$ and $\mathbf{r}(n)$ respectively. Equations (3.7) and (3.8) can be obtained by exploiting the shift invariance signal properties. In TLS-ESPRIT method, the data must be divided into two orthogonal subspaces namely signal and noise subspace. Singular value decomposition (SVD) technique is used to separate the data into two subspaces. Noise is assumed as zero mean white Gaussian.

$$\mathbf{R}_{yy} = E[\mathbf{y}(n)\mathbf{y}^*(n)]$$
$$= \mathbf{A}\mathbf{R}_\mathbf{s}\mathbf{A}^* + \sigma^2\mathbf{I} \tag{3.9}$$

Here $\mathbf{R}_s$ is the signal covariance matrix and σ^2 represents the variance of the noise. After application of SVD on the covariance matrix $\mathbf{R}_{yy}$, the following equation is obtained.

$$\mathbf{R}_{yy} = \mathbf{E}_\mathbf{s}\boldsymbol{\lambda}_\mathbf{s}\mathbf{E}_\mathbf{s}^* + \mathbf{E}_\mathbf{n}\boldsymbol{\lambda}_\mathbf{n}\mathbf{E}_\mathbf{n}^* \tag{3.10}$$

Where $\boldsymbol{\lambda}_\mathbf{s}$ is the singular value of the signal subspace and $\boldsymbol{\lambda}_\mathbf{n}$ is the singular value of the noise subspace. Since, $\mathbf{A}$ and $\mathbf{E}_\mathbf{s}$ span the same signal subspace, therefore a linear transform $\mathbf{T}$ exists such that $\mathbf{E}_\mathbf{s} = \mathbf{E}_\mathbf{p} = \mathbf{AT}$. Thus the basis corresponding to the data vectors $\mathbf{p}(n)$, $\mathbf{q}(n)$ and $\mathbf{r}(n)$ must satisfy the following equations

$$\begin{bmatrix} \mathbf{E}_p \\ \mathbf{E}_q \end{bmatrix} = \begin{bmatrix} \mathbf{AT} \\ \mathbf{A\Gamma T} \end{bmatrix} \tag{3.11}$$

$$\begin{bmatrix} \mathbf{E}_p \\ \mathbf{E}_r \end{bmatrix} = \begin{bmatrix} \mathbf{AT} \\ \mathbf{A\Gamma}^2\mathbf{T} \end{bmatrix} \tag{3.12}$$

The basis vectors for the signal subspace containing the data vectors $\mathbf{p}(n)$, $\mathbf{q}(n)$ and $\mathbf{r}(n)$ are represented in the columns of the matrices $\mathbf{E}_p$, $\mathbf{E}_q$ and $\mathbf{E}_r$ respectively. Equations (3.11) and (3.12) are obtained by exploiting the shift invariance properties of the signal [48]. Total least square method [81]

is used to get the approximated solution of these two equations having the objectives

$$min \parallel \begin{bmatrix} \mathbf{E}_p \\ \mathbf{E}_q \end{bmatrix} - \begin{bmatrix} \mathbf{AT} \\ \mathbf{A\Gamma T} \end{bmatrix} \parallel^2 \tag{3.13}$$

$$min \parallel \begin{bmatrix} \mathbf{E}_p \\ \mathbf{E}_r \end{bmatrix} - \begin{bmatrix} \mathbf{AT} \\ \mathbf{A\Gamma}^2\mathbf{T} \end{bmatrix} \parallel^2 \tag{3.14}$$

The modes estimated by the equation (3.13) and (3.14) are averaged to get the estimated modes by the modified TLS-ESPRIT.

3.3 Effects of outliers

Since the modified TLS-ESPRIT method is also based on least square approach, it is highly sensitive to the presence of an outlier. These outliers induces a change in the magnitudes of eigenvalues, direction of eigenvector and covariance structure of the matrix [82]. The covariance ellipsoid strongly changes its direction with respect to the position of outliers resulting in increase in the ellipsoidal area. The details about it has already been discussed in Section 2.3 of Chapter 2.

3.4 Proposed Robust TLS-ESPRIT

In the proposed robust TLS-ESPRIT, the classical covariance matrix as given by equation (3.9) is replaced by the estimated robust covariance as explained in the subsection below.

3.4.1 Robust Covariance using MM Estimator

The data matrix **D** is constructed from the given data samples as shown in the equation below

$$\mathbf{D} = \begin{bmatrix} y(0) & y(1) & ... & y(N-L+1) \\ y(1) & y(2) & ... & y(N-L+2) \\ \vdots & \vdots & \ddots & \vdots \\ y(L-1) & y(L) & ... & y(N) \end{bmatrix} = [\mathbf{x}_1, \mathbf{x}_2, ...\mathbf{x}_n] \tag{3.15}$$

Modified TLS-ESPRIT has utilized the covariance matrix $\mathbf{R}_{yy}$, which is observed to be sensitive towards the presence of outliers. To mitigate the effect of the presence of an outlier in the data matrix **D**, the present work uses MM estimator to estimate the robust covariance matrix ($\mathbf{R}_{yymodified}$), and hence the proposed robust TLS-ESPRIT method is found to be robust with the presence of an outlier.

3.4.2 MM Estimator

MM estimators are robust to outliers as well as efficient to normal data. At first a S estimator is used to obtain a robust scale estimate and then the shape matrix and the location vectors are determined by a much more efficient M estimator [89, 90]. The proposed method which provides the estimate of the covariance matrix based on S and M estimator, which is also known as MM estimator. The various steps involved in estimating the covariance matrix using the data matrix $\mathbf{D} = [\mathbf{x}_1, \mathbf{x}_2, ...\mathbf{x}_n]$ based on MM estimator are as follows:

Step 1: For independent and identically distributed observations $\mathbf{x}_1$,$\mathbf{x}_2$,....,$\mathbf{x}_n$, from a p- variate population, having location $\boldsymbol{\mu}_n$ and covariance $\boldsymbol{\Sigma}_n$, the multivariate S estimator ($\tilde{\boldsymbol{\mu}}_n$, $\tilde{\boldsymbol{\Sigma}}_n$) can be defined as the one that minimizes $|\mathbf{C}|$ subject to

$$\frac{1}{n}\sum_{i=1}^{n}\psi_0\left(\sqrt{(\mathbf{x}_i-\mathbf{T})^T\mathbf{C}^{-1}(\mathbf{x}_i-\mathbf{T})}\right) = b \tag{3.16}$$

over all $\mathbf{T} \in \mathbb{R}^p$ and $\mathbf{C} \in$ PDS (p). Here, PDS (p) denotes the class of positive definite symmetric $p \times p$ matrix.

To attain consistency at normal model, b is taken as $b = E_{N(\mathbf{0},\mathbf{I})}\psi(\| \mathbf{r} \|)$, where $\mathbf{r}$ has $N(\mathbf{0}, \mathbf{I})$ distribution, and

$$\psi_0(s) = \begin{cases} \frac{s^2}{2} - \frac{s^4}{2k_0^2} + \frac{s^6}{6k_0^4} & |\, s \,| \leq k_0 \\ \frac{k_0^2}{6} & |\, s \,| > k_0 \end{cases}$$

The default value of k_0 is 2.9366 so that the consistent scale estimate has 25% breakdown value. This gives ($\tilde{\boldsymbol{\mu}}_n$,$\tilde{\boldsymbol{\Sigma}}_n$). The robust scale estimate is then calculated as $\tilde{\boldsymbol{\sigma}}_n = |\tilde{\boldsymbol{\Sigma}}_n|^{1/2p}$.

Step 2: The minimizer ($\hat{\boldsymbol{\mu}}_n$,$\hat{\boldsymbol{\Gamma}}_n$) is found for $\frac{1}{n}\sum_{i=1}^{n}\psi_1\left(\frac{\sqrt{(\mathbf{x}_i-\mathbf{T})^T\mathbf{G}^{-1}(\mathbf{x}_i-\mathbf{T})}}{\tilde{\boldsymbol{\sigma}}_n}\right)$, over all $\mathbf{T} \in \mathbb{R}^p$ and $\mathbf{G} \in$ PDS (p), for which $|\mathbf{G}| = 1$, and

$$\psi_1(s) = \begin{cases} \frac{s^2}{2} - \frac{s^4}{2k_1^2} + \frac{s^6}{6k_1^4} & |\, s \,| \leq k_1 \\ \frac{k_1^2}{6} & |\, s \,| > k_1 \end{cases}$$

The default value of k_1 is 3.440 so that the MM estimate has 85% Gaussian asymptotic efficiency. The robust covariance matrix is then calculated as, $\hat{\boldsymbol{\Sigma}}_n = \hat{\boldsymbol{\sigma}}_n{}^2\hat{\boldsymbol{\Gamma}}_n$.

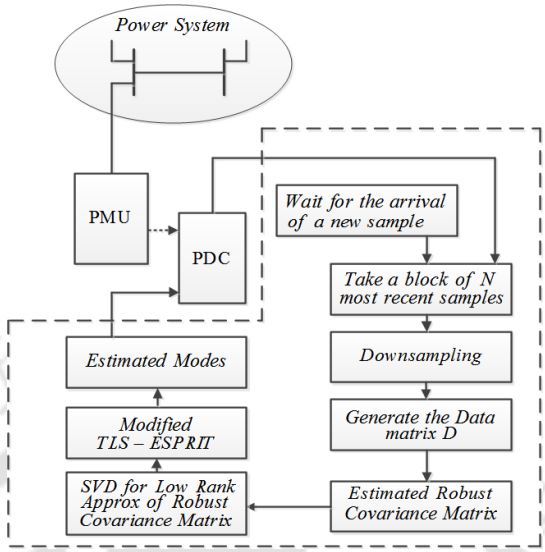

Figure 3.1: Block diagram of the proposed method i.e, robust TLS-ESPRIT for mode estimation.

3.4.3 Identification of Power System Modes using the Proposed robust TLS-ESPRIT Method

As the low frequency power oscillation corresponds to the electromechanical modes, the critical modes oscillation can be estimated using the power signal obtained from the PMU. These measurements from the PMU are provided to the PDC through various communication links. A block diagram for the proposed method as shown in Figure 3.1, describes the various steps for estimating the mode using the proposed method.

The steps for estimating the modes using the proposed method i.e, robust TLS-ESPRIT are described as follows:

Step 1: The proposed technique i.e., robust TLS-ESPRIT method utilizes a block of N number of measurements from PDC, corresponding to the active power of a particular line. The window size is typically taken as the ratio of PMU's reporting rate and lower limit of estimator's frequency [91].

Step 2: Perform down sampling to reduce the effect of noise and to decrease the computational complexity.

Step 3: Generate the data matrix **D** as given in equation (3.15).

Step 4: Estimate the robust covariance matrix using MM estimator as explained in sub-section 3.4.2.

Step 5: To further reduce the effect of noise, perform the low rank approximation [92] of the

estimated robust covariance matrix $\mathbf{R}_{yymodified}$. To get the model order, which is required for low rank approximation of the robust covariance matrix, the index [35] as given below is used by the proposed method.

$$K(i) = \left[\frac{\rho_1^2 + \rho_2^2 + \cdots + \rho_i^2}{\rho_1^2 + \rho_2^2 + \cdots + \rho_L^2}\right]^{\frac{1}{2}} \tag{3.17}$$

where $K(i)$ is monotonously increasing index and ρ_i is the i-th singular value. As i approaches to the actual signal order, $K(i)$ is almost close to unity.

Step 6: The low rank approximated robust covariance matrix is used by the modified TLS-ESPRIT to calculate the modes.

Step 7: The estimated modes corresponding to a block of N most recent samples, are stored in the PDC.

Step 8: The entire procedure is repeated after the arrival of N new samples.

3.5 Simulation Results

To illustrate the effectiveness of the proposed method i.e., robust TLS-ESPRIT, the simulations are done on two test signals with known attenuation factor and frequency in the presence of outlier. Out of the two, one of them corresponds to the local mode and the other corresponds to the inter-area mode, respectively. The performance evaluation of the modified TLS-ESPRIT method and the proposed method is done by simulating 10000 Monte Carlo runs for different noise levels. The simulation also includes the comparison of the proposed method with robust modified Prony on two-area system and real data obtained from the PMU connected in the WECC system. For a comparative analysis of the effect of an outlier, the present work has taken a signal corrupted with outlier at different position. For the synthetic test signal, a time window having a duration of 20 s with 251 samples of active power acquired from the PMU at the sampling frequency of 12.5 Hz. For the two-area system, a time window of 10.16 s with 128 samples and sampling rate of 12.5 Hz is used. For WECC system, the length of sample window is taken as 8.55 s.

3.5.1 Test signal Corresponding to Local Mode

A test signal $x(t) = e^{-0.1t}cos(2\pi t + \phi)$ corresponding to local mode is considered for the simulation.

Table 3.1: Mean and Variance of the estimated mode for the modified TLS-ESPRIT and the Proposed Method for outlier (=10 × peak value) placed towards the beginning of the signal at different SNR (Test signal- local mode)

Modified TLS-ESPRIT				
	Estimated Attenuation factor (True value= -0.1)		Estimated Frequency (True value= 1 Hz)	
SNR (dB)	μ (Mean)	σ^2 (Variance)	μ (Mean)	σ^2 (Variance)
40	-0.3627	3.37×10^{-7}	1.0085	2.43×10^{-9}
30	-0.3627	3.29×10^{-6}	1.0085	9.503×10^{-9}
20	-0.3627	3.24×10^{-5}	1.0085	8.32×10^{-8}
Proposed Method (Robust TLS-ESPRIT)				
	Estimated Attenuation factor (True value= -0.1)		Estimated Frequency (True value= 1 Hz)	
SNR (dB)	μ (Mean)	σ^2 (Variance)	μ (Mean)	σ^2 (Variance)
40	-0.1000	5.71×10^{-8}	1.0000	1.85×10^{-9}
30	-0.1000	5.10×10^{-7}	1.0000	1.37×10^{-8}
20	-0.0999	4.28×10^{-6}	1.0000	1.06×10^{-7}

3.5.1.1 Comparison of the Proposed Method With the modified TLS-ESPRIT for outlier placed towards the beginning of the test signal for different SNR

The mean and variance of the attenuation factor and frequency of the estimated modes on the test signal with outlier (=10 × peak value) placed towards the beginning is provided in Table 3.1 for the modified TLS-ESPRIT and the proposed method. It is observed that the estimated mean value of attenuation factor degrades significantly for the modified TLS-ESPRIT (i.e. estimated mean value of attenuation factor is equal to −0.3627) while the proposed method gives almost accurate results (which has a mean value of −0.1 for SNR = 40 and SNR = 30 dB and −0.0999 for SNR = 20 dB) with lesser variance than the modified TLS-ESPRIT. For frequency estimation, the proposed method gives exact value (i.e, estimated mean value of frequency is equal to 1 Hz) than the modified TLS-ESPRIT (which has a mean value of 1.0085 Hz) for all the SNR as shown in Table 3.1.

Table 3.2: Mean and Variance of the estimated mode for the modified TLS-ESPRIT and the Proposed Method for outlier (=10 × peak value) placed towards the end of the signal at different SNR (Test signal- local mode)

Modified TLS-ESPRIT				
	Estimated Attenuation factor (True value= -0.1)		Estimated Frequency (True value= 1 Hz)	
SNR (dB)	μ (Mean)	σ^2 (Variance)	μ (Mean)	σ^2 (Variance)
40	0.0170	7.69×10^{-8}	0.9972	3.26×10^{-9}
30	0.0170	7.49×10^{-7}	0.9972	2.51×10^{-8}
20	0.0171	7.58×10^{-6}	0.9972	2.37×10^{-7}
Proposed Method (Robust TLS-ESPRIT)				
	Estimated Attenuation factor (True value= -0.1)		Estimated Frequency (True value= 1 Hz)	
SNR (dB)	μ (Mean)	σ^2 (Variance)	μ (Mean)	σ^2 (Variance)
40	-0.1000	5.71×10^{-8}	1.0000	1.93×10^{-9}
30	-0.1000	5.102×10^{-7}	1.0000	1.36×10^{-8}
20	-0.1000	4.33×10^{-6}	1.0000	1.04×10^{-7}

3.5.1.2 Comparison of the Proposed Method With the modified TLS-ESPRIT for outlier placed towards the end of the test signal for different SNR

The mean and variance of the attenuation factor and frequency of the estimated modes on the test signal with outlier (=10 × peak value) placed towards the end is provided in Table 3.2 for the modified TLS-ESPRIT and the proposed method. Modified TLS-ESPRIT gives positive attenuation factor while the proposed method gives accurate attenuation factor (i.e, estimated mean value is equal to -0.1) with less variance for all noise levels. For estimating frequency, the proposed method gives accurate mean value (i.e, estimated mean value of frequency is equal to 1 Hz) than the modified TLS-ESPRIT (which has a mean value of 0.9972 Hz) and also has lesser variance than the later, for all noise levels as shown in Table 3.2.

Table 3.3: Mean and Variance of the estimated mode for the modified TLS-ESPRIT and the Proposed Method for outlier (=10 × peak value) placed towards the beginning of the signal at different SNR (Test signal- inter-area mode)

Modified TLS-ESPRIT				
	Estimated Attenuation factor (True value= -0.07)		Estimated Frequency (True value= 0.4 Hz)	
SNR (dB)	μ (Mean)	σ^2 (Variance)	μ (Mean)	σ^2 (Variance)
40	-0.2291	1.38×10^{-7}	0.4008	5.29×10^{-11}
30	-0.2291	1.39×10^{-6}	0.4008	3.95×10^{-9}
20	-0.2291	1.39×10^{-5}	0.4008	3.13×10^{-8}
Proposed Method (Robust TLS-ESPRIT)				
	Estimated Attenuation factor (True value= -0.07)		Estimated Frequency (True value= 0.4 Hz)	
SNR (dB)	μ (Mean)	σ^2 (Variance)	μ (Mean)	σ^2 (Variance)
40	-0.0700	4.32×10^{-8}	0.4000	1.13×10^{-9}
30	-0.0700	3.33×10^{-7}	0.4000	1.07×10^{-8}
20	-0.0699	3.32×10^{-6}	0.4000	7.78×10^{-8}

3.5.2 Test signal Corresponding to Inter-Area Mode

A test signal $x(t) = e^{-0.07t}cos(2\pi 0.4t + \phi)$ corresponding to inter-area mode is considered for the simulation.

3.5.2.1 Comparison of the Proposed method With the modified TLS-ESPRIT for outlier placed towards the beginning of the test signal for different SNR

The mean and variance of the attenuation factor and frequency of the estimated modes on the test signal with outlier (=10 × peak value) placed towards the beginning is provided in Table 3.3 for the modified TLS-ESPRIT and the proposed method. Attenuation factor estimation with modified TLS-ESPRIT gives incorrect results (i.e, estimated mean value is equal to -0.2291) while the proposed method gives better results (which has a mean value of -0.07 for SNR = 40 and SNR = 30 dB and -0.0699 for SNR = 20 dB) with less variance. Table 3.3 shows that for frequency estimation, the proposed method gives better results (which has a estimated mean value of 0.4000 Hz) than the modified TLS-ESPRIT (i.e, estimated mean value of frequency is equal to 0.4008 Hz) for all the SNR.

Table 3.4: Mean and Variance of the estimated mode for the modified TLS-ESPRIT and the Proposed Method for outlier (=10 × peak value) placed towards the end of the signal at different SNR (Test signal- inter-area mode)

Modified TLS-ESPRIT				
	Estimated Attenuation factor (True value= -0.07)		Estimated Frequency (True value= 0.4 Hz)	
SNR (dB)	μ (Mean)	σ^2 (Variance)	μ (Mean)	σ^2 (Variance)
40	-0.0174	4.17×10^{-8}	0.4055	3.12×10^{-9}
30	-0.0174	4.16×10^{-7}	0.4055	2.39×10^{-8}
20	-0.0174	4.09×10^{-6}	0.4055	2.31×10^{-7}
Proposed Method (Robust TLS-ESPRIT)				
	Estimated Attenuation factor (True value= -0.07)		Estimated Frequency (True value= 0.4 Hz)	
SNR (dB)	μ (Mean)	σ^2 (Variance)	μ (Mean)	σ^2 (Variance)
40	-0.0700	4.24×10^{-8}	0.4000	1.12×10^{-9}
30	-0.0700	3.53×10^{-7}	0.4000	1.107×10^{-8}
20	-0.0701	3.31×10^{-6}	0.4000	8.12×10^{-8}

3.5.2.2 Comparison of the Proposed method With the modified TLS-ESPRIT for outlier placed towards the end of the test signal for different SNR

The mean and variance of the attenuation factor and frequency of the estimated modes on the test signal with outlier (=10 × peak value) placed towards the end is provided in Table 3.4 for the modified TLS-ESPRIT and the proposed method. Modified TLS-ESPRIT gives inadequate attenuation factor (i.e, estimated mean value is equal to −0.0174) while the proposed method gives a better performance (which has a mean value of −0.07 for SNR = 40 and SNR = 30 dB and −0.0701 for SNR = 20 dB). It can be seen that for frequency estimation the proposed method performs better (i.e, estimated mean value of frequency is equal 0.4000 Hz) than the modified TLS-ESPRIT (which has a mean value of 0.4055 Hz) with lesser variance as compared to the other method.

Table 3.5: Mean and Variance of the estimated attenuation factor and frequency for the modified TLS-ESPRIT, robust modified Prony and the Proposed Method for the test signal for different position of outlier with SNR=40 dB (Test signal- local mode)

Estimated Attenuation factor (True value= -0.1)						
Outlier Position	Modified TLS-ESPRIT		Robust Modified Prony		Proposed Method	
(Sample No)	μ (Mean)	σ^2 (Variance)	μ (Mean)	σ^2 (Variance)	μ (Mean)	σ^2 (Variance)
50	-0.0676	1.881×10^{-8}	-0.1000	1.533×10^{-7}	-0.1000	1.195×10^{-7}
100	-0.0753	2.495×10^{-8}	-0.1000	1.109×10^{-7}	-0.1000	9.061×10^{-8}
150	-0.0818	2.878×10^{-8}	-0.1000	7.189×10^{-8}	-0.1000	6.000×10^{-8}
200	-0.0869	3.343×10^{-8}	-0.1000	5.414×10^{-8}	-0.1000	5.297×10^{-8}
Estimated Frequency (True value= 1 Hz)						
Outlier Position	Modified TLS-ESPRIT		Robust Modified Prony		Proposed Method	
(Sample No)	μ (Mean)	σ^2 (Variance)	μ (Mean)	σ^2 (Variance)	μ (Mean)	σ^2 (Variance)
50	1.0028	3.205×10^{-9}	1.0000	3.899×10^{-9}	1.0000	1.887×10^{-9}
100	1.0021	3.214×10^{-9}	1.0000	2.982×10^{-9}	1.0000	1.993×10^{-9}
150	1.0016	3.642×10^{-9}	1.0000	1.857×10^{-9}	1.0000	1.835×10^{-9}
200	1.0011	4.395×10^{-9}	1.0000	1.474×10^{-9}	1.0000	1.325×10^{-9}

3.5.3 Mode estimation for different position of outliers

The test signal of Section 3.5.1, i.e., $x(t) = e^{-0.1t}cos(2\pi t + \phi)$ is used for mode estimation in this section with a SNR of 40 dB. Table 3.5 shows the effectiveness of the proposed method in estimating modes for different position of outlier occurrence in the signal. It is observed that the proposed robust TLS-ESPRIT method gives better estimate of attenuation factor and frequency as compared to the robust modified Prony as shown by their variance values. As it is observed that the performance of the modified TLS-ESPRIT method in estimating the low frequency mode is highly sensitive to the presence of outlier, hence, in the subsequent sub-section of the work, the comparison of the proposed method is done with the robust modified Prony method.

3.5.4 Mode estimation for the two-area test system

The proposed method is compared with robust modified Prony for a two-area power system [9], as shown in Figure 3.2. Table 3.6 shows the estimated modes for the two-area system corresponding to low-frequency oscillations of the power in line $10-9$. The data for mode estimation is obtained by considering the loss of 40 MW of load at bus 8 which induces low-frequency oscillations. PMU installed at bus 9 provides measurements corresponding to the power oscillations. Table 3.6 shows the estimated mode at SNR= 20 dB by running 10000 Monte Carlo runs for outlier of magnitude 1.2 times the peak value of signal injected into the measurements. The modes estimated by the proposed method are very close to the values obtained from the small signal stability analysis (SSA) based on the eigen values of the state matrix [9] as compared to the robust modified Prony method. Table 3.7 shows the effect of large outlier (=10× the peak value) on the two methods. It is observed from the Table 3.7 that the proposed method performs better as compared to the robust modified Prony method.

Table 3.6: Estimated Critical Modes of Low-frequency oscillations for a 2-Area System with loss of 40 MW for SNR=20 dB with outlier (=1.2× peak value of the signal, Test signal- inter-area mode)

Mode 1 (Attenuation factor= -0.25, freq= 0.5374 Hz) obtained from SSA				
	Attenuation		Frequency	
Methods	μ (Mean)	σ^2 (Variance)	μ (Mean)	σ^2 (Variance)
Robust Modified Prony	-0.2482	1.890×10^{-4}	0.5355	4.515×10^{-6}
Proposed Method (Robust TLS-ESPRIT)	-0.2483	1.861×10^{-4}	0.5355	7.200×10^{-6}
Mode 2 (Attenuation factor= -0.25, freq= 1.1950 Hz) obtained from SSA				
	Attenuation		Frequency	
Methods	μ (Mean)	σ^2 (Variance)	μ (Mean)	σ^2 (Variance)
Robust Modified Prony	-0.2101	2.50×10^{-3}	1.1800	4.384×10^{-4}
Proposed Method (Robust TLS-ESPRIT)	-0.2390	1.31×10^{-2}	1.1839	2.647×10^{-4}
Mode 3 (Attenuation factor= -0.25, freq= 1.2047 Hz) obtained from SSA				
	Attenuation		Frequency	
Methods	μ (Mean)	σ^2 (Variance)	μ (Mean)	σ^2 (Variance)
Robust Modified Prony	-0.1772	5.70×10^{-3}	1.220	2.038×10^{-4}
Proposed Method (Robust TLS-ESPRIT)	-0.2242	1.00×10^{-2}	1.217	2.570×10^{-4}

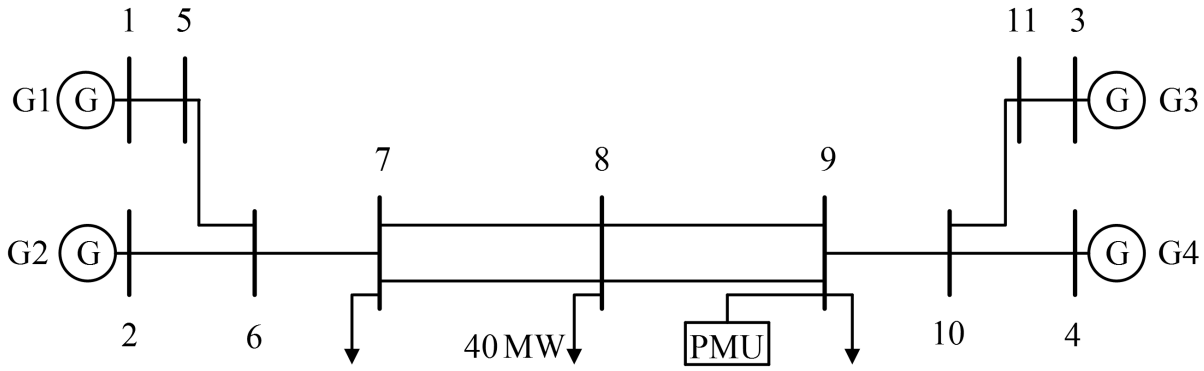

Figure 3.2: Single line diagram of the two-area system.

Table 3.7: Estimated Critical Modes of Low-frequency oscillations for a 2-Area System for outlier (=10× peak signal value) without noise

Mode 1 (Attenuation factor= -0.25, freq= 0.5374 Hz) obtained from SSA		
Methods	Attenuation	Frequency
Robust Modified Prony	-0.2651	0.5355
Proposed Method (Robust TLS-ESPRIT)	-0.2539	0.5360
Mode 1 (Attenuation factor= -0.25, freq= 1.1950 Hz) obtained from SSA		
Methods	Attenuation	Frequency
Robust Modified Prony	-0.1531	1.1813
Proposed Method (Robust TLS-ESPRIT)	-0.2496	1.1995
Mode 3 (Attenuation factor= -0.25, freq= 1.2047 Hz) obtained from SSA		
Methods	Attenuation	Frequency
Robust Modified Prony	-0.2443	1.2325
Proposed Method (Robust TLS-ESPRIT)	-0.2486	1.2001

3.5.5 Estimation of modes using the real test signal of the WECC system

A probing test data of the WECC system obtained on September 14, 2005 [78] is used for the performance evaluation of the proposed method as shown in Figure 3.3 [75]. The data set utilized for the analysis is given at the B.P.A website [79]. The estimated modes for the first and the second window was reported to be 0.318 Hz and 8.3% damping [79] for the North-South Swing.

The proposed method is compared with robust modified Prony method for a random outlier of strength 3 times the peak value injected into the sample as listed in Table 3.8. For the analysis widow 1, the proposed method gives better value of damping as compared to the robust modified Prony method. For the second analysis window, the proposed method gives the value of frequency and damping almost close to the reported value [79]. For analysis window 3, it has been observed that the proposed method gives a better estimate for the damping (6.13% damping) as compared to the robust modified Prony method.

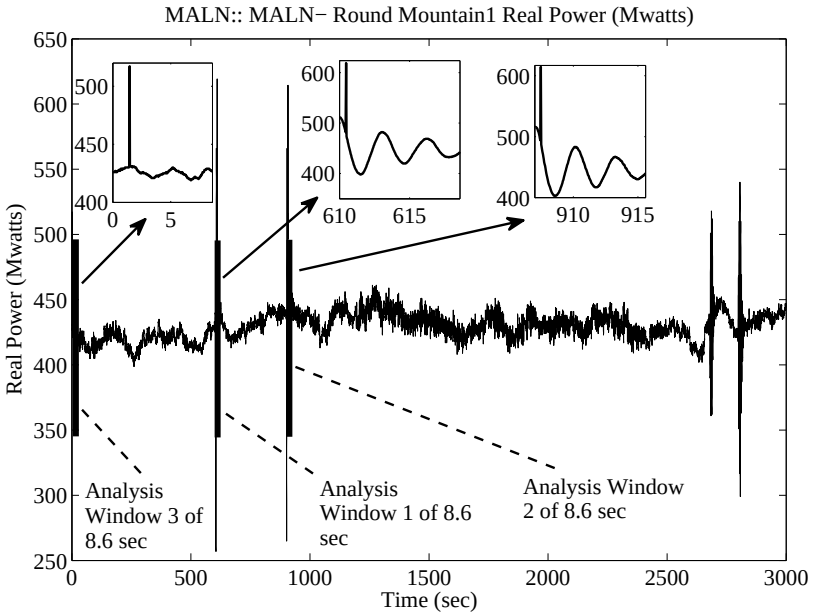

Figure 3.3: Probing data corresponding to the real power flow.

Table 3.8: Estimated Mode Analysis for outlier (= 3× peak signal value) placed in each window

Estimated mode for Analysis window 1			
	Attenuation	Frequency	% Damping
Robust Modified Prony	-0.1204	0.3179	6.01
Proposed Method (Robust TLS-ESPRIT)	-0.1401	0.3102	7.17
Estimated mode for Analysis window 2			
	Attenuation	Frequency	% Damping
Robust Modified Prony	-0.1753	0.3135	8.86
Proposed Method (Robust TLS-ESPRIT)	-0.1657	0.3223	8.15
Estimated mode for Analysis window 3			
	Attenuation	Frequency	% Damping
Robust Modified Prony	-0.0669	0.3199	3.32
Proposed Method (Robust TLS-ESPRIT)	-0.1237	0.3204	6.13

3.6 Conclusion

This chapter has proposed a robust TLS-ESPRIT method by employing a robust covariance matrix utilizing MM estimator, which is observed to be efficient than MCD estimator to handle the outliers in the sample data. Thus, the proposed method i.e., robust TLS-ESPRIT can mitigate the effect of the presence of outliers as well as high variance Gaussian noise. A comparative analysis of the proposed method is carried out with modified TLS-ESPRIT for the signals with different SNR values.

It is observed that the proposed method performs far better than the modified ESPRIT method and has the negligible bias in presence of outliers. Simulation results are also included for a test signal with different position of outliers in the data sample. It is observed that the proposed method performs better than the robust modified Prony method in terms of variance of the estimated modes. The effectiveness of the proposed method in identifying low-frequency modes is also provided on a two-area power system along with real time probing measurement signal of the WECC system. It can be observed through various simulations that the proposed method has some improvement over the robust modified Prony method.

4

Estimation of Low-Frequency Modes from Ambient Data using Wavelet, RD and TLS-ESPRIT

4.1 Introduction

The low frequency mode estimation methods as proposed in Chapter 2 & 3 of the thesis are based on the use of ringdown data generated during large disturbance in the power system. The events associated with major disturbances such as fault, adding/removing of a large load or generation provides the data associated with the free response that can be easily observed in the presence of ambient noise. As these major disturbance are less frequent, hence, the methods utilizing the ringdown data provides a very accurate estimation of the modes, but are updated typically after a long duration. Due to long and random update of the estimated modes, the current stability status of the system may not be provided, and hence, becomes a cause of concern for its suitability for providing the real-time stability of the system. On the other hand, the class of algorithms based on the use of ambient data i.e., the measurement data corresponding to the random load switching persistently excites the power system. These random perturbation of the system with nonlinear trends subtracted appears as noise with very small magnitude and is difficult to extract the impulse response out of it. Hence, the focus of this

chapter is on the ambient modal estimation known as operational modal analysis (OMA) to develop an algorithm which uses ambient data for getting the information about the stability of the system.

Extraction of the oscillatory modes from ambient data is difficult as the data has very low SNR and also corrupted with nonlinear trends. Various methods suitable for analysis of ambient signals are available in the literature, such as, in [53] ARMA model is used to estimate the oscillatory modes. Methods based on stochastic subspace identification [64] and distributed frequency domain [63] have also been used for identifying the oscillatory modes. The use of random decrement (RD) technique along with TLS-ESPRIT is proposed in [56]. In [66], combination of spectral independent component analysis and random decrement technique is described. A comparative study of subspace [64], wavelet [65] and independent component analysis methods [66] are illustrated in [67]. In [68], natural excitation technique (NExT) [69] in conjunction with eigensystem realization algorithm (ERA) [70] is used for identification of inter-area modes for ambient data of the power system. RD technique in combination with Ibrahim time domain (ITD) is presented in [71]. As the estimated modes using the ambient data are not very accurate, hence, significant improvement is required on the existing methods.

This chapter presents a robust method for identification of low frequency modes by utilizing a nonlinear filter and wavelet transform for detrending and de-noising the signal followed by random decrement (RD) technique for obtaining the free decay response. Finally, the modified TLS-ESPRIT is used to estimate the attenuation factor and frequency from the free decay response. The proposed method is compared with the nonlinear filtering [93], natural excitation technique- eigensystem realization (NExT-ERA) [68] and random decrement- Ibrahim time domain (RD-ITD) [71] methods for simulated data corresponding to ambient data and corrupted with nonlinear trends. The performance of the proposed method i.e., NwT-RD-TLS-ESPRIT is also carried out on the ambient data contaminated with nonlinear trends which is generated from an equivalent second order system representing a particular mode with dynamics corresponding to the modes present in a two-area power system [9] and also on the data obtained from a real time digital simulator (RTDS). The robustness of the proposed method is further established for real data obtained from North Eastern Regional Electricity Board (NEREB) and on the probing data of the Western Electricity Coordinating Council

(WECC) [78, 79].

This chapter motivates towards the application of wavelet technique to extract the significant and best set of coefficients for signal reconstruction, so that, it can provide reasonably good estimate of low frequency modes for the ambient data using the proposed method i.e., NwT-RD-TLS-ESPRIT. Section 4.2 gives a brief description of the techniques that constitutes the proposed method and presents an overview of the proposed method (NwT-RD-TLS-ESPRIT). Section 4.3 provides the simulation results and finally, the conclusion is presented in Section 4.4.

4.2 Methods for modal parameter estimation

4.2.1 Nonlinear filter

It is required to pre-filter the nonlinear trends present in the ambient data obtained from the PMU. The mathematical equation corresponding to the nonlinear pre-filter [93] proposed in this work for removing the nonlinear trends is given by the equation (4.1)

$$\begin{aligned} y[i] &= \frac{1}{2}\{(x[i] - \bar{w}(k-1)) + (x[i] - \bar{w}(k))\} \\ &= x[i] - \frac{1}{2}\{\bar{w}(k-1) + \bar{w}(k)\} \quad \forall i = w_s ... \infty \end{aligned} \tag{4.1}$$

where,

$w(k) \rightarrow k$-th window.

$l_w \rightarrow$ length of the window (W). The size of window in this work is always a multiple of 2.

$k \rightarrow$ index of the window, where $k = 2, ...\infty$.

$w_s \rightarrow$ samples by which the window is shifted, which is given as $w_s = l_w/2$.

$x[i] \rightarrow$ input sample to the nonlinear pre-filter.

$\bar{w}(k-1) \rightarrow$ mean of samples in window $w(k-1)$.

$\bar{w}(k) \rightarrow$ mean of samples in window $w(k)$.

$y[i] \rightarrow$ output of the nonlinear filtered signal.

It has been observed from the simulations that the nonlinear pre-filter has significantly mitigated the effect of the presence of nonlinear trends in the ambient data obtained from the PMU.

4.2.2 Wavelet based signal recovery technique

The pre-processed signal derived from the nonlinear pre-filter has very low SNR with very few modes present in it. A wavelet based recovery of the signal is then used to extract the signal lying in a very low dimensional space. A brief description of this technique is provided in this sub-section.

The basis of a wavelets [65] is defined as the families of functions $\psi_{a,b}(t)$ generated by scaling and translation of a single mother wavelet ψ as given below:

$$\psi_{a,b}(t) = \frac{1}{\sqrt{a}}\psi(\frac{t-b}{a}) \tag{4.2}$$

where a, b are the scaling and translation parameters. The function $x(t)$ can be represented as the linear combination of basis wavelet $\psi_{a,b}(t)$ as defined below:

$$x(t) = \sum_{a}\sum_{b} w_{a,b}\psi_{a,b}(t) \tag{4.3}$$

where, $w_{a,b}$ are the wavelet coefficients corresponding to the wavelet basis function. These wavelet coefficients $w_{a,b}$ of a signal $x(t)$ are given as:

$$w_{a,b} = \langle x(t), \psi_{a,b}(t) \rangle \tag{4.4}$$

The pre-processed signal are projected into the Beylkin wavelet basis vectors to get the wavelet coefficients corresponding to the ambient data using equation (4.4). From various simulation on ambient data, it has been observed that in wavelet transformed domain the energy of the signal is mostly concentrated in a few largest coefficients, while that of the noise is distributed throughout the coefficients. Hence, for selecting the most significant wavelet coefficients which mainly consist of dominant modes present in the signal, the present work has utilized VisuShrink [94] method of thresholding with slight modification. VisuShrink is an optimal thresholding technique with universal threshold T defined as $T = \sigma\sqrt{2ln(N)}$, where σ and N represents the standard deviation and the number of samples in the signal, respectively. In VisuShrink method, the threshold T is on the value of coefficients i.e., the significant coefficients are with absolute value greater than T , but a slightly modification is proposed to represent the corresponding number of coefficients as given in equation

below:

$$n_{TH} = (\sigma \sqrt{2ln(n)}) \times 0.683n \tag{4.5}$$

where, n_{TH} is the number of most significant wavelet coefficients which represents the dominant modes present in the signal, and n represents the effective number of wavelet coefficients with their absolute value greater than ϵ, where ϵ is positive real number with value close to zero.

As n_{TH}, may not be vary accurate, hence, estimated wavelet coefficients are arranged in decreasing order based on the absolute value of wavelet coefficients as given below.

$$w_1, w_2, ..., w_{n_{TH}}, w_{n_{TH+1}}, w_{n_{TH+2}}..., w_N \tag{4.6}$$

The energy in the remaining insignificant wavelet coefficients ($w_{n_{TH+1}}, w_{n_{TH+2}}..., w_N$) are calculated and is denoted as $E_1 = w^2_{n_{TH+1}} + w^2_{n_{TH+2}} + ... + w^2_N$ and also $E_2 = w^2_{n_{TH+2}} + w^2_{n_{TH+3}} + ... + w^2_N$. The value of n_{TH} is then incremented by one iteratively until $|E_2 - E_1| < \delta$. The updated value of n_{TH} is the number of significant wavelet coefficients used for the signal recovery.

4.2.3 Random decrement (RD) technique

After wavelet based de-noising of the measured ambient data, the next task is to get the impulse response. The random decrement (RD) technique developed by Cole was previously applied for space structures, aeroelastic systems [95], [96], large structures [97] and measuring dampings [98] of the soil.

Random decrement (RD) is a fast time-domain averaging technique utilized to estimate the correlation functions for the Gaussian process [99]. Estimation of random decrement signature or the impulse response is done by taking the sample wise average of the selected windows. The selection of window with a fixed number of samples is based on the sample value crossing a particular threshold. After selecting N number of window of length τ, random decrement signature or the impulse response is given as:

$$\delta(\tau) = \frac{1}{N} \sum_{r=1}^{N} y(t_r : t_r + \tau) \tag{4.7}$$

where N and τ are the number and length of the window, respectively. $\delta(\tau)$ is called the RD signature.

RD signature is proportional to the eigen or free response of the system perturbed with disturbance of Gaussian distribution [99]. These small perturbation of power system operating under ambient condition can be assumed to be uncorrelated and Gaussian. To have better estimate of modes by the RD signature, a proper selection of the threshold and the length τ is required. Details about the various techniques for choosing the threshold can be found in [100]. The proposed work has utilized a level crossing threshold defined as

$$T_{th} = c \tag{4.8}$$

where c is the threshold representing some fraction of the standard deviation σ of the signal. When the signal value become greater than or equal to c, a segment of length τ is collected and finally averaged to obtain the RD signature. The impulse response or RD signature thus obtained is then fed to the modified TLS-ESPRIT for mode estimation.

4.2.4 TLS-ESPRIT Estimation

The impulse response estimated by RD can be represented as a linear combination of exponentially damped sinusoidal signals with zero mean white Gaussian noise as referred in equation (4.9).

$$\begin{aligned} \delta(n) &= s(n) + w(n) \\ &= \sum_{j=1}^{M} \alpha_j e^{\beta_j n} + w(n) \end{aligned} \tag{4.9}$$

The low frequency modes present in the RD signature are estimated using modified TLS-ESPRIT [75]. A brief description of it has already been provided in Chapter 3, sub-section 3.2.2.

4.2.5 Identification of Power System Modes using the Proposed NwT-RD-TLS-ESPRIT Method

A Block diagram in Figure 4.1 illustrates the various steps for on-line identification of modes using the proposed method i.e., NwT-RD-TLS-ESPRIT. Low frequency oscillations are observed in ambient data as a result of random small mismatch between generation and demand. These small oscillations of power is measured from the phasor measurement units (PMU) which provides the data to the phasor data concentrator (PDC) connected through communication links.

To extract the modal information from the ambient data, the various steps of the NwT-RD-TLS-

ESPRIT, as shown in Figure 4.1, are described as follows:

Step 1: The proposed technique i.e., NwT-RD-TLS-ESPRIT at first uses a block of N samples of the active power obtained through the PDC.

Step 2: These samples are passed through the nonlinear filter. The nonlinear filter as described in Section 4.2.1 greatly helps in minimizing the nonlinear trends present in the ambient signals.

Step 3: It is observed that the filtered signal still has noise with high variance, hence, wavelet based signal de-noising technique is used as explained in Section 4.2.2.

Step 4: After de-noising of the measured ambient signal, the random decrement (RD) technique is applied to the reconstructed signal to get the RD signature as given in equation (4.7).

Step 5: The estimated RD signature corresponds to the impulse response which is given to the modified TLS-ESPRIT algorithm for mode estimation.

Step 6: The estimated modes which corresponds to a block of N most recent samples, are stored in the PDC.

Step 7: The entire process is repeated for the arrival of N new samples.

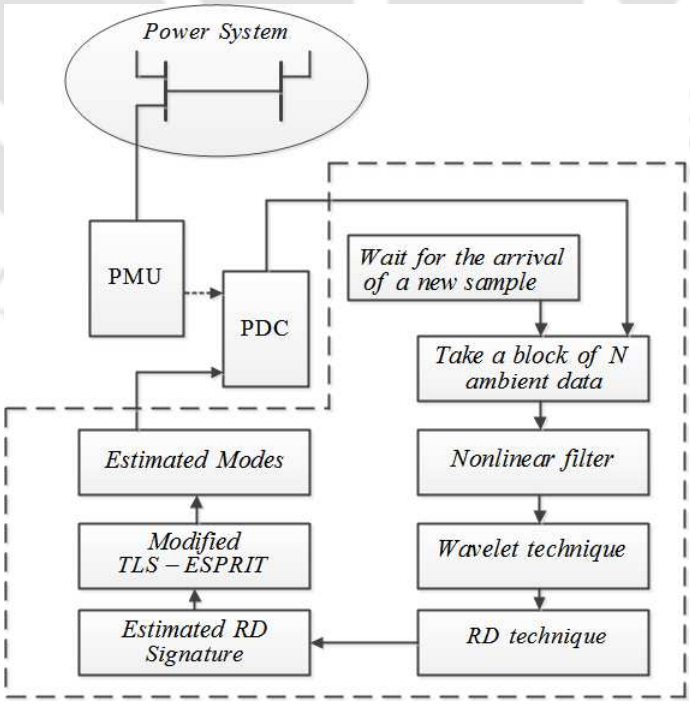

Figure 4.1: Block diagram of the proposed method i.e, NwT-RD-TLS-ESPRIT for mode estimation.

4.3 Simulation Results

For illustrating the effectiveness of the proposed method i.e., NwT-RD-TLS-ESPRIT, a comparison with nonlinear, NExT-ERA and RD-ITD methods are provided in the sub-section below for the test signals, simulated second order system corresponding to the modes present in a two-area system, two-area system simulated on RTDS facility at IIT Kanpur, and real time PMU data for Indian power systems and WECC. A performance identifier known as total vector error (TVE) [91] has been used for evaluating the accuracy of the proposed method.

$$\%TVE = \sqrt{\frac{(X_r^e - X_r^a)^2 + (X_i^e - X_i^a)^2}{(X_r^a)^2 + (X_i^a)^2}} \times 100 \tag{4.10}$$

where, X_r^e, X_i^e are the real and imaginary values of the estimated quantity and X_r^a, X_i^a are the real and imaginary values of the actual quantity respectively.

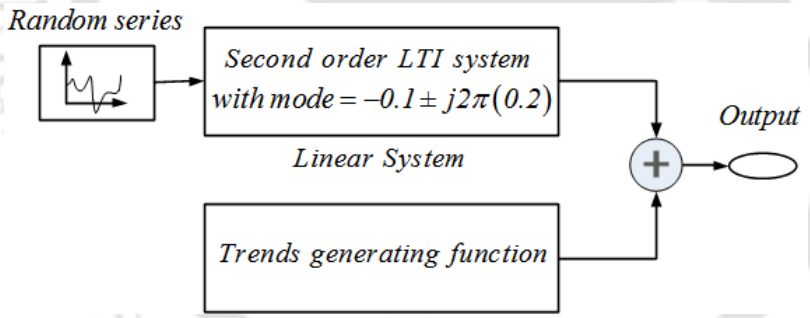

Figure 4.2: SIMULINK model used to generate ambient signal.

Table 4.1: Estimated Mode of Low-frequency oscillations for a test signal corresponding to ambient data

Attenuation factor=−0.1, freq=0.2 Hz			
Methods	Attenuation factor	Frequency	% TVE
Nonlinear	-0.1033	0.1982	0.9258
NExT-ERA	-0.1049	0.1970	1.5599
RD-ITD	-0.0870	0.2018	1.3554
Proposed Method (NwT-RD-TLS-ESPRIT)	-0.1049	0.2008	0.5718

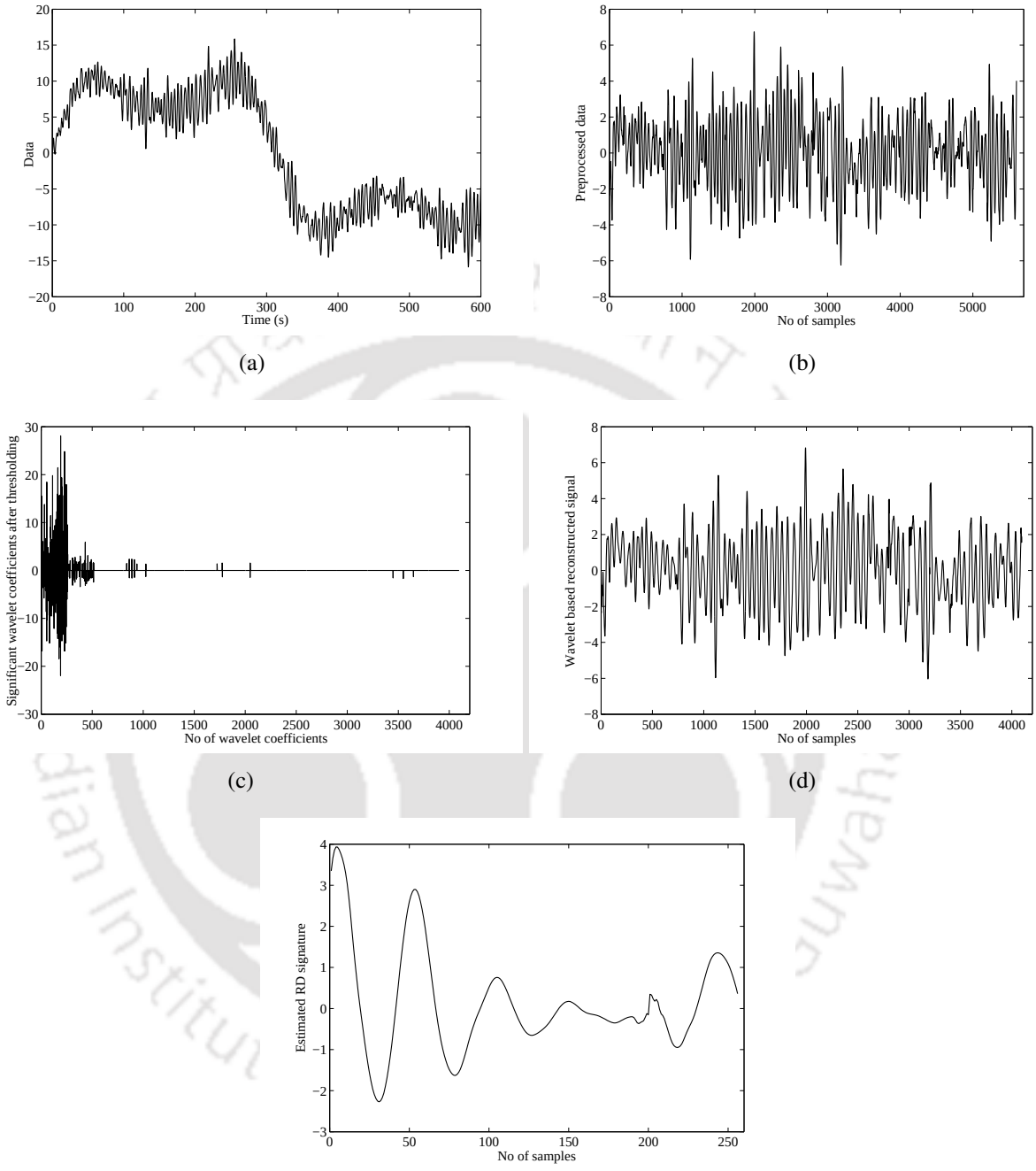

Figure 4.3: Plots for the generated test signal (a) Generated test signal resembling ambient data corrupted with nonlinear trends; (b) Signal obtained after nonlinear filtering; (c) Significant wavelet coefficients after thresholding; (d) Wavelet recovery signal; (e) Estimated RD signature.

4.3.1 Test signal corresponding to ambient data

A comparative analysis of the various methods with the proposed method i.e., NwT-RD-TLS-ESPRIT is done on the measurements resembling the system behavior under ambient conditions for

the test system. The data is generated for a time duration of 10 minutes with sampling frequency of 10 Hz. To generate the data which resembles ambient data along with nonlinear trends, a system with attenuation factor of (−0.1), frequency of (0.2 Hz) corresponding to a typical inter-area modes is excited with a random Gaussian noise as shown in 4.2. Further to simulate trends, a trend generating function is utilized. The output signal obtained from the simulink model corresponding to the ambient data is shown in Figure 4.3(a). This signal is then passed through the proposed nonlinear filter to obtain the pre-processed data, which is shown in Figure 4.3(b). The plot of the significant wavelet coefficients obtained after thresholding is shown in Figure 4.3(c). Figure 4.3(d) shows the signal reconstructed using the significant wavelet coefficients. The estimated impulse response of the ambient signal provided by the RD technique is shown in Figure 4.3(e). Table 4.1 shows the comparison of the proposed method with the nonlinear, NExT-ERA and RD-ITD methods for the test signal. It is seen that the proposed method provides a better estimate of the frequency (0.2008 Hz) with a total vector error (TVE) of 0.5718%, which is less as compared to the other methods.

4.3.2 Estimation of modes for the two-area system

In this section, two different approaches have been utilized to generate the test signal corresponding to the two-area ambient data. One is by exciting the models of the second order systems corresponding to the modes present in a two-area system and the other by using random variation of the load for a two-area system in real time digital simulator (RTDS). A comparative analysis of the various methods is provided in the subsequent sub-sections.

4.3.2.1 Mode estimation for the test signal corresponding to two-area data

The ambient signal is generated by using linear combination of 3 second order model with Mode 1 $= -0.25 \pm 7.5693\,j$, Mode 2 $= -0.25 \pm 3.3765\,j$, and Mode 3$= -0.25 \pm 7.5084\,j$, and a nonlinear trends generating functions, for 10 minutes duration with sampling frequency of 10 Hz. Figure 4.4 shows the block diagram of the model used to generate the two-area ambient data and the output signal obtained from the model is shown in Figure 4.5(a). The pre-processed data obtained after proposed nonlinear filtering is shown in Figure 4.5(b) and the significant wavelet coefficients obtained after thresholding is shown in Figure 4.5(c). Figure 4.5(d) and Figure 4.5(e) shows the reconstructed ambient signal and the estimated RD signature, respectively. Table 4.2 shows the comparison of the proposed method

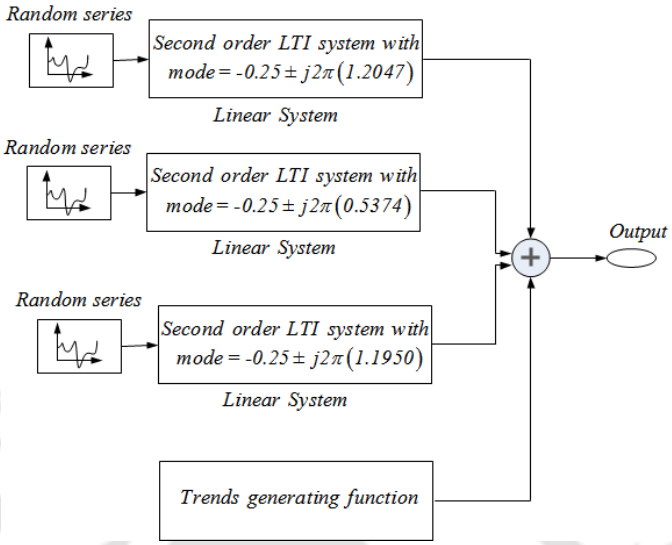

Figure 4.4: SIMULINK model used to generate two-area data.

Table 4.2: Estimated Mode of Low-frequency oscillations for generated two-area system

Attenuation factor=−0.25, freq=0.5374 Hz			
Methods	Attenuation factor	Frequency	% TVE
Nonlinear	-0.3188	0.5491	2.9724
NExT-ERA	-0.2063	0.5216	3.1961
RD-ITD	-0.3152	0.5192	3.8954
Proposed Method (NwT-RD-TLS-ESPRIT)	-0.2076	0.5272	2.2725

with the other methods. It is observed that the proposed method is able to identify the dominant mode more accurately with minimum TVE of 2.2725% as compared to the other methods.

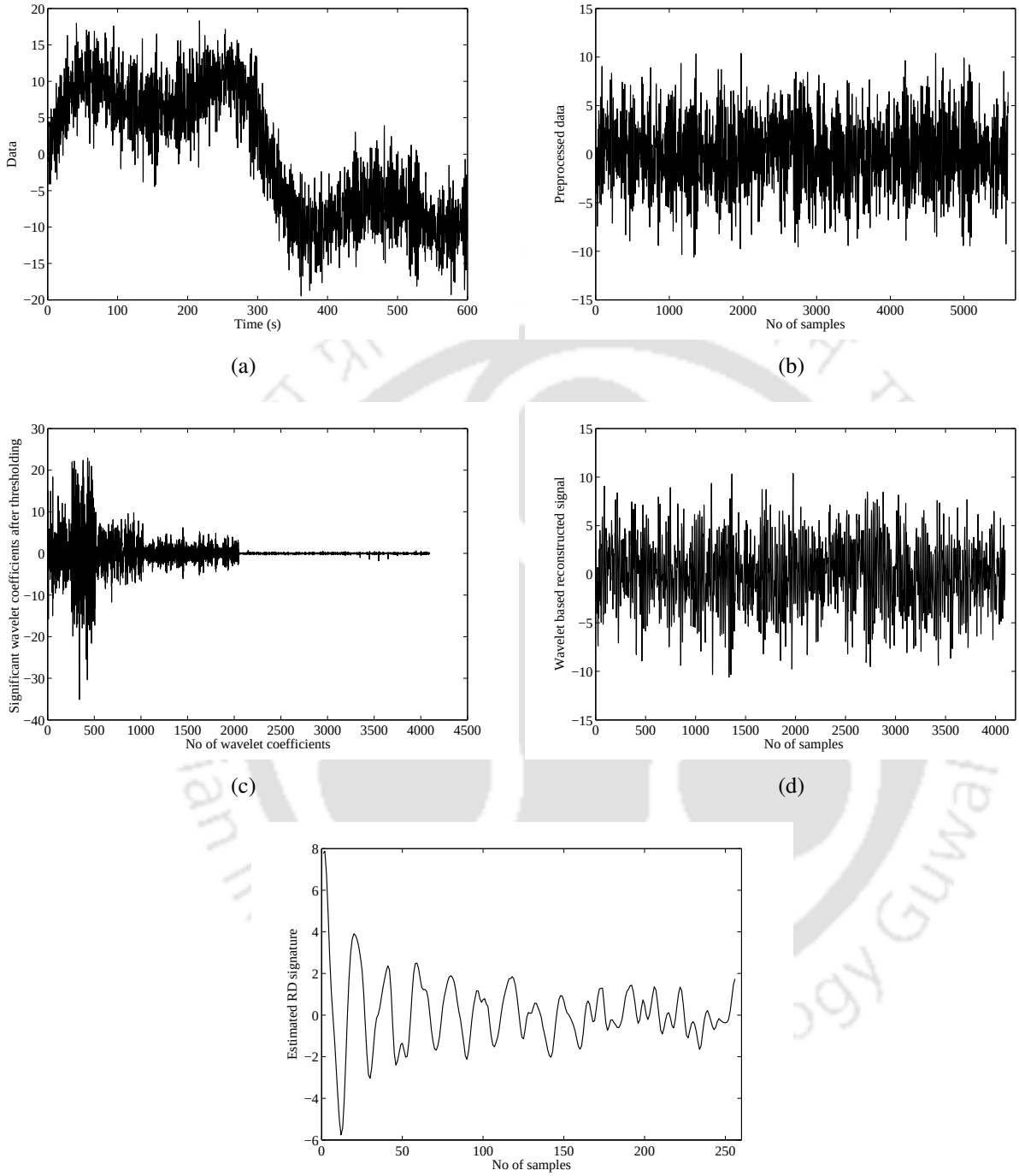

Figure 4.5: Plots for the generated two-area data (a) Generated test signal resembling two-area data corrupted with nonlinear trends; (b) Signal obtained after nonlinear filtering; (c) Significant wavelet coefficients after thresholding; (d) Wavelet recovery signal; (e) Estimated RD signature.

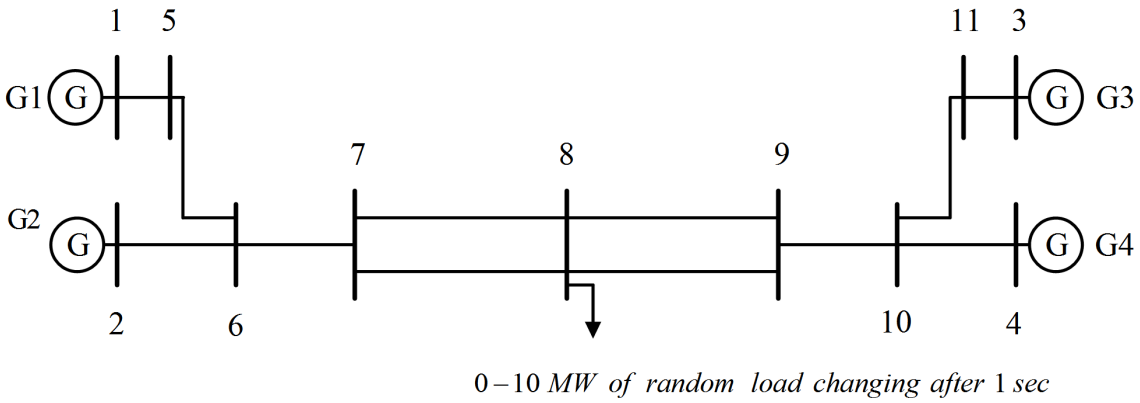

Figure 4.6: Two-area system for ambient data.

Table 4.3: Estimated Mode of Low-frequency oscillations with RTDS for two-area system

Attenuation factor=−0.25, freq=0.5374 Hz			
Methods	Attenuation factor	Frequency	% TVE
Nonlinear	-0.3410	0.2275	57.5793
NExT-ERA	-0.2888	0.5025	6.5703
RD-ITD	-0.3393	0.7821	45.4787
Proposed Method (NwT-RD-TLS-ESPRIT)	-0.2857	0.5673	5.6492

4.3.2.2 Mode estimation with RTDS data corresponding to two-area data simulated at the facility located at IIT Kanpur

Real time digital simulator (RTDS) is utilized to simulate real time signals corresponding to inter-area oscillations for a time duration of 20 minutes with sampling frequency of 50 Hz as shown in Figure 4.6. Figure 4.7(a) shows the RTDS data corresponding to low frequency oscillations of the active power flow. The low frequency oscillations takes place as a result of 0 − 10 MW of random load changing at bus 8 in an interval of 1 sec. Figure 4.7(b) and Figure 4.7(c) shows the pre-processed data and the dominant wavelet coefficients, respectively. The reconstructed signal and the estimated free response are depicted in Figure 4.7(d) and 4.7(e) respectively.

Table 4.3 shows that the proposed method provides a reasonably good estimate of the dominant oscillatory mode (i.e., attenuation factor= −0.2857, and frequency= 0.5673 Hz) and gives minimum TVE of 5.6492%, as compared to the other methods.

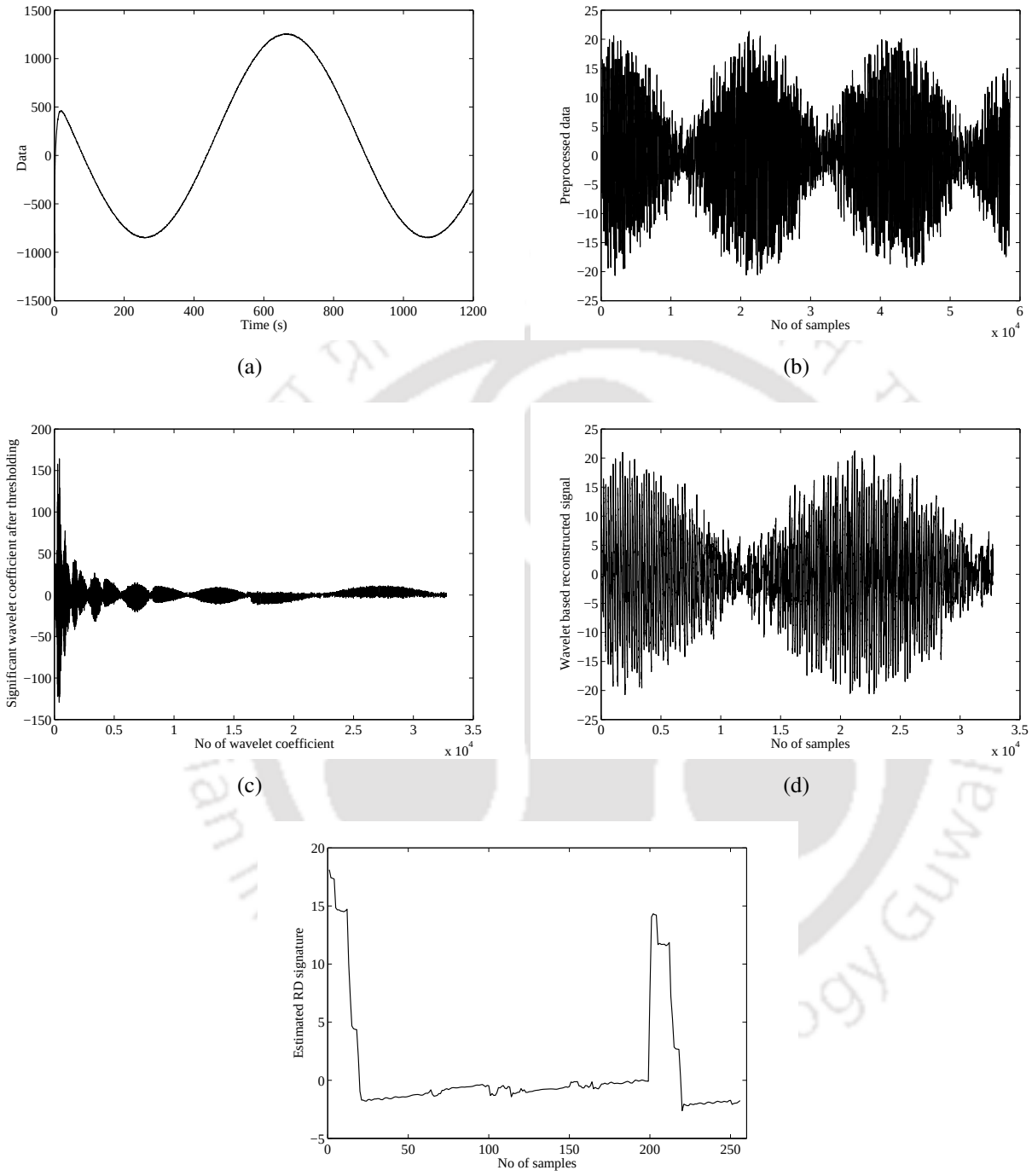

Figure 4.7: Plots for the RTDS data (a) RTDS data corresponding to active power flow of two-area system; (b) Signal obtained after nonlinear filtering; (c) Significant wavelet coefficients after thresholding; (d) Wavelet recovery signal; (e) Estimated RD signature.

4.3.3 Estimation of modes using the real PMU data from North Eastern Regional Electricity Board of Indian power grid

The effectiveness of the proposed method is further validated through real PMU measurements obtained from the North Eastern Regional Electricity Board. The data obtained from the PMU has a time duration of one hour and sampling frequency of 25 Hz. The data obtained from the PMU corresponds to the active power flow of the two lines connected to the same bus, which is shown in Figure 4.8(a) and 4.9(a), respectively. To calculate the TVE, the mean of the estimated modes for the two lines by the respective methods is considered as the true value of the estimated modes.

4.3.3.1 Mode estimation for power flow data in line one

The plot of the pre-processed data, prominent wavelet coefficients, reconstructed signal and the estimated free response for the data corresponding to line one are shown in Figure 4.8(b), 4.8(c), 4.8(d) and 4.8(e), respectively. Performance comparison of the proposed method with the nonlinear, NExT-ERA and RD-ITD method for power flow in line one corresponding to attenuation factor and frequency is shown in Table 4.4.

4.3.3.2 Mode estimation for power flow data in line two

The plot of the pre-processed data, prominent wavelet coefficients, reconstructed signal and the estimated free response for the data corresponding to line two are shown in Figure 4.9(b), 4.9(c), 4.9(d) and 4.9(e), respectively. Performance check of the proposed method with the nonlinear, NExT-ERA and RD-ITD method for power flow in line two is shown in Table 4.5.

As given in Tables 4.4 and 4.5, it is observed that the estimated modes by the proposed method are far better as compared with nonlinear and RD-ITD method and is comparable with the NExT-ERA method.

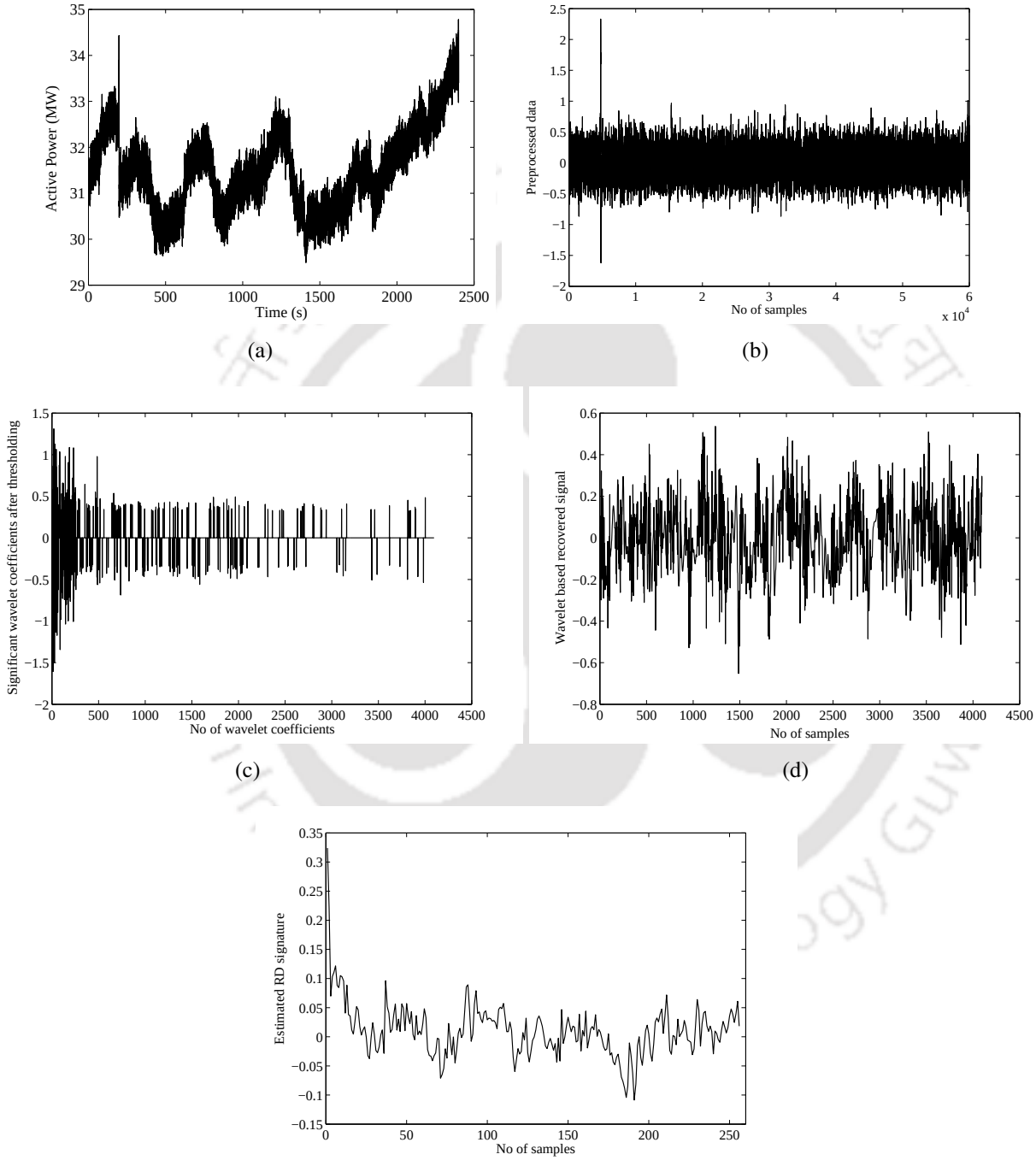

Figure 4.8: Plots for the Line 1 data (a) Active power flow of line one; (b) Signal obtained after nonlinear filtering; (c) Significant wavelet coefficients after thresholding; (d) Wavelet recovery signal; (e) Estimated RD signature.

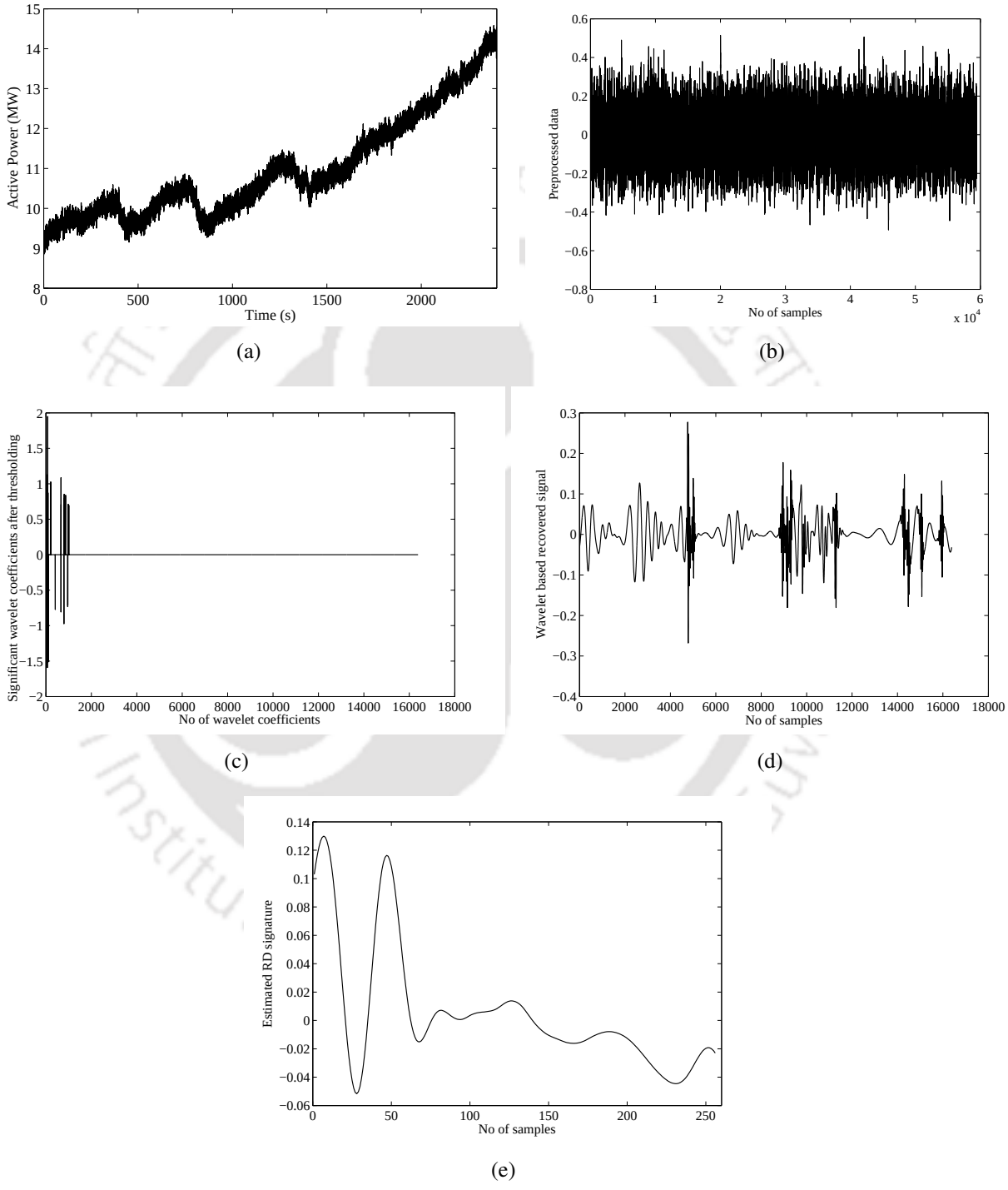

Figure 4.9: Plots for the Line 2 data (a) Active power flow of line two; (b) Signal obtained after nonlinear filtering; (c) Significant wavelet coefficients after thresholding; (d) Wavelet recovery signal; (e) Estimated RD signature.

Table 4.4: Mode estimation for line one power flow data

Methods	Attenuation factor	Frequency	% TVE
Nonlinear	-0.4672	0.2193	24.2883
NExT-ERA	-0.3938	0.2692	12.0351
RD-ITD	-0.4113	0.2250	19.3412
Proposed Method (NwT-RD-TLS-ESPRIT)	-0.4963	0.2716	12.2946

Table 4.5: Mode estimation for line two power flow data

Methods	Attenuation factor	Frequency	% TVE
Nonlinear	-1.2741	0.2570	24.2899
NExT-ERA	-0.8004	0.2526	12.0266
RD-ITD	-1.0342	0.2468	19.3407
Proposed Method (NwT-RD-TLS-ESPRIT)	-0.3266	0.2158	12.2800

4.3.4 Estimation of modes using the real test signal of the WECC system

A probing test signal of the WECC system, as shown in Figure 4.10 obtained on September 14, 2005 [78] is utilized to carry out the performance comparison of the proposed method with the other methods. The data used for the analysis purpose is provided at the B.P.A website [79]. The estimated modes for the ringdown data was reported in the literature as 0.318 Hz and 8.3 % damping [79].

Figure 4.11(a), 4.11(b), 4.11(c) and 4.11(d) shows the plot of the nonlinear filtered data, dominant wavelet coefficients, reconstructed signal and the estimated impulse response for the data corresponding to window 1 respectively. Similarly, the plots for the various steps of the proposed method applied to the data corresponding to the window 2 and window 3 are provided in Figure 4.12 and 4.13 respectively. Table 4.6 gives a comparison of the four methods for the real ambient data. For the analysis widow 1, the proposed method gives better mode estimate (0.2955 Hz at 8.0835 % damping) with a minimum TVE (7.087%) as compared to the other methods. The proposed method also gives better damping estimate (8.176% damping) in comparison with the other methods for analysis window 2.

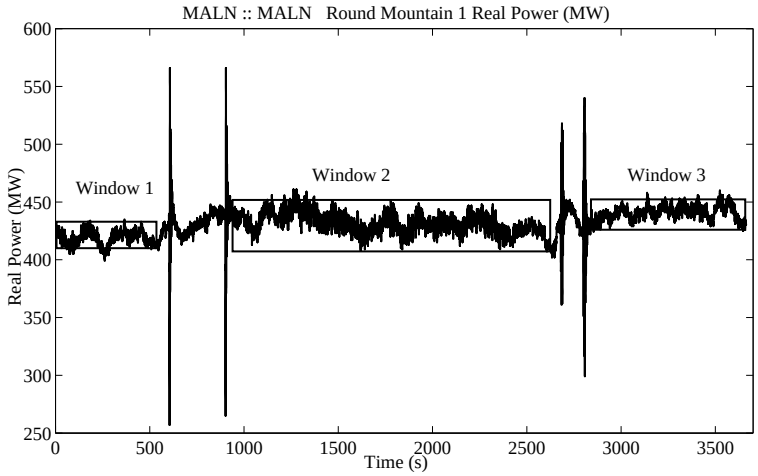

Figure 4.10: Probing data corresponding to real power flow.

The proposed method provides a more accurate frequency estimate (0.2982 Hz) as well as less TVE (6.2687%) in comparison with the other methods for analysis window 3. For analysis window 2, the TVE of the proposed method is comparable with the other methods.

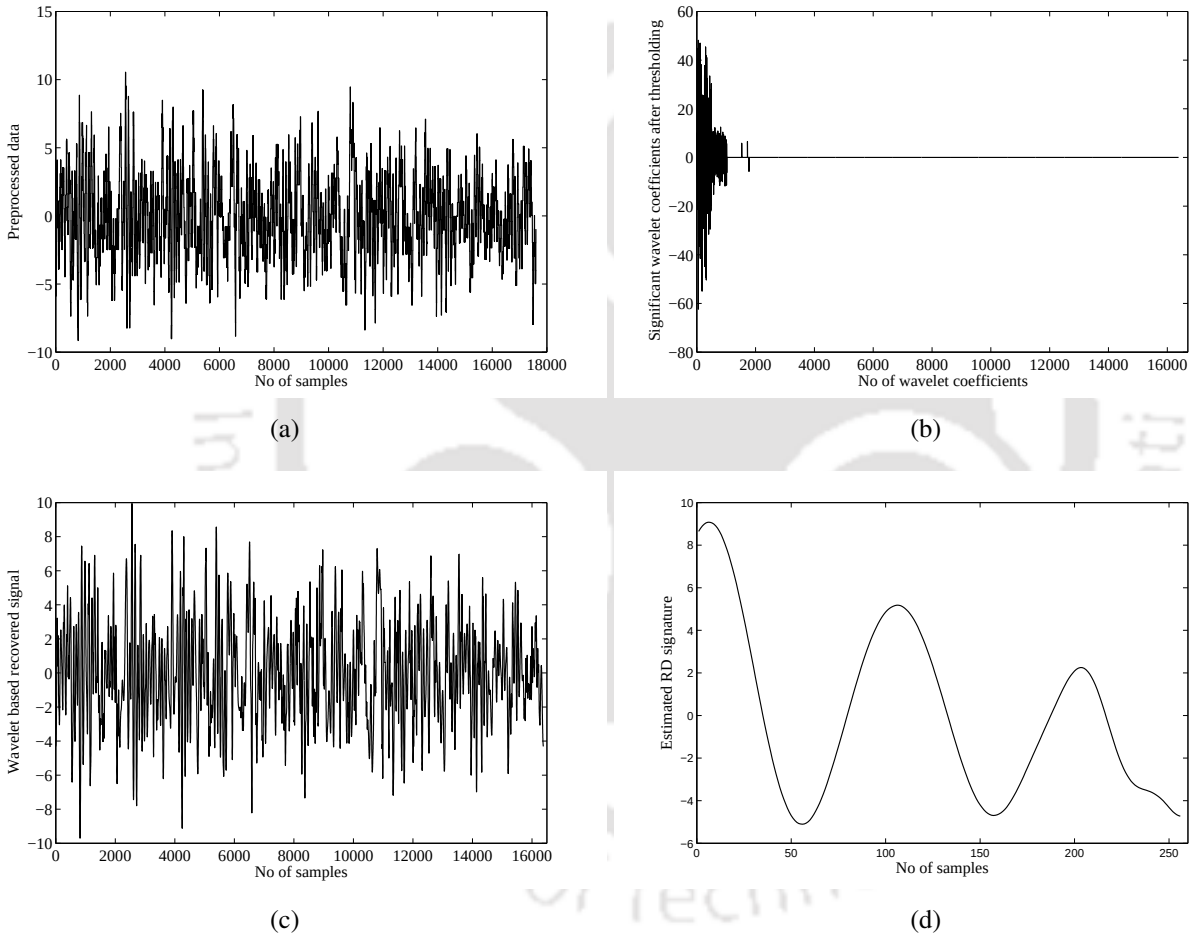

Figure 4.11: Plots for the window 1 data (a) Signal obtained after nonlinear filtering; (b) Significant wavelet coefficients after thresholding; (c) Wavelet recovery signal; (d) Estimated RD signature.

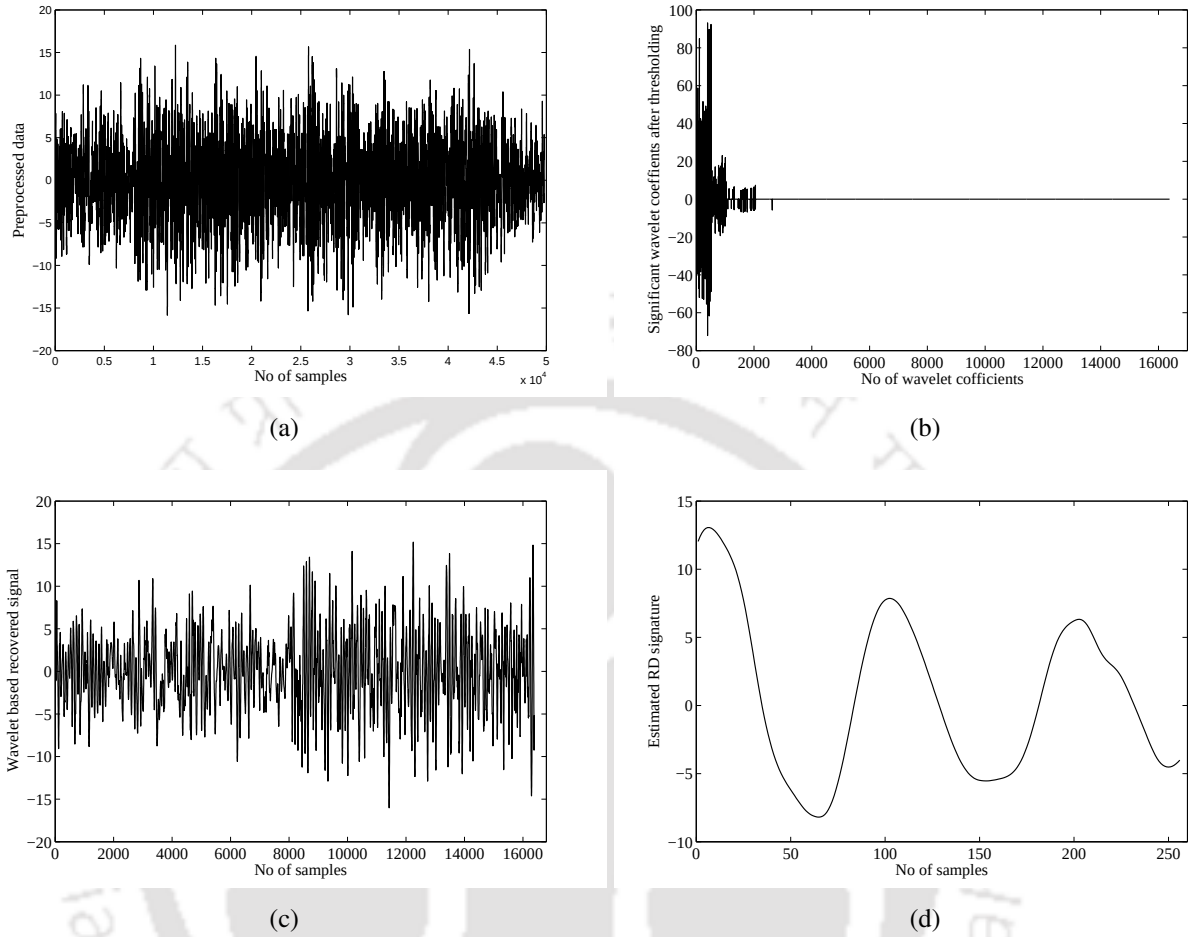

Figure 4.12: Plots for the window 2 data (a) Signal obtained after nonlinear filtering; (b) Significant wavelet coefficients after thresholding; (c) Wavelet recovery signal; (d) Estimated RD signature.

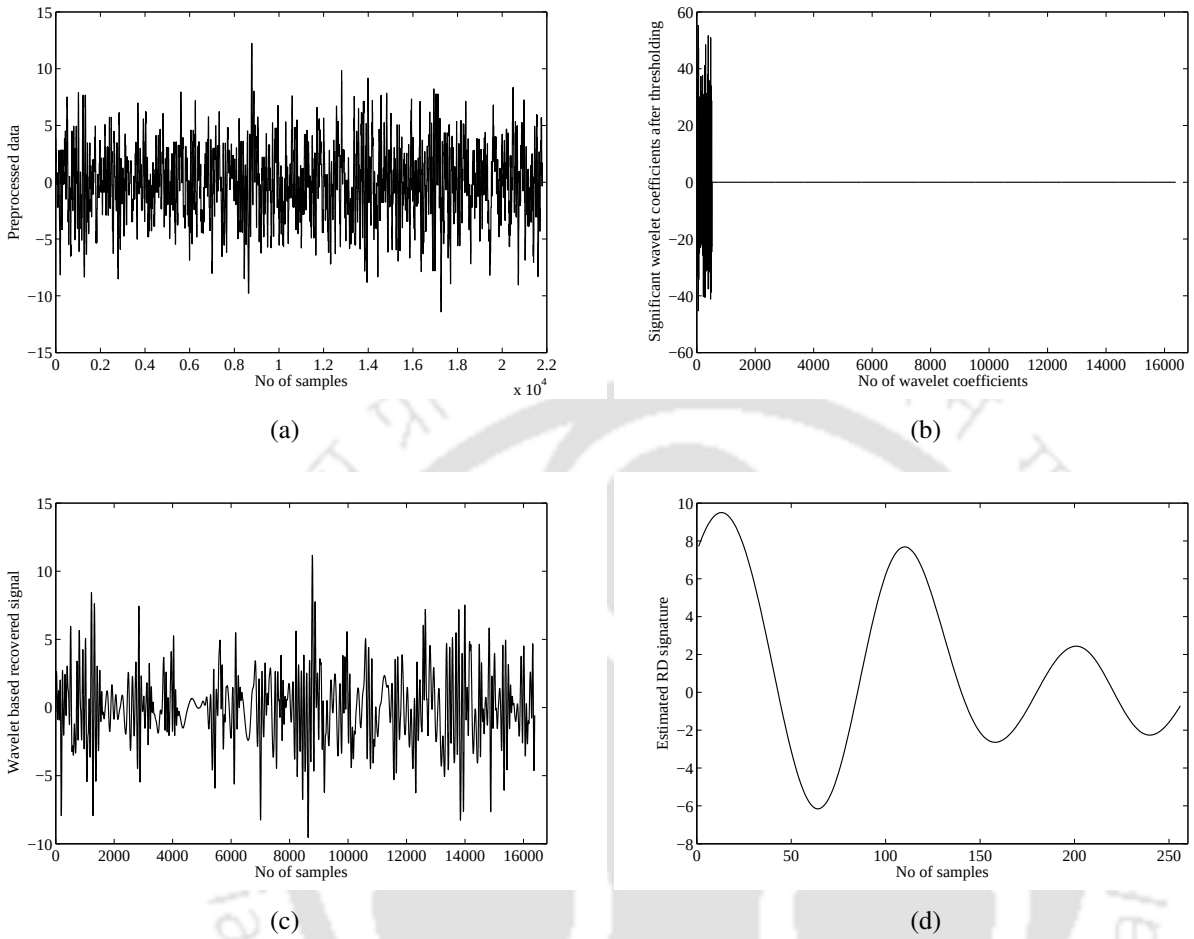

Figure 4.13: Plots for the window 3 data (a) Signal obtained after nonlinear filtering; (b) Significant wavelet coefficients after thresholding; (c) Wavelet recovery signal; (d) Estimated RD signature.

Table 4.6: Estimated Mode Analysis for WECC system

Estimated mode for Analysis window 1				
	Attenuation	Frequency	% Damping	% TVE
Nonlinear	-0.1394	0.2082	10.6004	34.4458
NExT-ERA	-0.2663	0.2483	16.8259	22.4014
RD-ITD	-0.1618	0.2871	8.9376	9.6991
Proposed Method (NwT-RD-TLS-ESPRIT)	-0.1506	0.2955	8.0835	7.0870
Estimated mode for Analysis window 2				
	Attenuation	Frequency	% Damping	% TVE
Nonlinear	-0.1704	0.3139	8.6056	1.2982
NExT-ERA	-0.1320	0.3193	6.5646	1.7639
RD-ITD	-0.1155	0.3286	5.5846	4.1717
Proposed Method (NwT-RD-TLS-ESPRIT)	-0.1604	0.3111	8.1760	2.1843
Estimated mode for Analysis window 3				
	Attenuation	Frequency	% Damping	% TVE
Nonlinear	-0.2607	0.2547	16.0807	20.3948
NExT-ERA	-0.2407	0.2928	12.9698	8.7112
RD-ITD	-0.1210	0.2736	7.0249	14.1090
Proposed Method (NwT-RD-TLS-ESPRIT)	-0.1849	0.2982	9.8222	6.2687

4.4 Conclusion

This chapter has proposed a mode estimation technique utilizing nonlinear filter, wavelet transform, random decrement and modified TLS-ESPRIT. The proposed method selects the best set of wavelet coefficients to represent the signal which makes it capable to withstand high noise and provides an unbias estimate of the modes present in a power system. To illustrate its effectiveness, the proposed method i.e., NwT-RD-TLS-ESPRIT is compared with nonlinear, NExT-ERA and RD-ITD methods on the test signals, simulated second order system corresponding to the modes present in

a two-area system, two-area system simulated on RTDS facility at IIT Kanpur. The robustness of the proposed method in identifying the oscillatory mode is also demonstrated on a real PMU data obtained from North Eastern Regional Electricity Board and probing data of the WECC system. The results provided in Section 4.3 shows the efficiency of the proposed method in withstanding high noise level and correctly identifying the oscillatory mode.

5

Estimation of Low-Frequency Modes from Ambient Data using Sparsity, RD and TLS-ESPRIT

5.1 Introduction

The use of wavelet along with random decrement and TLS-ESPRIT for low frequency critical mode identification, as proposed in Chapter 4, minimizes the nonlinear trends and extracts the signal from the noisy ambient data, and hence, performs better as compared to the nonlinear filtering, NExT-ERA and RD-ITD methods, as observed by the estimates of the attenuation factor, frequency and TVE of the estimator. However, the wavelet technique requires a proper thresholding criteria for the selection of the significant wavelet coefficients, which is to some extend utilize an heuristic approach, hence, there is a need to develop a more improved technique which can separate the signal from the noisy ambient data.

This chapter motivates towards the use of sparse technique, i.e, designing an efficient dictionary from a given input signal and thereby extracting sparse set of best coefficients to represent the signal, and hence, provides a fairly good estimate of low frequency modes in the presence of high noise in the measured data. The proposed method based on the sparse representation of signal along with RD

and TLS- ESPRIT i.e., S-RD-TLS-ESPRIT, consists of the following main steps to extract the modes corresponding to ambient data: At first, using a nonlinear filter to minimize the nonlinear trends, then by using sparse algorithm [101] [102] for de-noising followed by random decrement (RD) technique for obtaining the free response from the ambient data and lastly using these free decay responses as an input to the modified TLS-ESPRIT [75] for estimating the attenuation factor and frequency of the oscillatory modes.

The proposed method, i.e, S-RD-TLS-ESPRIT is compared with the NwT-RD-TLS-ESPRIT method, as proposed in Chapter 4, for simulated data corresponding to ambient data, followed by the estimation of the modes for a simulated dynamics of a two-area system [9]. Further, a comparative analysis of the proposed method with the NwT-RD-TLS-ESPRIT method is carried out for real measurement from PDC from the North Eastern Regional Electricity Board (NEREB) of India and real probing data of the Western Electricity Coordinating Council (WECC) system [79] [78].

This chapter motivates towards the application of sparse technique, i.e, to find a dictionary and the sparse coefficients that best represents the clean signal. Section 5.2 describes the theoretical background of the techniques utilized in the proposed method and also gives an outline of the proposed method for real time mode identification. The simulation results are provided in Section 5.3 followed by conclusion in Section 5.4.

5.2 Methods for modal parameter estimation

5.2.1 Nonlinear filter

It is required to pre-filter the nonlinear trends present in the ambient data obtained from the PMU. The mathematical equation corresponding to the pre-filter [93] for removing the nonlinear trends has been provided in Chapter 4, sub-section 4.2.1.

5.2.2 Sparse Technique for recovery of signal

The signal after getting pre-processed from the pre-filter has very low SNR with very few modes present in the signal. Hence, to extract the signal which lies in a very low dimensional space as compared to the dimension in which the ambient signal lies, the authors proposes to use sparse based recovery of the signal. A brief introduction to sparse based recovery is provided in this sub-section.

Sparse representation [101] [102] of vector **x** can be expressed as a linear combination of some of

the columns of the matrix **D**.

$$\mathbf{x} = \mathbf{D}\boldsymbol{\gamma} \tag{5.1}$$

satisfying

$$min \parallel \mathbf{x} - \mathbf{D}\boldsymbol{\gamma} \parallel_2 \tag{5.2}$$

such that $\parallel \boldsymbol{\gamma} \parallel_1 \leq B$, where **D** is the dictionary where each columns of the dictionary is called the atom. The vector $\boldsymbol{\gamma}$ is called as sparse vector in which some elements are non-zero and others are zero. B is the number of non-zero elements in the sparse vector $\boldsymbol{\gamma}$ which is also referred as the sparsity of the vector $\boldsymbol{\gamma}$. Dictionary **D** is created by exploiting the estimated structure of the signal using the measured data. The core idea of the sparse technique is to select the best possible combination of columns from the dictionary to represent the input signal. The main steps involved in the proposed method i.e., S-RD-TLS-ESPRIT are : (a) Creation of Dictionary (b) Determination of sparse vector (c) Signal reconstruction which are explained in the sub-section below.

5.2.2.1 Creation of Dictionary (D)

The core idea behind the construction of the dictionary is to represent the signal with minimum set of atoms or the column of the dictionary is to learn the dictionary to perform best on the signal.

Data matrix **X** i.e., $\mathbf{X} = [\mathbf{x_0}\ \mathbf{x_1}\ ...\mathbf{x_{n-1}}]$ is created from the pre-filtered data using the non-overlapping windows of samples creating a column vector $\mathbf{x_i}$ of length l for the data matrix **X**. The total number of samples utilized for mode estimation are, hence, given as $l \times n$. To get a low rank approximation of the data matrix, singular vector decomposition (SVD) along with the method proposed in [35] to get model order has been utilized. To get the model order, a index as proposed in [35] is defined in the equation below:

$$K(i) = \left[\frac{\rho_1^2 + \rho_2^2 + \cdots + \rho_i^2}{\rho_1^2 + \rho_2^2 + \cdots + \rho_D^2}\right]^{\frac{1}{2}} \tag{5.3}$$

where $K(i)$ is an index which increases monotonously and ρ_i is the i-th singular value. As i tends to the real signal order, $K(i)$ also tends to unity. The present work has utilized this index to calculate

the signal order. After determination of the approximated low rank data matrix, SVD is applied on it. The left singular vectors of the low rank data matrix forms the dictionary for the proposed method.

5.2.2.2 Determination of sparse vector

Sparse vector $\boldsymbol{\gamma}_i$ with respect to the dictionary $\mathbf{D}$ is determined for each column vector $\mathbf{x_i}$ corresponding to the data matrix $\mathbf{X} = [\mathbf{x_0}\ \mathbf{x_1}\ ...\mathbf{x_{n-1}}]$ using batch omp [103–105]. Orthogonal matching pursuit (OMP) selects the atoms having the highest correlation to the current residual iteratively from the dictionary. But it uses the current approximate an orthogonal projection onto the subspace spanned by the selected atoms so far. Batch OMP performs faster than OMP as it involves computation of the projection of the residual onto the dictionary and not the residual itself.

Terms used in the algorithm are given below:

$n \rightarrow$ no of iteration

$I^n \rightarrow$ indices of the atom selected

$\boldsymbol{\gamma}^n \rightarrow$ sparse representation of $\mathbf{x}$

$\mathbf{r}^n \rightarrow$ residue $(\mathbf{x} - \mathbf{D}\boldsymbol{\gamma}^n)$

$\boldsymbol{\zeta}^n \rightarrow$ product of $\mathbf{D}^T\mathbf{r}^n$

$\mathbf{G} \rightarrow \mathbf{D}^T\mathbf{D}$

$\boldsymbol{\Upsilon}^n \rightarrow$ product of $\mathbf{G}\boldsymbol{\gamma}^n$

$\mathbf{L}^n \rightarrow$ Cholesky factorization of $\mathbf{G}_{I^n,I^n}$

$\mathbf{c}^n \rightarrow$ non zero coefficients of $\boldsymbol{\gamma}^n$, numbered by I^n

The computation steps are as follows [105],

1. Input: $\boldsymbol{\zeta}^0 = \mathbf{D}^T\mathbf{x}$, $\mathbf{G}$ and target sparsity $=B$
2. Output: The sparse vector $\boldsymbol{\gamma}$
3. Initialization: Set $I := ()$, $\mathbf{L}^1 := [1]$, $n := 1$
4. while $n \leqslant B$ do
5. $\hat{k} := \underset{k}{argmax}\left\{\left|\zeta_k^{n-1}\right|\right\}$
6. $\mathbf{g} := \mathbf{G}_{I^n,\hat{k}}$
7. if $n > 1$ then
8. $\mathbf{w}$:=Solve for $\mathbf{w}\left\{\mathbf{L}^{n-1}\mathbf{w} = \mathbf{g}_{I_n}\right\}$

9.

$$\mathbf{L}^n := \begin{bmatrix} \mathbf{L}^{n-1} & 0 \\ \mathbf{w}^T & \sqrt{1 - \mathbf{w}^T\mathbf{w}} \end{bmatrix}$$

10. end if

11. $I^n := (I^{n-1}, \hat{k})$

12. $\mathbf{c}^n$:=Solve for $\mathbf{c}\left\{\mathbf{L}^n(\mathbf{L}^n)^T\mathbf{c} = \zeta^0_{I^n}\right\}$

13. $\Upsilon^n = \mathbf{G}_{I^n}\mathbf{c}^n$

14. $\zeta^n := \zeta^0 - \Upsilon^n$

15. $n = n + 1$

16. end while

17. $\boldsymbol{\gamma} := 0$

18. $\boldsymbol{\gamma}_{I^n} := \mathbf{c}^n$

Each sparse vector $\boldsymbol{\gamma_i}$ corresponding to each of the column vector $\mathbf{x_i}$ of the data matrix $\mathbf{X} = [\mathbf{x_0}\ \mathbf{x_1}\ ...\mathbf{x_{n-1}}]$ obtained through batch omp, are arranged column wise to get the resultant sparse matrix $\mathbf{\Phi} = [\gamma_0\ \gamma_1 ...\ \gamma_{n-1}]$.

5.2.2.3 Signal reconstruction

The dictionary **D** is multiplied with the estimated sparse matrix **Φ** to get the reconstructed signal matrix $\mathbf{Y_{reconstruct}}$. The resultant signal vector **y** is obtained by appending all the columns of the reconstructed signal matrix $\mathbf{Y_{reconstruct}}$.

5.2.3 Random decrement (RD) technique

After extracting the signal from the noisy ambient data, the next step is to get the impulse response of the system from the reconstructed signal obtained by the sparse recovery technique. Here, the RD technique is utilized to get the impulse response of the system and is described in detail in Chapter 4, sub-section 4.2.3. The equation corresponding to RD signature is

$$\delta(\tau) = \frac{1}{N}\sum_{r=1}^{N} y(t_r : t_r + \tau) \tag{5.4}$$

A level crossing threshold $T_{th} = c$, representing a fraction of the standard deviation σ of the signal has been used.

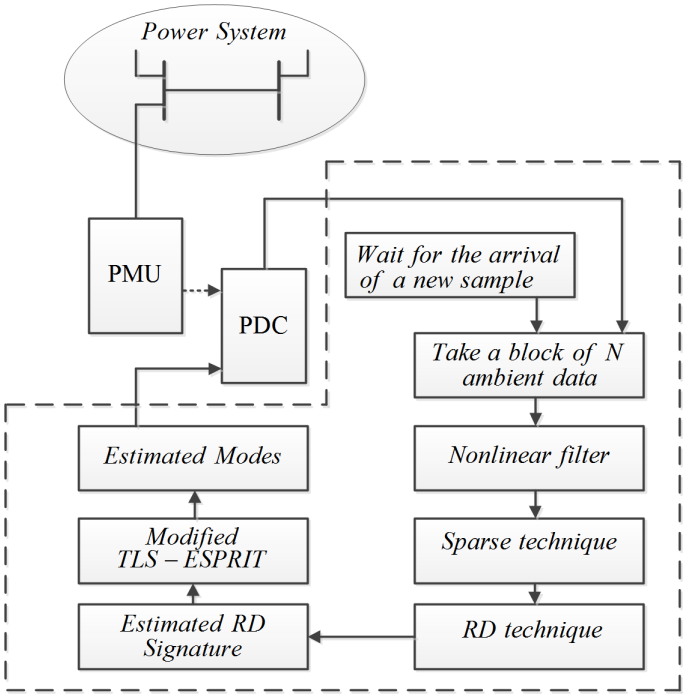

Figure 5.1: Block diagram of the proposed method i.e, S-RD-TLS-ESPRIT for mode estimation.

5.2.4 TLS-ESPRIT Estimation

The impulse response obtained through RD, is expressed as a linear combination of exponentially damped sinusoids with white Gaussian noise of zero mean, as given in equation (5.5).

$$\begin{aligned}\delta(n) &= s(n) + w(n) \\ &= \sum_{j=1}^{M} \alpha_j e^{\beta_j n} + w(n)\end{aligned} \tag{5.5}$$

Modified TLS-ESPRIT [75] method has been used to estimate the attenuation factor and frequency and a brief description of this method has been presented in Chapter 3, sub-section 3.2.2.

5.2.5 Identification of Power System Modes using the Proposed S-RD-TLS-ESPRIT Method

A Block diagram in Figure. 5.1 depicts the various steps for on-line mode identification of power system utilizing the proposed method. Small and sudden mismatch between generated power and load demand results into the excitation of low frequency modes which are measured from the phasor measurement units (PMU). These measured data corresponding to the power swing are send to the

phasor data concentrator (PDC) through the communication links. To extract the modal information from the ambient data, a method is proposed as shown in Figure. 5.1. The steps for mode estimation utilizing the proposed method are described briefly as follows:

Step 1: The proposed technique at first uses a block of N samples of the active power obtained through the PDC.

Step 2: These samples are passed through the nonlinear filter. The nonlinear filter as explained in Section 4.2.1 is found to be very effective in filtering the nonlinear trends, and hence resulting into a signal which is weakly stationary.

Step 3: The filtered signal still has noise with high variance, hence, sparse based technique is used to de-noise the signal as explained in Section 5.2.2.

Step 4: After de-noising of the measured ambient signal, the random decrement (RD) technique is applied to the reconstructed sparse signal to obtain RD signature as given in equation (5.4).

Step 5: The estimated RD signature corresponds to the impulse response and hence, it can be fed as an input to the modified TLS-ESPRIT method for estimating the frequency and attenuation factor.

Step 6: The estimated modes thus obtained corresponds to a block of N most recent samples and are stored in the PDC.

Step 7: The whole procedure is repeated for the arrival of N new samples.

5.3 Simulation Results

For illustrating the effectiveness of the proposed method, a comparison with NwT-RD-TLS-ESPRIT method is provided in the sub-section below for the test signals, two-area system, and real time PMU data for WECC and Indian Power Systems. The accuracy of the proposed method in estimating the modes, has been evaluated by a performance identifier known as total vector error (TVE) [91].

$$\%TVE = \sqrt{\frac{(X_r^e - X_r^a)^2 + (X_i^e - X_i^a)^2}{(X_r^a)^2 + (X_i^a)^2}} \times 100 \tag{5.6}$$

where, X_r^e, X_i^e are the real and imaginary values of the estimated quantity and X_r^a, X_i^a are the real and imaginary values of the actual quantity respectively.

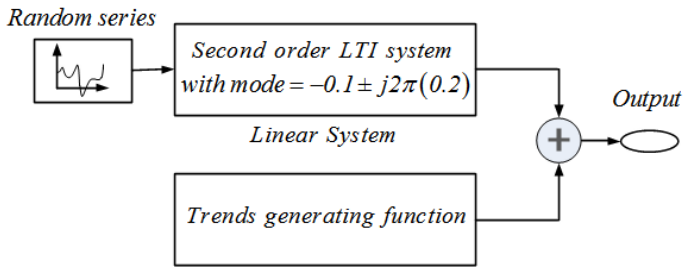

Figure 5.2: SIMULINK model used to generate ambient signal.

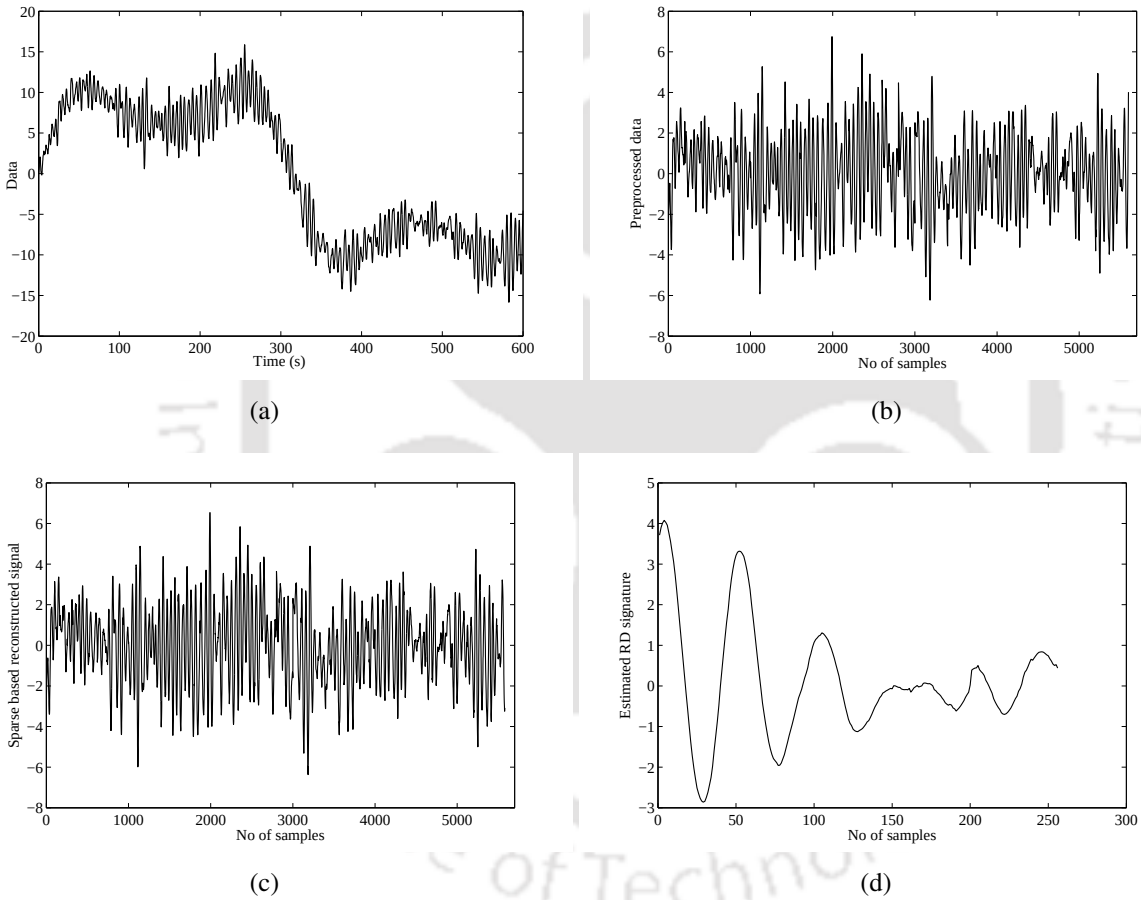

Figure 5.3: Plots for the generated test signal (a) Generated test signal resembling ambient data corrupted with nonlinear trends; (b) Signal obtained after nonlinear filtering; (c) Sparse recovery signal; (d) Estimated RD signature.

5.3.1 Test signal corresponding to ambient data

To generate the test signal corresponding to the ambient data, a second order system with an attenuation factor of −0.1, and frequency of 0.2 Hz as shown in Figure 5.2 is excited by Gaussian noise and corrupted with nonlinear trends. Finally, to get the test signal corresponding to the ambient data, the output response of the system shown in Figure 5.3(a), is sampled with a sampling frequency

Table 5.1: Estimated Mode of Low-frequency oscillations for a test signal corresponding to ambient data

Attenuation factor=−0.1, freq=0.2 Hz			
Methods	Attenuation factor	Frequency	% TVE
NwT-RD-TLS-ESPRIT	-0.1049	0.2008	0.5718
Proposed Method (S-RD-TLS-ESPRIT)	-0.0990	0.1992	0.4025

of 10 Hz. The pre-processed signal obtained after the use of a nonlinear filter is shown in Figure 5.3(b). Figure 5.3(c) and 5.3(d) shows the signal reconstructed using the sparse coefficients and the estimated impulse response of the ambient signal provided by the RD technique respectively. Table 5.1 shows the comparison of the proposed method, i.e., S-RD-TLS-ESPRIT with the NwT-RD-TLS-ESPRIT method for the test signal. It is observed that the proposed method provides more accurate estimation of modes (i.e., attenuation factor= −0.0990 and frequency= 0.1992 Hz) with a total vector error (TVE) of 0.4025%, which is less as compared to the other method.

5.3.2 Estimation of modes for the two-area system

To generate the test signal corresponding to the two-area ambient data, the authors have utilized two approach. One by exciting the models of the second order systems corresponding to the modes present in a two-area system and the other using random variation of load for a two-area system in real time digital simulator (RTDS).

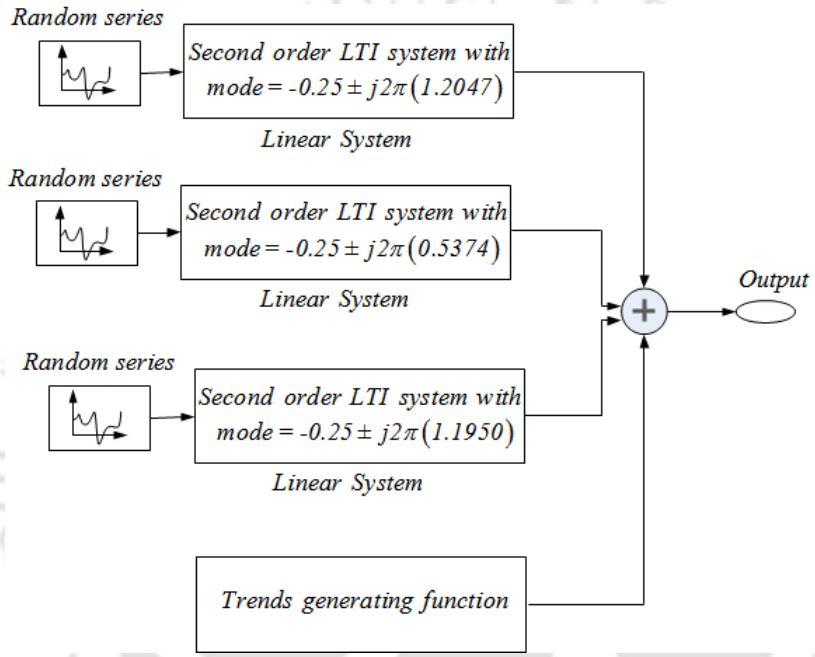

Figure 5.4: SIMULINK model used to generate two-area data.

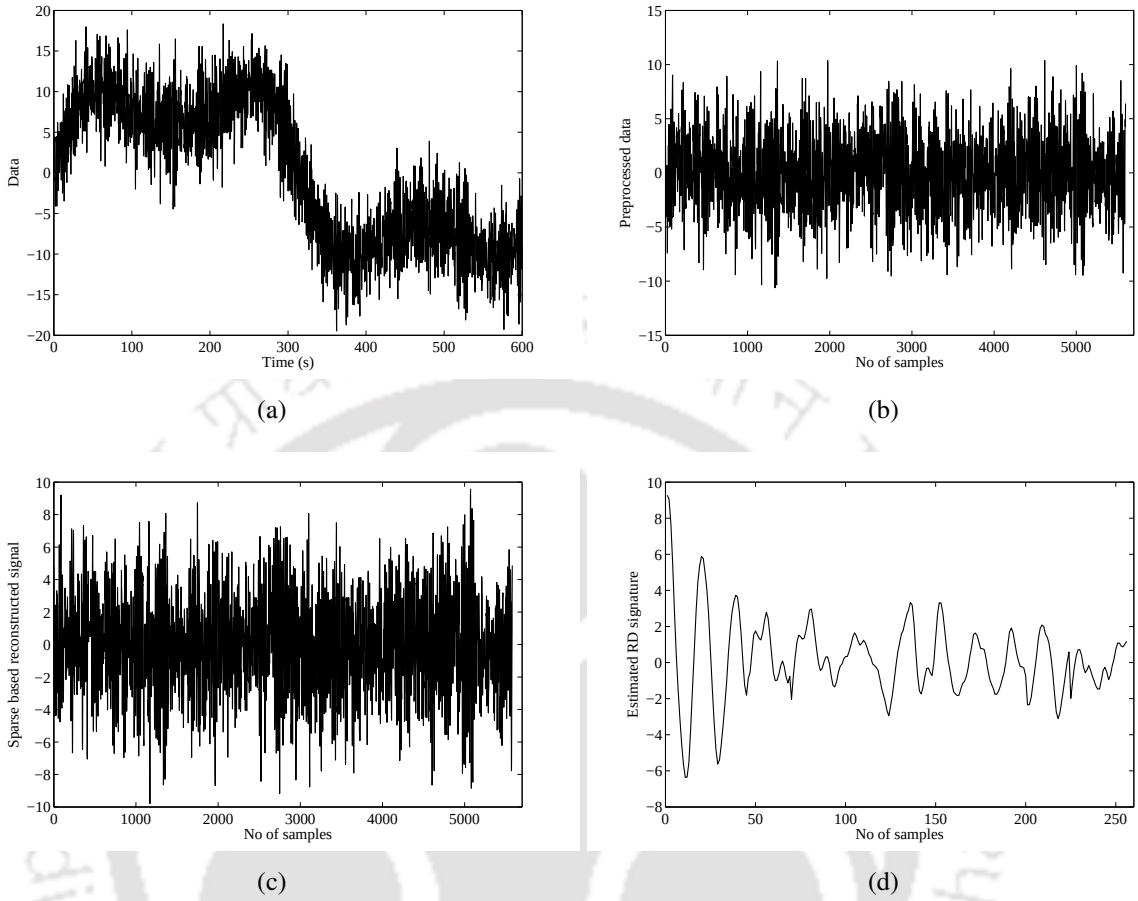

Figure 5.5: Plots for the generated two-area data (a) Generated test signal resembling two-area data corrupted with nonlinear trends; (b) Signal obtained after nonlinear filtering; (c) Sparse recovery signal; (d) Estimated RD signature.

Table 5.2: Estimated Mode of Low-frequency oscillations for generated two-area system

Attenuation factor=−0.25, freq=0.5374 Hz			
Methods	Attenuation factor	Frequency	% TVE
NwT-RD-TLS-ESPRIT	-0.2076	0.5272	2.2725
Proposed Method (S-RD-TLS-ESPRIT)	-0.2093	0.5283	2.0760

5.3.2.1 Mode estimation for the test signal corresponding to two-area data

The ambient signal for a two-area power system is generated using linear combination of 3 second order model with Mode 1 = $-0.25\pm7.5693\,j$, Mode 2 = $-0.25\pm3.3765\,j$, and Mode 3= $-0.25\pm7.5084\,j$ and nonlinearity generating functions as shown in Figure 5.4. The output response of the system as

plotted in Figure 5.5(a) is sampled with a frequency of 10 Hz over a duration of 10 minutes, after which the signal is passed through the nonlinear filter to obtain the filtered data as shown in Figure 5.5(b). Figure 5.5(c) and Figure 5.5(d) shows the reconstructed ambient signal and the estimated RD signature respectively. This data is used to show a comparison of the proposed method with the other method. Table 5.2 shows the estimated dominant mode for the two-area system by the two methods. It is observed that the proposed method is able to estimate the dominant mode more accurately (i.e., attenuation factor= -0.2093, and frequency= 0.5283 Hz) with less total vector error (TVE) of 2.076%.

5.3.2.2 Mode estimation with RTDS corresponding to two-area data

Real time digital simulator (RTDS) is used to generate real time signals corresponding to inter-area oscillations. The data is generated for a time duration of 20 min with sampling frequency of 50 Hz as shown in Fig. 5.6. Figure 5.7(a) shows the RTDS data corresponding to low frequency oscillations of the active power flow. The low frequency oscillations have occurred due to $0-10$ MW of random load changing at bus 8 in the interval of 1 sec. Figure 5.7(b), 5.7(c) and 5.7(d) shows the plot of the nonlinear filtered data, reconstructed signal and the estimated impulse response for the RTDS data respectively. It is seen from Table 5.3 that the proposed method provides a reasonably good estimate of the attenuation factor (-0.2524) with a TVE of 5.6416%, which is less as compared to the NwT-RD-TLS-ESPRIT method.

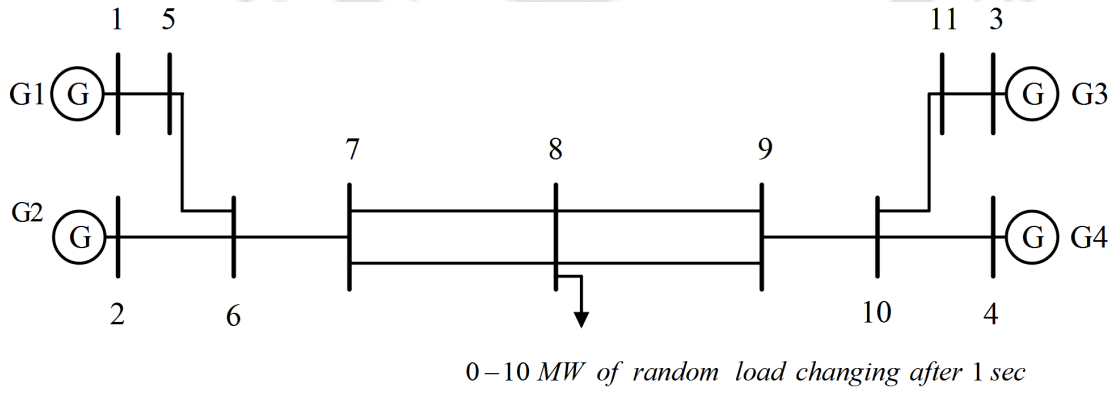

Figure 5.6: Two-area system for ambient data.

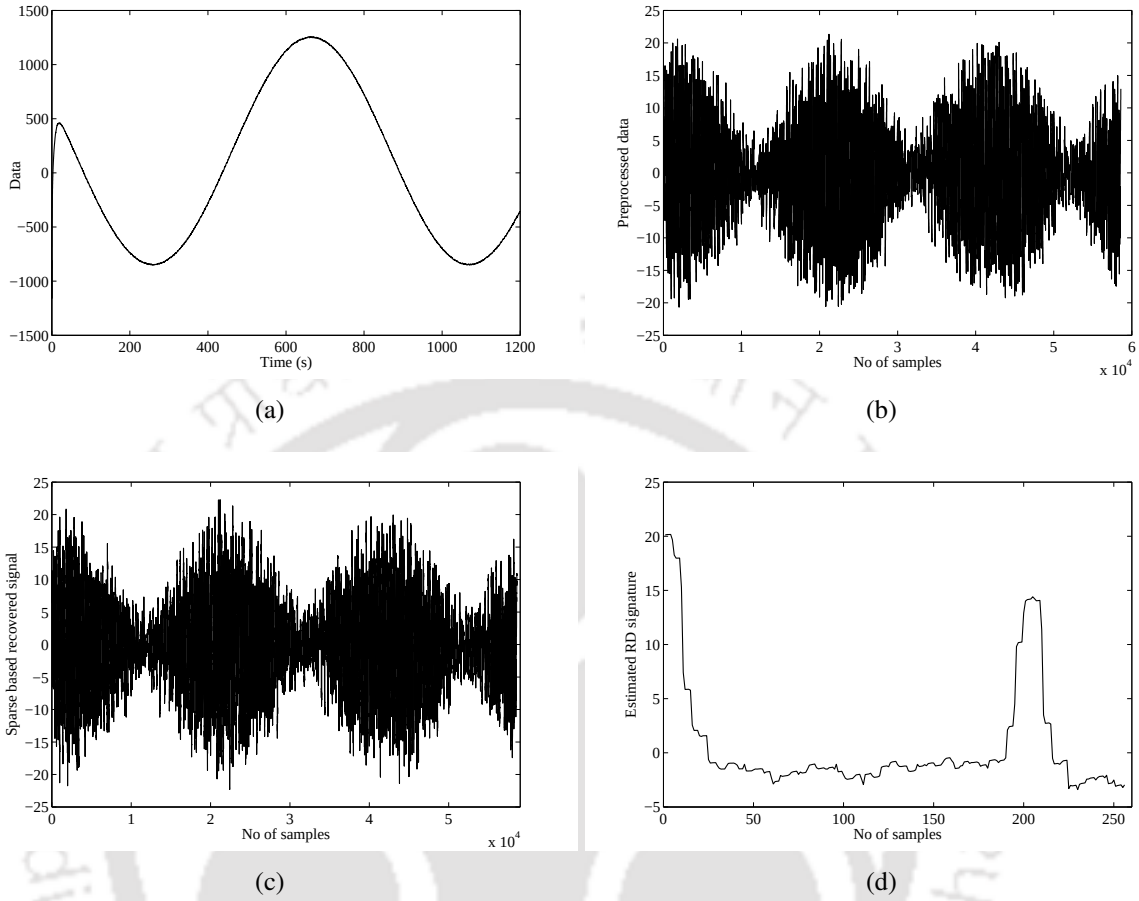

Figure 5.7: Plots for the RTDS data (a) RTDS data corresponding to active power flow of two-area system; (b) Signal obtained after nonlinear filtering; (c) Sparse recovery signal; (d) Estimated RD signature.

Table 5.3: Estimated Mode of Low-frequency oscillations with RTDS for two-area system

Attenuation factor=−0.25, freq=0.5374 Hz			
Methods	Attenuation factor	Frequency	% TVE
NwT-RD-TLS-ESPRIT	-0.2857	0.5673	5.6492
Proposed Method (S-RD-TLS-ESPRIT)	-0.2524	0.5070	5.6416

5.3.3 Estimation of modes using the real PMU data from North Eastern Regional Electricity Board of Indian power grid

To further validate the effectiveness of the proposed method, PMU data with phasor reporting rate of 25 frames/second from the North Eastern Regional Electricity Board is used for mode estimation. The data measured from the PMU corresponds to the active power flow of the two lines incident on the same bus is provided in Figure 5.8(a) and Figure 5.9(a), respectively. Here for calculating the TVE, we have assumed true value of the estimated modes as the average of the estimated modes for the two lines by the respective methods.

5.3.3.1 Mode estimation for power flow data in line one

The plot of the pre-processed data, reconstructed signal and the estimated free response for the data corresponding to line one are shown in Figure 5.8(b), 5.8(c) and 5.8(d) respectively. Performance comparison of the proposed method with the NwT-RD-TLS-ESPRIT method for power flow in line one corresponding to attenuation factor and frequency are shown in Table 5.4.

5.3.3.2 Mode estimation for power flow data in line two

The plot of the pre-processed data, reconstructed signal and the estimated free response for the data corresponding to line two are shown in Figure 5.9(b), 5.9(c) and 5.9(d) respectively. Performance check of the proposed method with the NwT-RD-TLS-ESPRIT method for power flow in line two are shown in Table 5.5.

It is observed from the estimated modes corresponding to the power flows for the two lines connected to a single bus as provided in Table 5.4 and Table 5.5, that the estimated modes for the data corresponding to the active power flow in the two lines is more consistent for the proposed method as compared to the NwT-RD-TLS-ESPRIT method. The TVE for the proposed method provided in Tables 5.4 and 5.5 is less in comparison with the other method.

Table 5.4: Mode estimation for line one power flow data

Methods	Attenuation factor	Frequency	% TVE
NwT-RD-TLS-ESPRIT	-0.4963	0.2716	12.2946
Proposed Method (S-RD-TLS-ESPRIT)	-0.4094	0.2470	11.0336

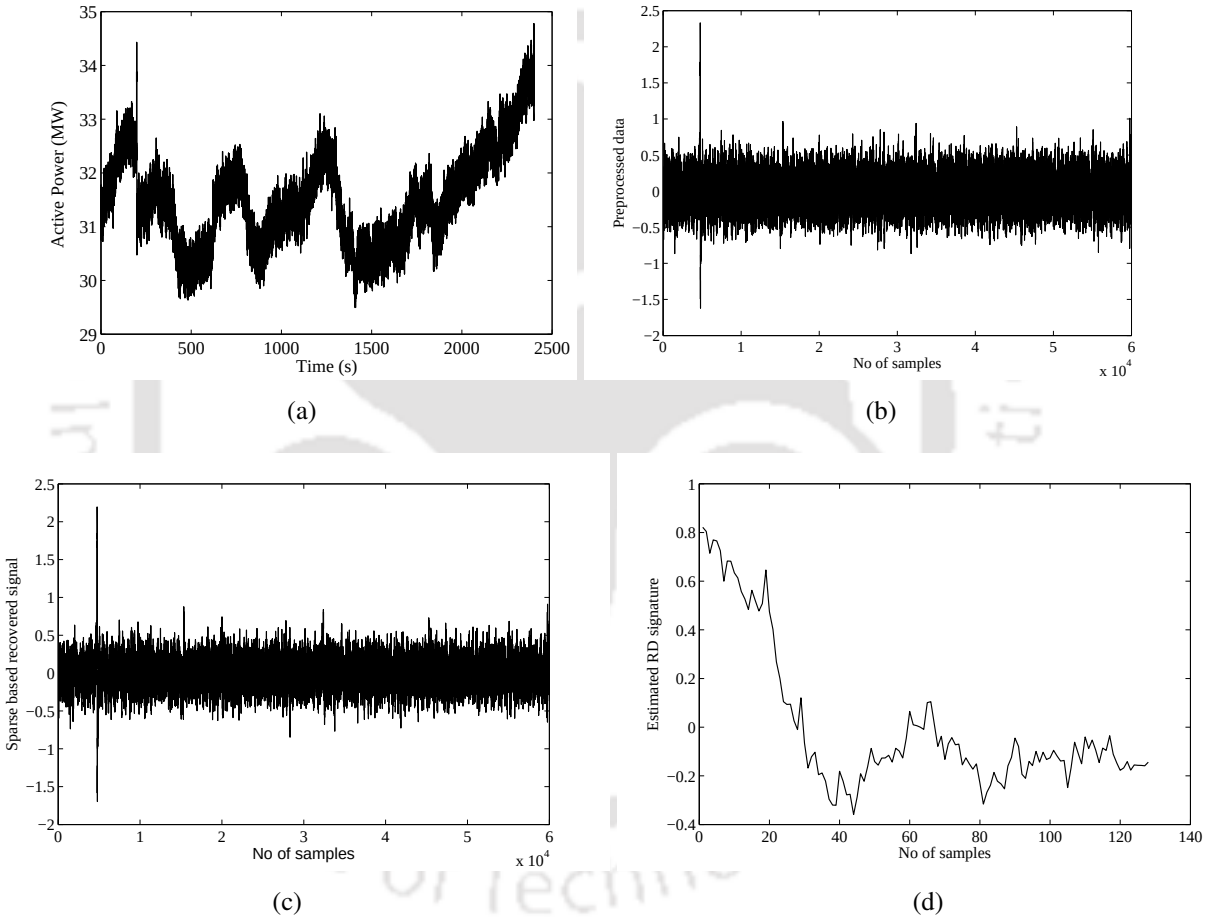

Figure 5.8: Plots for the Line 1 data (a) Active power flow of line one; (b) Signal obtained after nonlinear filtering; (c) Sparse recovery signal; (d) Estimated RD signature.

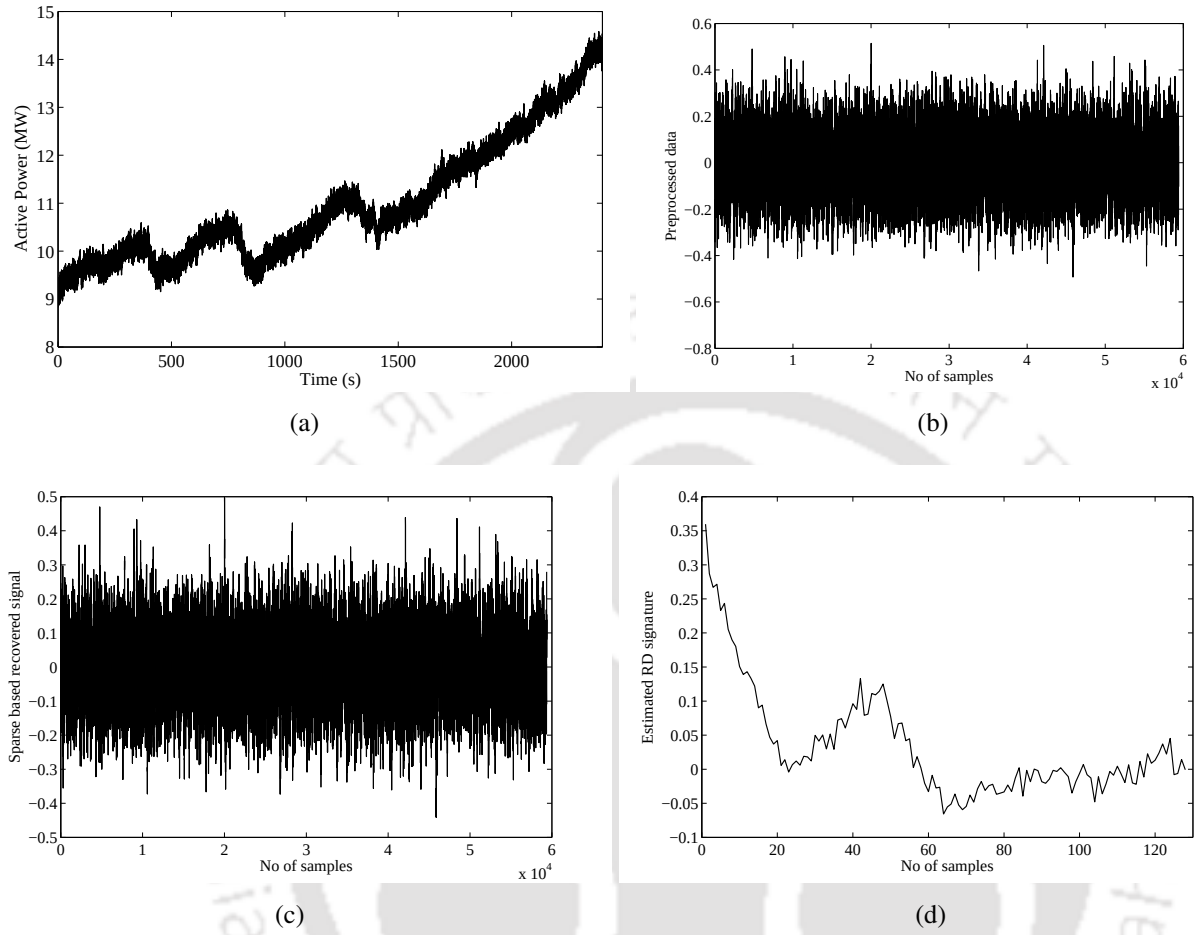

Figure 5.9: Plots for the Line 2 data (a) Active power flow of line two; (b) Signal obtained after nonlinear filtering; (c) Sparse recovery signal; (d) Estimated RD signature.

Table 5.5: Mode estimation for line two power flow data

Methods	Attenuation factor	Frequency	% TVE
NwT-RD-TLS-ESPRIT	-0.3266	0.2158	12.2800
Proposed Method (S-RD-TLS-ESPRIT)	-0.7644	0.2375	11.0340

5.3.4 Estimation of modes using the real test signal of the WECC system

A probing test data of the WECC system, as shown in Figure 5.10, obtained on September 14, 2005 [78] is utilized for comparing the performance of the proposed method with the other method. The data used for the estimation purpose is taken from the B.P.A website [79]. The estimated modes as reported in the literature for the probing test signal is 0.318 Hz and 8.3% damping [79]. The plots

for the various steps of the proposed applied to the data corresponding to window 1, 2 and 3 are provided in Figure 5.11, 5.12 and 5.13 respectively. Table 5.6 gives a comparison of the methods for the real ambient data. For the analysis widow 1, the proposed method gives better damping estimate (8.1768% damping) as compared to the other method. For analysis window 2, the proposed method gives the value of damping (8.3896 % damping) approximately close to the reported value [79] and minimum TVE (2.1607%) in comparison with the other method. The proposed method is able to estimate the damping almost accurately (7.8704% damping) as compared to the other methods for analysis window 3. For analysis window 1 and 3, the TVE for the estimated modes is comparable with the other method.

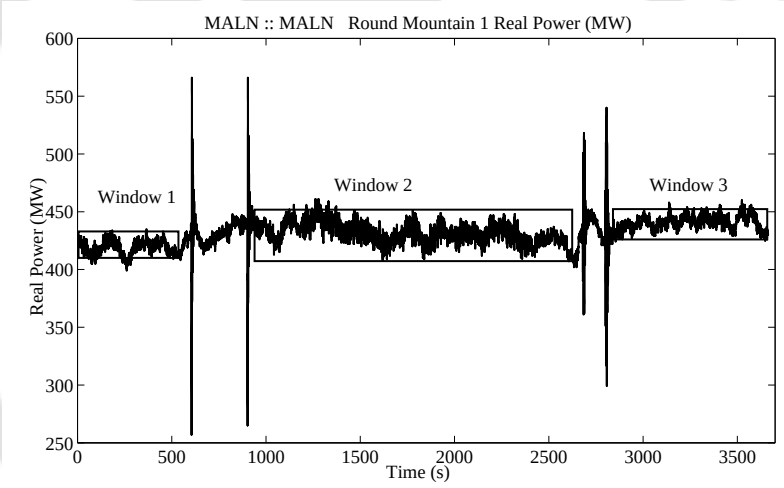

Figure 5.10: Probing data corresponding to real power flow.

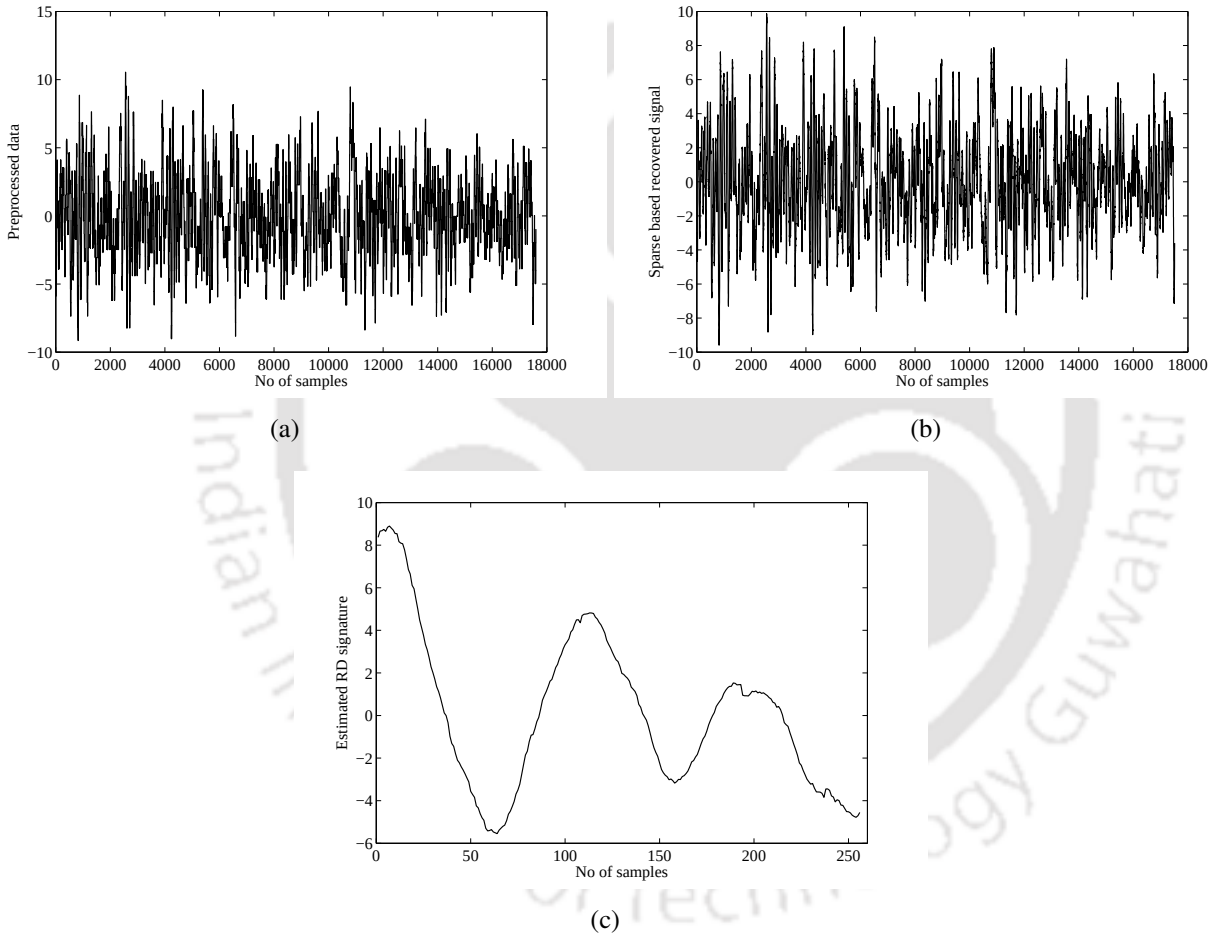

Figure 5.11: Plots for the window 1 data (a) Signal obtained after nonlinear filtering; (b) Sparse recovery signal; (c) Estimated RD signature.

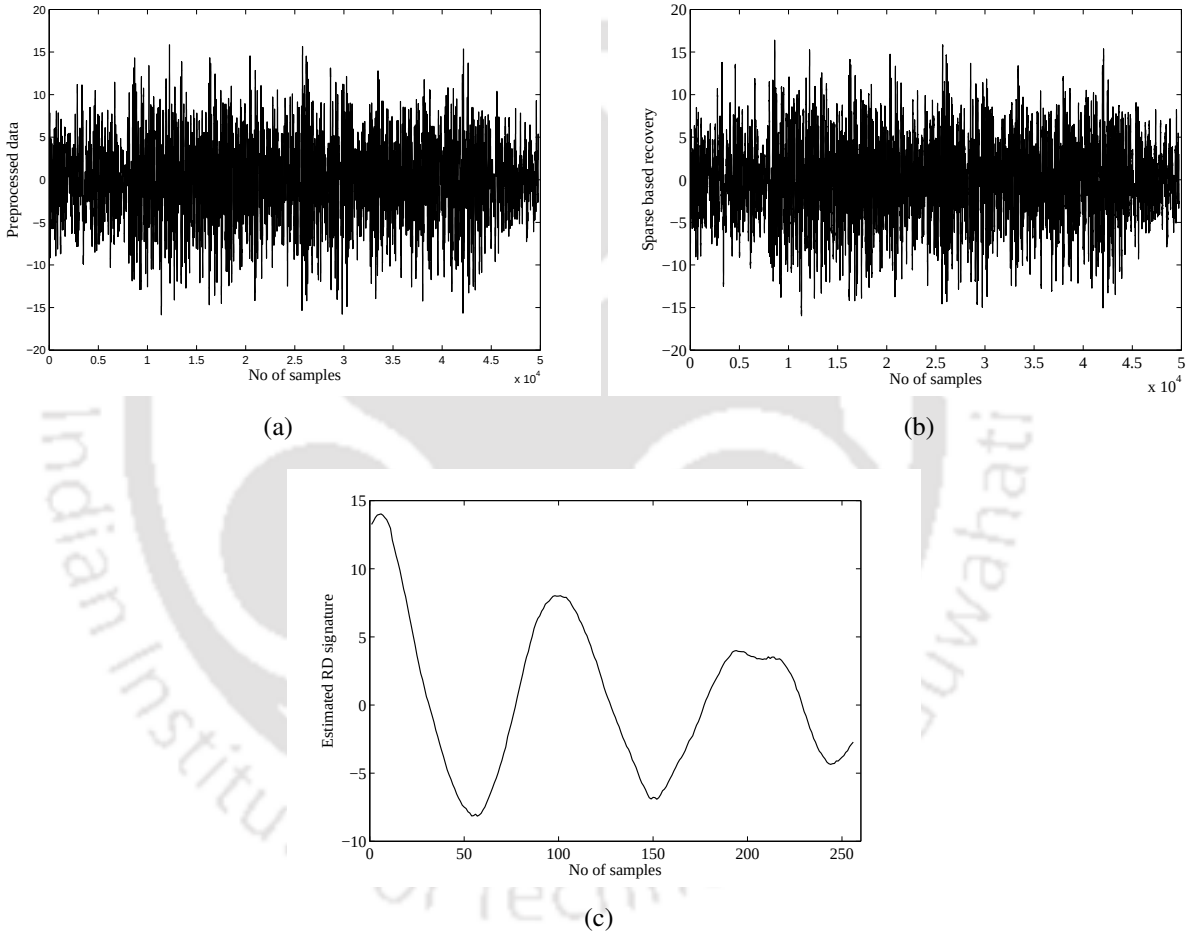

Figure 5.12: Plots for the window 2 data (a) Signal obtained after nonlinear filtering; (b) Sparse recovery signal; (c) Estimated RD signature.

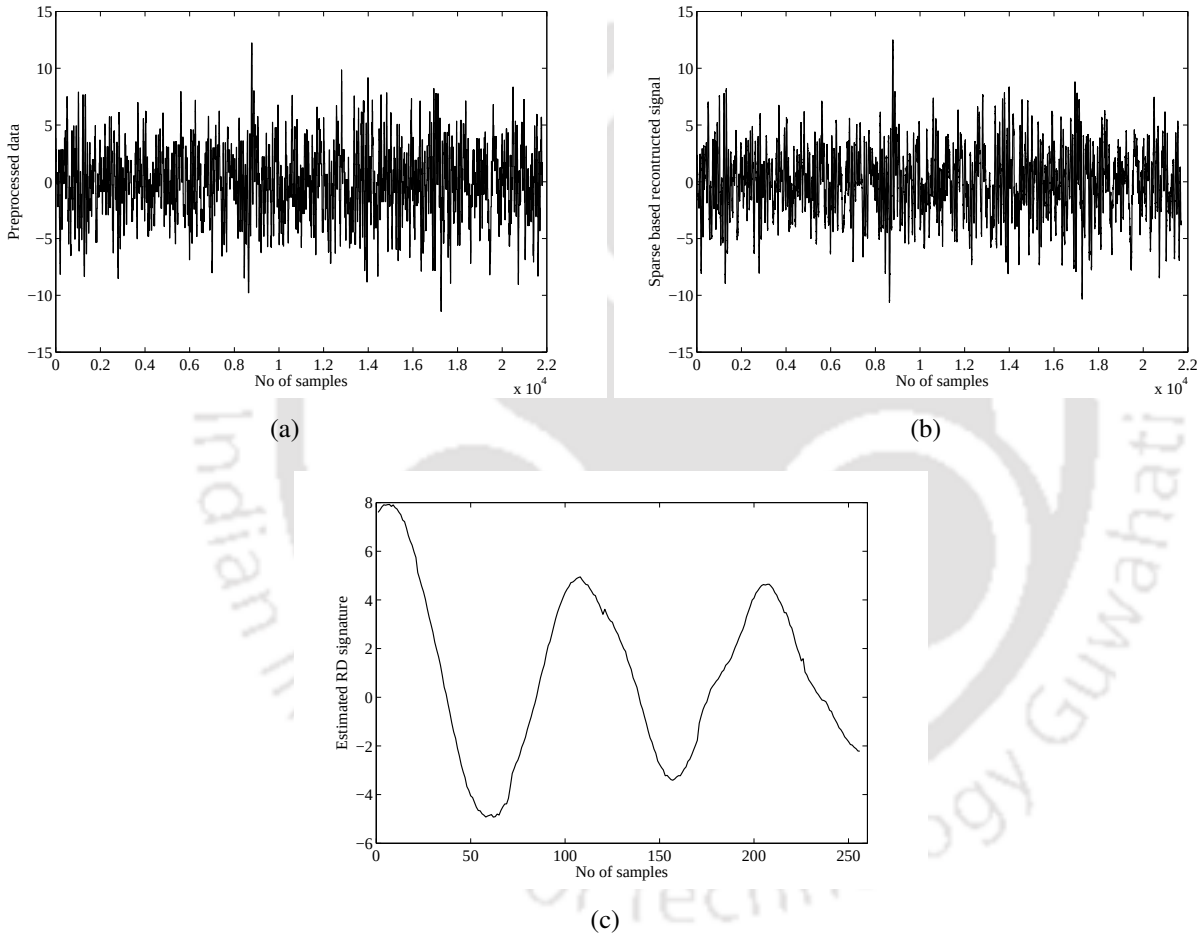

Figure 5.13: Plots for the window 3 data (a) Signal obtained after nonlinear filtering; (b) Sparse recovery signal; (c) Estimated RD signature.

Table 5.6: Estimated Mode Analysis for WECC system

Estimated mode for Analysis window 1				
	Attenuation	Frequency	% Damping	% TVE
NwT-RD-TLS-ESPRIT	-0.1506	0.2955	8.0835	7.0870
Proposed Method (S-RD-TLS-ESPRIT)	-0.1498	0.2906	8.1768	8.6377
Estimated mode for Analysis window 2				
	Attenuation	Frequency	% Damping	% TVE
NwT-RD-TLS-ESPRIT	-0.1604	0.3111	8.1760	2.1843
Proposed Method (S-RD-TLS-ESPRIT)	-0.1646	0.3111	8.3896	2.1607
Estimated mode for Analysis window 3				
	Attenuation	Frequency	% Damping	% TVE
NwT-RD-TLS-ESPRIT	-0.1849	0.2982	9.8222	6.2687
Proposed Method (S-RD-TLS-ESPRIT)	-0.1458	0.2939	7.8704	7.6254

5.4 Conclusion

This chapter proposes a robust estimation technique by utilizing sparsity, random decrement and modified TLS-ESPRIT to estimate modes corresponding to the low frequency oscillations in power system for the ambient data. The proposed method chooses a proper dictionary and selects the best set of sparse coefficients to extract the clean signal, and hence, has significantly improved its robustness towards the presence of high level of noise. To show its robustness, the proposed method is compared with NwT-RD-TLS-ESPRIT on the simulated data corresponding to ambient data, followed by the estimation of the modes for a simulated dynamics of a two-area system. Further, a comparative analysis of the proposed method with the NwT-RD-TLS-ESPRIT method is carried out for real measurement from PDC from the North Eastern Regional Electricity Board (NEREB) of India and real probing data of the Western Electricity Coordinating Council (WECC) system. From the results presented in Section 5.3, it is observed that the proposed method provides a more accurate and robust estimation of low frequency modes in the power system.

6

Conclusions

6.1 General

The synchrophasor based wide area monitoring system (WAMS) consist of phasor measurement units (PMUs), which are geographically distributed and time synchronized via GPS clock. These devices have the ability to measure both the magnitude and the phase angle of the voltages and currents in the power system. It delivers the time stamped data to the phasor data concentrator (PDC) at a high refresh rate, which has made WAMS capable enough to provide the dynamic states of the power system.

For secure and reliable operation of power system, it is required to have suitable stability margin. Since, the dynamics of interconnected power system is very complex, it is required to classify the phenomena of instability as voltage stability, frequency stability and rotor angle stability. The rotor angle stability is, further, categorized as the small signal stability and transient stability. Traditional approaches for analyzing the small signal rotor angle stability is based on eigenvalue analysis of the linearized time invariant model. These off-line based methods are suitable for system design and analysis, but cannot be applied for real time monitoring purpose. This thesis has mainly focussed on the development of synchrophasor based on-line monitoring of the small signal rotor angle stability of the system for ringdown and ambient data. The main contributions of the thesis are as follows:

- Development of a robust low frequency mode estimator for the ringdown signal corrupted with high variance noise and outliers using minimum covariance determinant (MCD) to robustify the improved Prony method.

- Development of a covariance approach based robust and fast estimator of low frequency mode using MM estimator with modified TLS-ESPRIT method.

- Development of a nonlinear filter and wavelet based low frequency mode estimator to remove the nonlinear trends and extract the signal from the noisy ambient data.

- Development of an improved low frequency mode estimator based on sparsity to separate the signal from the high amplitude noise in the ambient data.

6.2 Summary of Important Findings

In Chapter 2, a method based on the improved Prony, for estimating the low frequency modes, has been proposed. It utilizes the real time synchrophasor measurements derived from the phasor measurement unit (PMU) via phasor data concentrator (PDC). The proposed robust modified Prony method uses a minimum covariance determinant technique to find a robust covariance matrix, to mitigate the effect of bad data. A comparative analysis of the proposed method with the improved Prony and modified total least squares estimation of signal parameters via rotational invariance techniques (TLS-ESPRIT) has been carried out by running the Monte-Carlo simulations on the test signal corresponding to the inter-area and the local modes of oscillations at different noise levels with and without outliers. The effectiveness of the proposed method is also validated for two-area system. Comparison of the proposed method with the improved Prony, modified TLS-ESPRIT and eigensystem realization algorithm (ERA)/Prony are also obtained on the real time probing test data obtained from a PDC connected in the Western Electricity Coordinating Council (WECC) system. The main conclusions of the work, in this chapter, are as follows.

- It has been observed that the proposed method provides a better damping estimate in terms of the mean and variance and also a better frequency estimate in terms of variance, which clearly shows that it has negligible bias towards the presence of the high variance noise and outliers.

- The modes estimated by the proposed method is close to those obtained using the conventional eigenvalue analysis for a two-area system.

- The proposed method has provided very accurate mode estimates for the probing test data of the WECC system.

In Chapter 3, a robust total least squares estimation of signal parameters via rotational invariance techniques (TLS-ESPRIT), for estimating the low frequency modes, has been proposed. It utilizes a MM estimator to robustify the covariance matrix. A comparative analysis of the proposed method with the modified TLS-ESPRIT and robust modified Prony has been carried out on the test signal corresponding to the inter-area and the local modes of oscillations. The results are also obtained on the two-area system and on the real time probing test data obtained from a PDC connected in the WECC system. The main conclusions of this proposed work are as follows.

- The variance in the attenuation and frequency in the estimated modes of the proposed method are less as compared with the robust modified Prony method.

- The modes identified by the proposed method is quite close to those obtained by the small signal stability analysis for a two-area system.

- The proposed method has provided a more accurate estimate of the modes for the real time probing data of the WECC system as compared to the robust modified Prony method. It has also provided a fairly good estimate of the damping of the mode corresponding to the ambient data window of the probing test data.

Chapter 4 has proposed a mode estimation technique using nonlinear filter, wavelet transform, random decrement and modified TLS-ESPRIT. The proposed method selects the best set of wavelet coefficients to represent the signal which makes it capable to withstand high noise and provides an unbias estimate of the modes present in a power system. To illustrate its effectiveness, the proposed method i.e., NwT-RD-TLS-ESPRIT is compared with nonlinear filtering, natural excitation technique- eigen-system realization algorithm (NExT-ERA) and random decrement technique- Ibrahim time domain (RD-ITD) methods on the test signals, simulated second order system corresponding to the modes

present in a two-area system, two-area system simulated on real time digital simulator (RTDS) facility at IIT Kanpur. The robustness of the proposed method in identifying the oscillatory mode is also demonstrated on a real PMU data obtained from North Eastern Regional Electricity Board (NEREB) and probing data of the WECC system. The main conclusions are provided below:

- The proposed method utilizes a nonlinear filter to mitigate the non-linear trends and a wavelet based signal de-noising technique to extract the significant wavelet coefficients to represent the clean signal.
- It has been observed from the simulations that the proposed method performs better than the nonlinear filter, NExT-ERA and RD-ITD in estimating the modes.
- The proposed method has provided fairly good estimate of the modes for real ambient data of NEREB and WECC.

Chapter 5 has proposed a robust estimation technique by utilizing sparsity, random decrement and modified TLS-ESPRIT to estimate modes corresponding to the low frequency oscillations in power system for the ambient data. The proposed method chooses a proper dictionary and selects the best set of sparse coefficients to extract the clean signal, and hence, has significantly improved its robustness towards the presence of high level of noise. To show its robustness, the proposed method is compared with NwT-RD-TLS-ESPRIT on the simulated data corresponding to ambient data, followed by the estimation of the modes for a simulated dynamics of a two-area system. Further, a comparative analysis of the proposed method with the NwT-RD-TLS-ESPRIT method is carried out for real measurement from PDC from the North Eastern Regional Electricity Board (NEREB) of India and real probing data of the Western Electricity Coordinating Council (WECC) system. The main conclusions drawn from the proposed work are as follows.

- The proposed method utilizes sparsity, which involves designing an efficient dictionary from a given input signal and thereby extracting the representation coefficients from it, that best represents the noise free signal. Hence, it provides a reasonably good estimate of low frequency modes in the presence of high noise in the measured data.

- It has been observed from the simulations that the proposed method performs better than the wavelet method in estimating the modes.

- The proposed method also provides fairly good estimate of the modes for real ambient data of NEREB and WECC.

6.3 Scope for Future Research

From the result of the investigations carried out in this thesis, the following topics have been found out for future research in this area:

1. The proposed robust modified Prony and robust TLS-ESPRIT based low frequency estimator has been effective towards the presence of high variance noise and outliers. The effect of missing data can also be studied and accordingly a more robust estimator can be designed.

2. The proposed wavelet and sparse based estimator for low frequency mode estimation for ambient data has used RD method, which assumes Gaussian excitation for correct estimation of the impulse response of the system. A robust estimator can be developed which accounts for non-Gaussian excitation in the system.

3. The present thesis has primarily focussed on application of the synchrophasor technology to the small signal rotor angle stability prediction. The work may also be expanded to develop effective techniques for voltage instability prediction and other possible power system applications.

A

Data for the 11-bus, Two-Area System

A. Data for the 11-bus, Two-Area System

The two-area power system data is taken from [9]. This system comprises of 4 generators and 11 buses. The single line diagram is given in Figure A.1. Generators 1 and 2 forms the first area and the generators 3 and 4 forms the second area. Tables A.1 and A.2 shows the bus data and the line data respectively. Synchronous machine and exciter data are listed in Tables A.3 and A.4. All the system data are in p.u. The conventional power system stabilizers data are taken from reference [11].

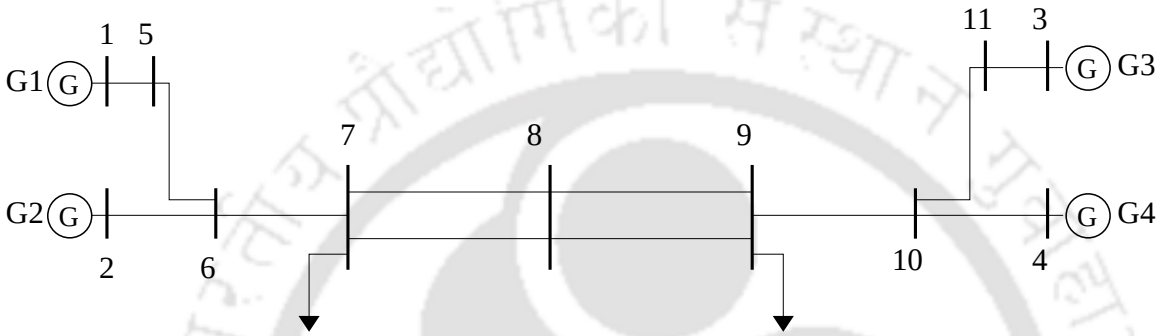

Figure A.1: Single line diagram of the two-area system.

Table A.1: Bus data (in p.u.)

Bus	V_M	P_G	P_L	Q_G	Q_L	Q_{Gmax}	Q_{Gmin}
1	1.03	7	0	1.61	0	10	-10
2	1.01	7	0	1.76	0	10	-10
7	0.98	0	9.76	0	1	0	0
5	1.01	0	0	0	0	0	0
3	1.03	7.16	0	1.49	0	10	-10
4	1.01	7	0	1.39	0	10	-10
9	0.99	0	17.7	0	1	0	0
6	0.99	0	0	0	0	0	0
8	1	0	0	1.09	0	0	0
11	1.01	0	0	0	0	0	0
10	0.99	0	0	0	0	0	0

Table A.2: Line data (in p.u.)

From Bus	To Bus	R	X	B_{SH}	Tap Ratio
1	5	0	0.0167	0	1
2	6	0	0.0167	0	1
7	6	0.0010	0.0100	0.0175	1
7	8	0.0110	0.1100	0.1925	1
7	8	0.0110	0.1100	0.1925	1
5	6	0.0025	0.0250	0.0437	1
3	11	0	0.0167	0	1
4	10	0	0.0167	0	1
9	8	0.0110	0.1100	0.1925	1
9	8	0.0110	0.1100	0.1925	1
9	10	0.0010	0.0100	0.0175	1
11	10	0.0025	0.0250	0.0437	1

Table A.3: Synchronous Machine Data

Gen. no.	Bus. no.	MVA BASE	X_L	R_A	X_d	X'_d	T'_{d0}	X_q	X'_q	T'_{q0}	H	D
1	1	900	0.2	0.0025	1.8	0.3	8	1.7	0.55	0.4	6.5	6.5
2	2	900	0.2	0.0025	1.8	0.3	8	1.7	0.55	0.4	6.5	6.5
3	3	900	0.2	0.0025	1.8	0.3	8	1.7	0.55	0.4	6.5	6.5
4	4	900	0.2	0.0025	1.8	0.3	8	1.7	0.55	0.4	6.5	6.5

Table A.4: First Order Exciter Data

Exciter at gen. no.	K_A	T_A	E_{fd}^{max}	E_{fd}^{min}
1	0.01	200	5	-5
2	0.01	200	5	-5
3	0.01	200	5	-5
4	0.01	200	5	-5

Table A.5: Power System Stabilizer Data

PSS no.	Exciter no.	K_{PSS}	T_W	T_1	T_2	T_3	T_4	PSS_OUT_{MAX}	PSS_OUT_{MIN}
1	1	400	10	0.2	0.1	0.2	0.1	0.2	-0.05
2	2	400	10	0.2	0.1	0.2	0.1	0.2	-0.05

List of Symbols:

V_M : Voltage magnitude (pu)

P_G : Real power generation (pu)

P_L : Real power load (pu)

Q_G : Reactive power generation (pu)

Q_L : Reactive power load (pu)

Q_{Gmax} : Maximum reactive power generation (pu)

Q_{Gmin} : Minimum reactive power generation (pu)

R : Resistance (pu)

X : Reactance (pu)

B_{SH} : Full line charging (pu)

X_L : Leakage reactance (pu)

R_A : Synchronous machine stator resistance (pu)

X_d : D-axis synchronous reactance (pu)

X'_d : D-axis transient reactance (pu)

T'_{d0} : D-axis open-circuit time constant (seconds)

X_q : Q-axis synchronous reactance (pu)

X'_q : Q-axis transient reactance (pu)

T'_{q0} : Q-axis open-circuit time constant (seconds)

H : Inertia constant (seconds)

D : Load damping coefficient (pu)

T_R : Exciter input filter time constant (seconds)

K_A : Voltage regulator gain

E_{fd}^{max} : Maximum exciter output voltage (pu)

E_{fd}^{min} : Minimum exciter output voltage (pu)

K_{PSS} : PSS gain

T_W : PSS washout filter time constant (seconds)

$T_1 - T_4$: PSS lead-lag network time constants (pu)

PSS_OUT_{MAX} : PSS maximum output (pu)

PSS_OUT_{MIN} : PSS minimum output (pu)

Bibliography

[1] Y. Kokai, F. Masuda, S. Horiike, and Y. Sekine, "Recent development in open systems for EMS/SCADA," *International Journal of Electrical Power & Energy Systems*, vol. 20, no. 2, pp. 111 – 123, 1998.

[2] A. Bose, "Smart Transmission Grid Applications and Their Supporting Infrastructure," *IEEE Trans. Smart Grid.*, vol. 1, no. 1, pp. 11–19, June 2010.

[3] J. Du, S. Ma, Y. C. Wu, and H. V. Poor, "Distributed Hybrid Power State Estimation under PMU Sampling Phase Errors," *IEEE Trans. Signal Process.*, vol. 62, no. 16, pp. 4052–4063, Aug 2014.

[4] C. W. Taylor, D. C. Erickson, K. E. Martin, R. E. Wilson, and V. Venkatasubramanian, "WACS-Wide-Area Stability and Voltage Control System: R & D and Online Demonstration," *Proc. IEEE*, vol. 93, no. 5, pp. 892–906, May 2005.

[5] R. B. Sharma and G. M. Dhole, "Synchrophasor measurement network and its applications in indian grid," in *2016 International Conference on Emerging Trends in Electrical Electronics Sustainable Energy Systems (ICETEESES)*, March 2016, pp. 30–34.

[6] G. Benmouyal, E. O. Schweitzer, and A. Guzman, "Synchronized phasor measurement in protective relays for protection, control, and analysis of electric power systems," in *57th Annual Conference for Protective Relay Engineers, 2004*, April 2004, pp. 419–450.

[7] R. J. Best, D. J. Morrow, D. M. Laverty, and P. A. Crossley, "Synchrophasor Broadcast Over Internet Protocol for Distributed Generator Synchronization," *IEEE Trans. Power Del.*, vol. 25, no. 4, pp. 2835–2841, Oct 2010.

[8] P. Kundur, J. Paserba, V. Ajjarapu, G. Andersson, A. Bose, C. Canizares, N. Hatziargyriou, D. Hill, A. Stankovic, C. Taylor, T. V. Cutsem, and V. Vittal, "Definition and classification of power system stability IEEE/CIGRE joint task force on stability terms and definitions," *IEEE Trans. Power Syst.*, vol. 19, no. 3, pp. 1387–1401, Aug 2004.

[9] P. Kundur, *Power System Stability and Control.* New York: McGraw-Hill, 1994.

[10] W. S. Peter and M. A. Pai, *Power System Dynamics and Stability.* New Jersey, U.S.A.: Prentice Hall, 1998.

[11] G. Rogers, *Power System Oscillations.* Norwell, MA: Kluwar, 2000.

[12] R. Messina, *Inter-area Oscillations in Power Systems: A Nonlinear and Nonstationary Perspective.* New York: Springer, 2009.

[13] Z. Dong, P. Zhang, J. Ma, J. Zhao, M. Ali, K. Meng, and X. Yin, *Emerging Techniques in Power System Analysis.* London: Springer, 2010.

[14] R. T. Byerly, R. J. Bennon, and D. E. Sherman, "Eigenvalue Analysis of Synchronizing Power Flow Oscillations in Large Electric Power Systems," *IEEE Trans. Power App. Syst.*, vol. PAS-101, no. 1, pp. 235–243, Jan 1982.

[15] D. Y. Wong, G. J. Rogers, B. Porretta, and P. Kundur, "Eigenvalue analysis of very large power systems," *IEEE Trans. Power Syst.*, vol. 3, no. 2, pp. 472–480, May 1988.

[16] P. Kundur, G. J. Rogers, D. Y. Wong, L. Wang, and M. G. Lauby, "A comprehensive computer program package for small signal stability analysis of power systems," *IEEE Trans. Power Syst.*, vol. 5, no. 4, pp. 1076–1083, Nov 1990.

[17] L. Wang and A. Semlyen, "Application of sparse eigenvalue techniques to the small signal stability analysis of large power systems," *IEEE Trans. Power Syst.*, vol. 5, no. 2, pp. 635–642, May 1990.

[18] P. L. Dandeno and P. Kundur, "Practical application of eigenvalue techniques in the analysis of power system dynamic stability problems," *Canadian Electrical Engineering Journal*, vol. 1, no. 1, pp. 35–46, Jan 1976.

[19] G. J. Rogers, "Methods for small signal analysis of very large power systems," in *26th IEEE Conference on Decision and Control, 1987.*, vol. 26, Dec 1987, pp. 393–398.

[20] Y. Obata, S. Takeda, and H. Suzuki, "An Efficient Eigenvalue Estimation Technique for Multimachine Power System Dynamic Stability Analysis," *IEEE Trans. Power App. Syst.*, vol. PAS-100, no. 1, pp. 259–263, Jan 1981.

[21] D. M. Lam, H. Yee, and B. Campbell, "An efficient improvement of the AESOPS algorithm for power system eigenvalue calculation," *IEEE Trans. Power Syst.*, vol. 9, no. 4, pp. 1880–1885, Nov 1994.

[22] N. Uchida and T. Nagao, "A new eigen-analysis method of steady-state stability studies for large power systems: S matrix method," *IEEE Trans. Power Syst.*, vol. 3, no. 2, pp. 706–714, May 1988.

[23] K. K. P. Poon and K. C. Lee, "Analysis of transient stability swings in large interconnected power systems by Fourier transformation," *IEEE Trans. Power Syst.*, vol. 3, no. 4, pp. 1573–1581, Nov 1988.

[24] A. A. Girgis and F. M. Ham, "A Quantitative Study of Pitfalls in the FFT," *IEEE Trans. Aerosp. Electron. Syst.*, vol. AES-16, no. 4, pp. 434–439, Jul 1980.

[25] F. Zhang, Z. Geng, and W. Yuan, "The algorithm of interpolating windowed FFT for harmonic analysis of electric power system," *IEEE Trans. Power Del.*, vol. 16, no. 2, pp. 160–164, Apr 2001.

[26] P. Korba, M. Larsson, and C. Rehtanz, "Detection of oscillations in power systems using Kalman filtering techniques," in *Proc. 2003 IEEE Conf. Control Applications, 2003.*, vol. 1, pp. 183–188.

[27] R. de Prony, "Essai experimentale et analytique," *J. Ecole Polytechnique (Paris)*, pp. 24–76, 1795.

[28] D. A. Pierre, D. J. Trudnowski, and J. F. Hauer, "Identifying Reduced-Order Models for Large Non-linear Systems with Arbitrary Initial Conditions and Multiple Outputs using Prony Signal Analysis," in *American Control Conference, 1990*, May 1990, pp. 149–154.

[29] J. F. Hauer, C. J. Demeure, and L. L. Scharf, "Initial results in Prony analysis of power system response signals," *IEEE Trans. Power Syst.*, vol. 5, no. 1, pp. 80–89, Feb 1990.

[30] J. F. Hauer, "Application of Prony analysis to the determination of modal content and equivalent models for measured power system response," *IEEE Trans. Power Syst.*, vol. 6, no. 3, pp. 1062–1068, Aug 1991.

[31] D. A. Pierre, D. J. Trudnowski, and J. F. Hauer, "Identifying linear reduced-order models for systems with arbitrary initial conditions using Prony signal analysis," *IEEE Trans. Autom. Control.*, vol. 37, no. 6, pp. 831–835, Jun 1992.

[32] D. Trudnowski, "Order reduction of large-scale linear oscillatory system models," *IEEE Trans. Power Syst.*, vol. 9, no. 1, pp. 451–458, Feb 1994.

[33] M. Amono, M. Watanabe, and M. Banjo, "Self-testing and self-tuning of power system stabilizers using Prony analysis," in *Proc. IEEE Power Eng. Soc. 1999 Winter Meeting*, vol. 1, Jan 1999, pp. 655–660.

[34] D. J. Trudnowski, J. Johnson, and J. Hauer, "Making Prony analysis more accurate using multiple signals," *IEEE Trans. Power Syst.*, vol. 14, no. 1, pp. 226–231, Feb 1999.

[35] J. Xiao, X. Xie, Y. Han, and J. Wu, "Dynamic tracking of low-frequency oscillations with improved Prony method in wide-area measurement system," in *Proc. IEEE Power Eng. Soc. General Meeting, Jun 2004*, pp. 1104–1109 Vol.1.

[36] L. Qi, L. Qian, S. Woodruff, and D. Cartes, "Prony analysis for power-system transient harmonics," *EURASIP J. Appl. Signal Process*, no. 1, pp. 170–181, 2007.

[37] J. J. Sanchez-Gasca and J. H. Chow, "Performance comparison of three identification methods for the analysis of electromechanical oscillations," *IEEE Trans. Power Syst.*, vol. 14, no. 3, pp. 995–1002, Aug 1999.

[38] R. Kumaresan and D. Tufts, "Estimating the parameters of exponentially damped sinusoids and pole-zero modeling in noise," *IEEE Trans. Acoust., Speech, Signal Processing*, vol. 30, no. 6, pp. 833–840, 1982.

[39] R. Kumaresan, "On the zeros of the linear prediction-error filter for deterministic signals," *IEEE Trans. Acoust., Speech, Signal Processing*, vol. 31, no. 1, pp. 217–220, Feb 1983.

[40] P. Tripathy, S. C. Srivastava, and S. N. Singh, "An improved Prony method for identifying low frequency oscillations using synchro-phasor measurements," *International conference on Power Systems, 2009. Dec. 2009.*, pp. 1–5.

[41] S. M. Zali and J. V. Milanovic, "Dynamic equivalent model of Distribution Network Cell using Prony analysis and Nonlinear least square optimization," in *PowerTech, 2009 IEEE Bucharest*, June 2009, pp. 1–6.

[42] P. N. Papadopoulos, T. A. Papadopoulos, P. Crolla, A. J. Roscoe, G. K. Papagiannis, and G. M. Burt, "Black-box dynamic equivalent model for microgrids using measurement data," *IET Gener. Transm. Distrib.*, vol. 8, no. 5, pp. 851–861, May 2014.

[43] M. R. Osborne and G. Smyth, "A modified prony algorithm for exponential function fitting," *SIAM J. Comput.*, vol. 16, no. 1, pp. 119–138, 1995.

[44] M. Perron, I. Kamwa, and L. A. Dessaint, "Development of a portable software tool for time domain modal analysis," *11th Int. Conf. on Information Science, Signal Processing and their Applications, Montreal, QC, 2009. July. 2012.*, pp. 1371–1376.

[45] A. R. Borden and B. C. Lesieutre, "Variable Projection Method for Power System Modal Identification," *IEEE Trans. Power Syst.*, vol. 29, no. 6, pp. 2613–2620, Nov 2014.

[46] T. J. Browne, V. Vittal, G. T. Heydt, and A. R. Messina, "A Comparative Assessment of Two Techniques for Modal Identification From Power System Measurements," *IEEE Trans. Power Syst.*, vol. 23, no. 3, pp. 1408–1415, Aug 2008.

[47] "On the HHT, its problems, and some solutions," *Mechanical Systems and Signal Processing*, vol. 22, no. 6, pp. 1374 – 1394, 2008, special Issue: Mechatronics.

[48] A. L. Swindlehurst, B. Ottersten, R. Roy, and T. Kailath, "Multiple invariance ESPRIT," *IEEE Trans. Signal Process.*, vol. 40, no. 4, pp. 867–881, Apr 1992.

[49] A. L. Swindlehurst, P. Stoica, and M. Jansson, "Exploiting arrays with multiple invariances using MUSIC and MODE," *IEEE Trans. Signal Process.*, vol. 49, no. 11, pp. 2511–2521, Nov 2001.

[50] H. Zeineldin, T. Abdel-Galil, E. El-Saadany, and M. Salama, "Islanding detection of grid connected distributed generators using TLS-ESPRIT," *Electric Power Systems Research*, vol. 77, no. 2, pp. 155 – 162, 2007.

[51] I. Y. H. Gu and M. H. J. Bollen, "Estimating Interharmonics by Using Sliding-Window ESPRIT," *IEEE Trans. Power Del.*, vol. 23, no. 1, pp. 13–23, Jan 2008.

[52] J. W. Pierre, D. J. Trudnowski, and M. K. Donnelly, "Initial results in electromechanical mode identification from ambient data," *IEEE Trans. Power Syst.*, vol. 12, no. 3, pp. 1245–1251, Aug 1997.

[53] R. W. Wies, J. W. Pierre, and D. J. Trudnowski, "Use of ARMA block processing for estimating stationary low-frequency electromechanical modes of power systems," *IEEE Trans. Power Syst.*, vol. 18, no. 1, pp. 167–173, Feb 2003.

[54] R. W. Wies, J. W. Pierre, and D. J. Trudnowski., "Use of least mean squares (LMS) adaptive filtering technique for estimating low-frequency electromechanical modes in power systems," in *Proc. IEEE Power Eng. Soc. General Meeting*, June 2004, pp. 1863–1870 Vol.2.

[55] R. W. Wies, A. Balasubramanian, and J. W. Pierre, "Using adaptive step-size least mean squares (ASLMS) for estimating low-frequency electromechanical modes in power systems," in *Proc. 9th International Conference on Probabilistic Methods Applied to Power Systems*, June 2006, pp. 1–8.

[56] X. Wang, F. Tang, X. Wang, and P. Zhang, "Estimation of electromechanical modes under ambient condition via random decrement technique and TLS-ESPRIT algorithm," in *Power System Technology (POWERCON), 2014 International Conference on*, Oct 2014, pp. 588–593.

[57] N. Zhou, J. W. Pierre, D. J. Trudnowski, and R. T. Guttromson, "Robust RLS Methods for Online Estimation of Power System Electromechanical Modes," *IEEE Trans. Power Syst.*, vol. 22, no. 3, pp. 1240–1249, Aug 2007.

[58] N. Zhou, D. J. Trudnowski, J. W. Pierre, and W. A. Mittelstadt, "Electromechanical Mode Online Estimation Using Regularized Robust RLS Methods," *IEEE Trans. Power Syst.*, vol. 23, no. 4, pp. 1670–1680, Nov 2008.

[59] J. Turunen, M. Larsson, P. Korba, J. Jyrinsalo, and L. Haarla, "Experiences and future plans in monitoring the inter-area power oscillation damping," in *IEEE Power and Energy Society General Meeting, 2008*, July 2008, pp. 1–8.

[60] D. J. Trudnowski, J. W. Pierre, N. Zhou, J. F. Hauer, and M. Parashar, "Performance of three modemeter block-processing algorithms for automated dynamic stability assessment," *IEEE Trans. Power Syst.*, vol. 23, no. 2, pp. 680–690, May 2008.

[61] N. Zhou, J. Pierre, and R. Wies, "Estimation of low-frequency electromechanical modes of power systems from ambient measurements using a subspace method," in *Proc. North American Power Symp.*, 2003, pp. 1–4.

[62] G. Liu and V. Venkatasubramanian, "Oscillation monitoring from ambient pmu measurements by frequency domain decomposition," in *Proc. IEEE Int. Symp. on Circuits and Systems*, May 2008, pp. 2821–2824.

[63] J. Ning, X. Pan, and V. Venkatasubramanian, "Oscillation modal analysis from ambient synchrophasor data using distributed frequency domain optimization," *IEEE Trans. Power Syst.*, vol. 28, no. 2, pp. 1960–1968, May 2013.

[64] M. Larsson and D. S. Laila, "Monitoring of inter-area oscillations under ambient conditions using subspace identification," in *Proc. IEEE Power Energy Society General Meeting*, July 2009, pp. 1–6.

[65] J. Turunen, T. Rauhala, and L. Haarla, "Selecting wavelets for damping estimation of ambient-excited electromechanical oscillations," in *Power and Energy Society General Meeting, 2010 IEEE*, July 2010, pp. 1–8.

[66] J. Thambirajah, N. Thornhill, and B. Pal, "A Multivariate Approach Towards Interarea Oscillation Damping Estimation Under Ambient Conditions Via Independent Component Analysis and Random Decrement," *IEEE Trans. Power Syst.*, vol. 26, no. 1, pp. 315–322, Feb 2011.

[67] J. Turunen, J. Thambirajah, M. Larsson, B. Pal, N. Thornhill, L. Haarla, W. Hung, A. Carter, and T. Rauhala, "Comparison of Three Electromechanical Oscillation Damping Estimation Methods," *IEEE Trans. Power Syst.*, vol. 26, no. 4, pp. 2398–2407, Nov 2011.

[68] J. Seppanen, J. Turunen, M. Koivisto, N. Kishor, and L. Haarla, "Modal Analysis of Power Systems Through Natural Excitation Technique," *IEEE Trans. Power Syst.*, vol. 29, no. 4, pp. 1642–1652, July 2014.

[69] G. H. James, T. G. Carne, and J. P. Lauffer, "The natural excitation technique for modal parameter extraction from operating wind turbines," *Sandia National Laboratories,SAND92-1666 UC-261. Albuquerque, NM, USA*, 1993.

[70] J. N. Juang and R. S. Pappa, "An eigensystem realization algorithm for modal parameter identification and model reduction," *J. Guidance Control*, vol. 8, pp. 620–627, 1985.

[71] P. Zhang, Y. Teng, X. Wang, and X. Wang, "Estimation of interarea electromechanical modes during ambient operation of the power systems using the RDT-ITD method," *International Journal of Electrical Power and Energy Systems*, vol. 71, no. Complete, pp. 285–296, 2015.

[72] R. G. Farmer and E. H. Allen, "Power system dynamic performance advancement from history of north american blackouts," in *Proc. IEEE PES Power Systems Conference and Exposition*, Oct 2006, pp. 293–300.

[73] R. Roy and T. Kailath, "ESPRIT-estimation of signal parameters via rotational invariance techniques," *IEEE Trans. Acoust., Speech, Signal Processing*, vol. 37, no. 7, pp. 984–995, Jul 1989.

[74] N. Zhou, J. W. Pierre, and J. F. Hauer, "Initial results in power system identification from injected probing signals using a subspace method," *IEEE Trans. Power Syst.*, vol. 21, no. 3, pp. 1296–1302, Aug 2006.

[75] P. Tripathy, S. C. Srivastava, and S. N. Singh., "A modified TLS-ESPRIT-based method for low-frequency mode identification in power systems utilizing synchrophasor measurements," *IEEE Trans. Power Syst.*, vol. 26, no. 2, pp. 719–727, May 2011.

[76] P. Huber, *Robust Statistics*. Wiley Series in Probability and Statistics, John Wiley & Sons, 2004.

[77] R. Maronna, R. Martin, and V. Yohai, *Robust Statistics:Theory and Methods*. Wiley Series in Probability and Statistics,Wiley, 2006.

[78] PDCI Probe Testing Plan, 2005 [Online]. Available: http://www.transmission.bpa.gov/business/operations/SystemNews/.

[79] Report and data of WECC. [Online]. Available: ftp://ftp.bpa.gov/pub/WAMS_Information/.

[80] F. Hildebrand, *Introduction to Numerical Analysis*. Dover Books on Advanced Mahematics, Dover Publications, Incorporated, 1956.

[81] G. Golub and C. F. V. Loan, *Matrix Computations*. Baltimore, MD: Johns Hopkins Univ. Press, 1989.

[82] M. Daszykowski, K. Kaczmarek, Y.V.Heyden, and B. Walczak, "Robust statistics in data analysis- A review: Basic concepts," *Chemometrics and intelligent Laboratory Systems*, vol. 85, no. 2, pp. 203–219, 2007.

[83] M. Hubert and P. J. Rousseeuw, "ROBPCA: A new approach to robust principal component analysis," *Technometrics*, vol. 47, no. 1, pp. 64–79, 2005.

[84] P. J. Rousseeuw and K. V. Driessen, "A Fast algorithm for the minimum covariance determinant estimator," *Technometrics*, vol. 41, no. 3, pp. 212–223, 1999.

[85] I. Jolliffe, "Principal Component Analysis," *Springer Series in Statistics, Springer*, 2002.

[86] V. Verardi and A. McCathie, "The S-estimator of multivariate location and scatter in Stata," *Stata Journal*, vol. 12, no. 2, 2012.

[87] C. Croux and G. Haesbroeck, "Influence Function and Efficiency of the Minimum Covariance Determinant Scatter Matrix Estimator," *Journal of Multivariate Analysis*, vol. 71, no. 2, pp. 161–190, 1999.

[88] K. S. Tatsuoka and D. E. Tyler, "On the uniqueness of S-functionals and M-functionals under Nonelliptical Distributions," *The Annals of Statistics*, vol. 28, no. 4, pp. 1219–1243, Aug. 2000.

[89] M. Salibián-Barrera, S. Van Aelst, and G. Willems, "Principal components analysis based on multivariate MM estimators with fast and robust bootstrap," *J Am Stat Assoc*, vol. 101, no. 475, pp. 1198–1211, 2006.

[90] C. Chen, "Robust regression and outlier detection with the ROBUSTREG procedure," *SUGI Paper*, no. 265-27, 2002.

[91] *IEEE Standard for Synchrophasor Measurements for Power Systems*. IEEE Standard C37.118.1aTM-2014, Mar 2014.

[92] L. L. Scharf, "The SVD and reduced rank signal processing," *Signal Processing*, vol. 25, no. 2, pp. 113–133, 1991.

[93] S. Rai, S. K. Nayak, and P. Tripathy, "A Nonlinear Filtering Technique along with RD and TLS-ESPRIT for Mode Identification of ambient Data," in *2015 Annual IEEE India Conference (INDICON)*, Dec 2015, pp. 1–6.

[94] D. Donoho, I. Johnstone, and I. M. Johnstone, "Ideal spatial adaptation by wavelet shrinkage," *Biometrika*, vol. 81, pp. 425–455, 1993.

[95] C. S. Chang and NASA, *Study of Dynamic Characteristics of Aerodynamic Systems Utilizing Random dec Signatures*. CR-132563, 1975.

[96] A. H. Cole and NASA, *On-line Failure Detection and Damping Measurements of Space Structures by Random Decrement Signatures*. CR-2205, 1973.

[97] S. R. Ibrahim, "Random Decrement technique for modal identifications of structures," *J. Spacecrafts and Rockets*, vol. 14, pp. 696–700, 1977.

[98] A. A. Al-Sanad, M. S. Aggour, and M. I. Amer, "Use of random loading in soil testing," *Indian Geotech. J*, vol. 16, no. 2, pp. 126–135, 1986.

[99] R. Brincker, S. Krenk, P. H. Kirkegaard, and A. Rytter, "Identification of dynamic properties from correlation function estimates," *Bygningsstatiske Meddelelser*, vol. 63, no. 1, pp. 1–38, 1992.

[100] J. C. Amussen, S. R. Ibrahim, and R. Brinker, "Random Decrement Identification of Structures Subjected to Ambient Excitation," *Proc. of 16h IMAC*, pp. 914–921, 1998.

[101] M. Aharon, M. Elad, and A. Bruckstein, "K -SVD: An Algorithm for Designing Overcomplete Dictionaries for Sparse Representation," *IEEE Trans. Signal Process.*, vol. 54, no. 11, pp. 4311–4322, Nov 2006.

[102] R. Rubinstein, A. Bruckstein, and M. Elad, "Dictionaries for Sparse Representation Modeling," *Proc. IEEE*, vol. 98, no. 6, pp. 1045–1057, June 2010.

[103] J. Tropp and A. Gilbert, "Signal Recovery From Random Measurements Via Orthogonal Matching Pursuit," *IEEE Trans. Inf. Theory.*, vol. 53, no. 12, pp. 4655–4666, Dec 2007.

[104] J. Wang, S. Kwon, and B. Shim, "Generalized Orthogonal Matching Pursuit," *IEEE Trans. Signal Process.*, vol. 60, no. 12, pp. 6202–6216, Dec 2012.

[105] R. Rubinstein, M. Zibulevsky, and M. Elad, "Efficient implementation of the K-SVD algorithm and the Batch-OMP method," *Department of Computer Science, Technion, Israel, Tech. Rep*, 2008.

Curriculam Vitae

Shekha Rai

Educational Qualifications

Doctor of Philosophy (Ph.D.): from the Department of Electronics & Electrical Engineering, Indian Institute of Technology Guwahati, India. Thesis submission: April 2017, Cumulative Performance Index (CPI): 8.83/10.

Bachelor of Engineering (B. E): in Electrical Engineering, Jorhat Engineering College, Assam, India. Year of completion: 2009, Percentage of Marks: 74.10%.

Research Papers (Published)

Referred Journal:

(i) **S. Rai**, D. Lalani, S. K. Nayak, T. Jacob and P. Tripathy "Estimation of Low-Frequency Modes in Power System using Robust Modified Prony", *IET Generation Transmission and Distribution*, vol. 10, no.6, 2016, pp. 1401-1409.

Conference Proceedings:

(i) **S. Rai**, P. Tripathy and S. K. Nayak, " A Robust TLS-ESPRIT Method using Covariance Approach for Identification of Low-Frequency Oscillatory Mode in Power Systems," *IEEE NPSC-2014*, 18-20 Dec-2014, Guwahati, India.

(ii) **S. Rai**, S. K. Nayak and P. Tripathy, " A Nonlinear Filtering Technique along with RD and TLS-ESPRIT for Mode Identification of Ambient Data," *IEEE INDICON-2015*, 17-20 Dec-2015, New Delhi, India.

(iii) **S. Rai**, P. Tripathy and S. K. Nayak, " An efficient wavelet based technique for oscillatory mode identification of ambient data via RD and TLS-ESPRIT," *IEEE NPSC-2016*, 19-21 Dec-2016, Bhubaneshwar, India. (**2nd Best poster award**)

Manuscript Communicated:

(i) **S. Rai**, P. Tripathy and S. K. Nayak, "Using sparsity to estimate Low frequency mode from Ambient Data via Random Decrement and TLS-ESPRIT", (*in International Transactions on Electrical Energy Systems*)